



MARMARA UNIVERSITY
INSTITUTE FOR GRADUATE STUDIES
IN PURE AND APPLIED SCIENCES



**RECOVERY OF PHOSPHORUS FROM
SEWAGE SLUDGE ASH WITH
SEQUENCING BIOLEACHING AND
ELECTRODIALYSIS**

BÜŞRA KUNT

MASTER THESIS

Department of Environmental Engineering

Thesis Supervisor

Assoc. Prof. Dr. Neslihan Semerci

ISTANBUL, 2018



MARMARA UNIVERSITY
INSTITUTE FOR GRADUATE STUDIES
IN PURE AND APPLIED SCIENCES



**RECOVERY OF PHOSPHORUS FROM
SEWAGE SLUDGE ASH WITH
SEQUENCING BIOLEACHING AND
ELECTRODIALYSIS**

BÜŞRA KUNT
(524314007)

MASTER THESIS

Department of Environmental Engineering

Thesis Supervisor

Assoc. Prof. Dr. Neslihan Semerci

ISTANBUL, 2018

MARMARA UNIVERSITY
INSTITUTE FOR GRADUATE STUDIES
IN PURE AND APPLIED SCIENCES

Büşra KUNT, a Master of Science student of Marmara University Institute for Graduate Studies in Pure and Applied Sciences, defended her thesis entitled “**Recovery of Phosphorus from Sewage Sludge Ash with Sequencing Bioleaching and Electrodialysis**”, on Jan 17, 2018 and has been found to be satisfactory by the jury members.

Jury Members

Assoc. Prof. Dr. Neslihan SEMERCI (Advisor)

Marmara University(SIGN).....

Prof. Dr. Barış ÇALLI (Jury Member)

Marmara University(SIGN).....


Assoc. Prof. Dr. Özgür AKTAŞ (Jury Member)

İstanbul Medeniyet University(SIGN).....

APPROVAL

Marmara University Institute for Graduate Studies in Pure and Applied Sciences Executive Committee approves that Büşra KUNT be granted the degree of Master of Science in Department of Environmental Engineering Program on 22.01.2018.
(Resolution no: 2018/02-03)

Director of the Institute


Prof. Dr. Süleyman EKİCİ
Enstitu Müdürü


ACKNOWLEDGEMENT

I would like to express my gratitude to my advisor, Assoc. Prof. Dr. Neslihan SEMERCI, for her guidance, motivation, support and advices from the beginning of the study to the end of it. It was a good experience for me to study with her.

Besides my advisor, I would also thank to Prof. Dr. Barış ÇALLI for his comments and advices throughout the study. It was a good pleasure for me to get ideas from him.

Also, special thanks to Assoc. Prof. Dr. Serdar AKTAŞ and his team MC365 for their helps.

I thank to all of the members of the Environmental Engineering Laboratory and also my friends for their helps.

I would like to express my appreciation to my family for their understanding, support and encouragement during all of my education.

Lastly, special thanks to Research Fund of Marmara University (BAPKO) for supporting this study (Project Number: FEN-C-YLP-100616-0278).

December, 2017

Büşra KUNT

TABLE OF CONTENTS

	PAGE
ACKNOWLEDGEMENT	i
TABLE OF CONTENTS	ii
ABSTRACT	vi
ÖZET	vii
SYMBOLS	viii
ABBREVIATIONS	ix
LIST OF FIGURES	x
LIST OF TABLES	xv
1. INTRODUCTION	1
1.1. Aim and Scope of the Study	1
1.2. Phosphorus	2
1.2.1. Phosphorus cycle	3
1.2.2. Phosphorus production	4
1.2.3. Usage areas of phosphorus	8
1.2.4. Phosphorus removal in wastewater treatment plants.....	10
1.2.4.1. Biological phosphorus removal	10
1.2.4.2. Chemical phosphorus removal	12
1.3. Phosphorus Recovery	13
1.3.1. Phosphorus recovery from meat and bone meal.....	13
1.3.2. Phosphorus recovery from manure.....	15
1.3.3. Phosphorus recovery from agricultural waste	18
1.3.4. Phosphorus recovery from wastewater treatment plants	20

1.4. Final Products of Phosphorus Recovery Processes	22
1.4.1. Struvite	22
1.4.2. Calcium phosphate	25
1.5. Main Phosphorus Recovery Processes from Municipal Wastewater	27
1.5.1. Chemical precipitation.....	27
1.5.2. Adsorption	28
1.5.3. Wet chemical process	28
1.5.4. Thermochemical process	29
1.6. Phosphorus Recovery from Municipal Wastewater	31
1.6.1. Phosphorus recovery from aqueous phase.....	31
1.6.2. Phosphorus recovery from sewage sludge.....	36
1.6.3. Phosphorus recovery from sewage sludge ash	37
1.7. Sewage Sludge Management.....	39
1.8. Sewage Sludge Ash	43
1.8.1. Sewage sludge ash characteristics	43
1.9. Bioleaching.....	45
1.9.1. Microorganisms in bioleaching	46
1.9.2. Mechanisms of bioleaching.....	47
1.9.3. Studies about bioleaching.....	49
1.10. Electrodialysis	51
1.10.1. Ion exchange membranes	53
1.10.2. Electrodes and electrode reactions	54
1.10.3. Transport mechanisms.....	55
1.10.4. Studies about electrodialysis	56
2. MATERIAL AND METHOD	58

2.1. Sewage Sludge Ash	58
2.1.1. Characterization of sewage sludge ash	59
2.2. Isolation and Enrichment of Bioleaching Bacteria.....	59
2.2.1. Isolation and enrichment of Iron oxidizing bacteria.....	59
2.2.2. Isolation and enrichment of Sulfur oxidizing bacteria	60
2.3. Bioleaching Experiments.....	61
2.4. Electrodialysis Experiments	65
2.4.1. Electrodes	66
2.4.2. Anion and cation exchange membranes	67
2.4.3. Power supply	67
2.5. Analytical Methods	68
2.5.1. pH and conductivity	68
2.5.2. Phosphate.....	68
2.5.3. Sulfate.....	68
2.5.4. Heavy metals	68
2.5.5. Calcium and Magnesium.....	69
2.6. Calculations	69
3. RESULTS AND DISCUSSION	70
3.1. Characterization of Sewage Sludge Ash	70
3.1.1. Physical-chemical characterization of sewage sludge ash	70
3.1.2. Phosphorus and heavy metal content of sewage sludge ash.....	72
3.2. Isolation and Enrichment of the Bioleaching Bacteria.....	72
3.3. Bioleaching Studies	74
3.3.1. Determination of optimum ash amount.....	74
3.3.1.1. Bioleaching with Iron oxidizing bacteria	75

3.3.1.2. Bioleaching with Sulfur oxidizing bacteria	80
3.3.1.3. Bioleaching with mixture of Sulfur&Iron oxidizing bacteria	83
3.3.1.4. Optimum ash amount	86
3.3.2. Determination of optimum inocula volume.....	86
3.3.2.1. Bioleaching with Sulfur oxidizing bacteria	86
3.3.2.2. Bioleaching with mixture of Sulfur&Iron oxidizing bacteria	89
3.3.2.3. Optimum inocula volume	93
3.3.3. Determination of optimum amount of sulfur.....	93
3.3.4. Bioleaching in 2 L reactor	96
3.4. Electrodialysis Studies.....	99
3.4.1. Electrodialysis with graphite electrodes	99
3.4.2. Electrodialysis with gold coated copper electrodes.....	102
3.4.2.1. Electrodialysis with the synthetic phosphate containing solution	102
3.4.2.2. Electrodialysis with bioleaching solution.....	104
4. CONCLUSIONS	112
REFERENCES	114

ABSTRACT

RECOVERY OF PHOSPHORUS FROM SEWAGE SLUDGE ASH WITH SEQUENCING BIOLEACHING AND ELECTRODIALYSIS

Phosphorus is an essential element for all living organisms and also for plants. However, phosphate rock which is the main source of the phosphorus is limited, thus it must be recovered from its secondary sources like sewage sludge ash. Sewage sludge ash is one of the most promising secondary sources because it contains considerable amounts of phosphorus. The drawback of the sewage sludge ash as being secondary source is the presence of the heavy metals beside phosphorus. Thus, in this study, recovery of the phosphorus from sewage sludge ash with bioleaching and electro dialysis processes was investigated. Bioleaching process was applied to dissolve the phosphorus inside the sewage sludge ash and with electro dialysis process separation of the dissolved phosphorus from the heavy metals that become soluble after bioleaching was aimed. Batch bioleaching experiments were carried out with Sulfur and Iron oxidizing bacteria to optimize the process in terms of phosphorus dissolution. Maximum phosphorus dissolution was obtained from the experiment realized with Sulfur oxidizing bacteria with 81.7% of the phosphorus dissolution after 30 days with solid to liquid ratio of 1:100. Electro dialysis experiments were performed in 3 compartment electro dialysis reactor with graphite and gold coated copper electrodes. Phosphorus passage to anode part was only 6.6% with graphite electrodes because anode electrode was damaged at the 2nd day after introducing electrical current. However, experiment with gold coated copper electrodes lasted 14 days and 24.6% of the phosphorus transported to the anode part.

December, 2017

Büşra KUNT

ÖZET

ARITMA ÇAMURU KÜLÜNDE BİYOLİÇ VE ELEKTRODİYALİZ İLE FOSFOR GERİ KAZANIMI

Fosfor tüm canlılar ve bitkiler için çok önemli bir elementtir. Fakat, fosforun temel kaynağı olan fosfat kayaları sınırlıdır ve bu nedenle fosforun arıtma çamuru külü gibi ikincil kaynaklarından geri kazanımı oldukça önemlidir. Arıtma çamuru külü içerisindeki yüksek fosfor miktarı nedeniyle umut verici bir ikincil kaynaktır. Ancak, fosfor açısından ikincil kaynak olan arıtma çamuru fosforun yanı sıra ağır metaller de içermektedir. Bu nedenle, bu çalışmada biyoliç ve elektrodializ prosesleri ile arıtma çamuru külünden fosfor geri kazanımı incelenmiştir. Biyoliç prosesi ile arıtma çamuru içerisindeki fosforun çözünmesi amaçlanırken, elektrodializ prosesi ile biyoliç prosesi sonrası fosfor ile eş zamanlı çözünen ağır metallerin fosfordan ayrılması amaçlanmıştır. Biyoliç deneyleri, kesikli sistemlerde Kükürt ve Demir oksitleyen bakteriler kullanılarak gerçekleştirilerek maksimum fosfor çözünmesini elde etmek amacıyla proses optimize edilmeye çalışılmıştır. Yapılan çalışmalar sonucunda maksimum fosfor çözünmesi, 30 gün sonunda, katı sıvı oranı 1:100 olan ve Kükürt bakterilerinin kullanıldığı sistemden %81.7 olarak elde edilmiştir. Elektrodializ çalışmaları 3 bölmeli bir reaktörde, grafit ve altın kaplamalı bakır elektrotlar kullanılarak gerçekleştirilmiştir. Grafit elektrotlarla gerçekleştirilen deneyde grafit elektrotun sisteme akım verilmeye başladıktan 2 gün sonra zarar görmesi nedeniyle anot kısma taşınan fosfor %6.6 olmuştur. Ancak, altın kaplamalı bakır elektrotlar ile gerçekleştirilen deney 14 gün boyunca sürdürülmüş ve anot kısımda toplanan fosfor %24.6 olmuştur.

Aralık, 2017

Büşra KUNT

SYMBOLS

A	: Ampere
cm	: Centimeter
e⁻	: Electron
Fe²⁺	: Ferrous ion
Fe³⁺	: Ferric ion
g	: Gram
I	: Electric current (A)
kg	: Kilogram
L	: Liter
LoI	: Loss on Ignition (%)
M	: Molarity
mA	: Milliampere
Me	: Metal
meq	: Milliequivalent
mg	: Milligram
MJ	: Megajoule
mL	: Milliliter
mm	: Millimeter
mS	: Millisiemens
MT	: Megaton
PO₄³⁻	: Phosphate ion (mg/L)
R	: Partial resistances (Ω)
rpm	: Revolution per minute
sec	: Second
SO₄²⁻	: Sulfate ion (mg/L, g/L)
U	: Voltage (V)
V	: Volt
w%	: Weight Percent
μm	: Micrometer
~	: Almost equal to

ABBREVIATIONS

ACP	: Amorphous Calcium Phosphate
AEDS	: <i>Acidithiobacillus sp.</i> Enriched Digested Sludge
AN	: Anion Exchange Membrane
ATP	: Adenosine Triphosphate
AWBs	: Agricultural Waste/ Byproducts
CAT	: Cation Exchange Membrane
CMIA	: Chicken Manure Incinerated Ash
COD	: Chemical Oxygen Demand
CSH	: Calcium Silicate Hydrate
DAP	: Diammonium Phosphate
DCPA	: Dicalcium Phosphate Anhydrate
DCPD	: Dicalcium Phosphate Dihydrate
DNA	: Deoxyribonucleic Acid
HAP	: Hydroxyapatite
ICP-OES	: Inductively Coupled Plasma- Optical Emission Spectrometry
MAP	: Monoammonium Phosphate
MBM	: Meat and Bone Meal
OCP	: Octocalcium Phosphate
P	: Phosphorus
PAOs	: Phosphorus Accumulating Organisms
PHB	: Polyhydroxybutyrate
S.D.	: Standard Deviation
SS	: Sewage Sludge
SSA	: Sewage Sludge Ash
SRM	: Specified Risk Materials
SWO	: Supercritical Water Oxidation
TCP	: Tricalcium Phosphate
TS	: Total Solids
TSE	: Transmissible Spongiform Encephalopathy
TSP	: Triple Superphosphate
XRD	: X-Ray Powder Diffraction

LIST OF FIGURES

	PAGE
Figure 1.1. A schematic diagram of aquatic phosphorus cycle (Worsfold et al., 2016)..	3
Figure 1.2. Phosphorus flow in urban areas (Pearce, 2015)	4
Figure 1.3. Phosphorus production curve (Cordell et al., 2009).....	5
Figure 1.4. World phosphate rock reserves in 2016 (Data: United States Geological Survey, 2017)	5
Figure 1.5. Share of world rock phosphate production in 2016 (Data: United States Geological Survey, 2017).....	6
Figure 1.6. Production of phosphoric acid with wet chemical method (Villalba et al., 2008).....	7
Figure 1.7. Share of phosphate rock use (Scholz et al., 2014)	8
Figure 1.8. Technical use of phosphorus (Gantner et al., 2014).....	9
Figure 1.9. Biological phosphorus removal (Henze et al., 2008).....	10
Figure 1.10. Biochemical model for PAOs under anaerobic conditions (Henze et al., 2008).....	11
Figure 1.11. Biochemical model for PAOs under aerobic (or anoxic) conditions (Henze et al., 2008).....	11
Figure 1.12. Phosphorus content for different materials (Roy, 2017).....	13
Figure 1.13. Evolution of dairy manure management (Tao et al., 2016)	16
Figure 1.14. Schematic of quick wash process (Szögi et al., 2015)	18
Figure 1.15. Schematic of AWBs based biosorbents usage for phosphorus removal and recovery from aqueous solutions (Nguyen et al., 2014).....	20
Figure 1.16. Possible phosphorus recovery points from wastewater treatment plants (Egle et al., 2016)	21
Figure 1.17. Occurrence and development of MAP crystals (Liu et al., 2013).....	23

Figure 1.18. Calcium phosphate precipitation for phosphorus recovery (Metcalf & Eddy, 2014)	26
Figure 1.19. Schematic of the phosphorus recovery from sewage sludge ash by thermochemical process (Adam et al., 2009)	30
Figure 1.20. Gaseous fractions of some heavy metal chlorides (Vapor pressure of some heavy metals oxides are lower by several orders of magnitude. Thus, only PbO and CdO are visible in the graph) (Vogel et al., 2011)	30
Figure 1.21. Schematic of REM-NUT [®] process (Liberti et al., 2001)	32
Figure 1.22. Schematic of AirPrex [®] process (AirPrex [®] , 2015).....	33
Figure 1.23. Schematic of Ostara Pearl [®] process (Desmidt et al., 2015)	33
Figure 1.24. Schematic of Crystalactor [®] process (Giesen et al., 2009).....	34
Figure 1.25. Schematic of In P-RoC [®] process (Berg et al., 2005)	35
Figure 1.26. Schematic of NuReSys [®] process for phosphorus recovery (Ye et al., 2017)	35
Figure 1.27. Schematic of AshDec [®] process (AshDec [®] , 2015)	38
Figure 1.28. Schematic of LEACHPHOS [®] process (LEACHPHOS [®] , 2015).....	39
Figure 1.29. Schematic example of gasification process (Viader et al., 2015)	41
Figure 1.30. Schematic of sewage sludge incineration in fluidized bed reactor (Donatello and Cheeseman, 2013)	42
Figure 1.31. Principle of electro dialysis process (Bernardes et al., 2014)	52
Figure 1.32. Schematic presentation of transport mechanisms in electro dialysis (AN: Anion exchange membrane, CAT: Cation exchange membrane) (Gonçalves, 2015)....	55
Figure 1.33. 3-compartment electro dialysis cell (Guedes et al., 2014)	56
Figure 1.34. Schematic of (a) 3-compartment and (b) 2-compartment electro dialysis cells (Ebbbers et al., 2015a)	57

Figure 2.1. Dried sewage sludge and incinerated sewage sludge ash (from left to right)	58
Figure 2.2. Iron oxidizing bacteria	60
Figure 2.3. Sulfur oxidizing bacteria	61
Figure 2.4. Bioleaching experiments performed in incubator shaker.....	62
Figure 2.5. Performed bioleaching experiments.....	62
Figure 2.6. Electrodialysis reactor and system	66
Figure 2.7. Graphite and gold coated copper electrodes (from left to right).....	67
Figure 2.8. Power supply used in this study	68
Figure 3.1. X-Ray diffractogram of the sewage sludge ash	71
Figure 3.2. pH change during enrichment of Iron oxidizing bacteria	73
Figure 3.3. pH change during enrichment of Sulfur oxidizing bacteria	74
Figure 3.4. pH profile of trial with Iron oxidizing bacteria	77
Figure 3.5. Conductivity profile of trial with Iron oxidizing bacteria	78
Figure 3.6. X-Ray diffractogram of the residue obtained after the bioleaching of the sewage sludge ash with Iron oxidizing bacteria	79
Figure 3.7. pH profile of trial with Sulfur oxidizing bacteria.....	80
Figure 3.8. Conductivity profile of trial with Sulfur oxidizing bacteria.....	81
Figure 3.9. Sulfate concentration profile for bioleaching with Sulfur oxidizing bacteria	82
Figure 3.10. Phosphorus dissolution profile for bioleaching with Sulfur oxidizing bacteria.....	83
Figure 3.11. pH profile of trial with mixture of Sulfur&Iron oxidizing bacteria	84
Figure 3.12. Conductivity profile of trial with mixture of Sulfur&Iron oxidizing bacteria.....	84

Figure 3.13. Sulfate concentration profile for bioleaching with mixture of Sulfur&Iron oxidizing bacteria	85
Figure 3.14. Phosphorus dissolution profile for bioleaching with mixture of Sulfur&Iron oxidizing bacteria.....	86
Figure 3.15. pH profile for bioleaching with different Sulfur oxidizing bacteria inocula volumes.....	87
Figure 3.16. Conductivity profile for bioleaching with different Sulfur oxidizing bacteria inocula volumes	88
Figure 3.17. Sulfate concentration profile for bioleaching with different Sulfur oxidizing bacteria inocula volumes	88
Figure 3.18. Phosphorus dissolution profile for bioleaching with different Sulfur oxidizing bacteria inocula volumes	89
Figure 3.19. pH profile for bioleaching with mixture of Sulfur&Iron oxidizing bacteria with different inocula volumes	90
Figure 3.20. Conductivity profile for bioleaching with mixture of Sulfur&Iron oxidizing bacteria with different inocula volumes	91
Figure 3.21. Sulfate concentration profile for bioleaching with mixture of Sulfur&Iron oxidizing bacteria with different inocula volumes	92
Figure 3.22. Phosphorus dissolution profile for bioleaching with mixture of Sulfur&Iron oxidizing bacteria with different inocula volumes	92
Figure 3.23. pH profile for bioleaching with different sulfur amounts	93
Figure 3.24. Conductivity profile for bioleaching with different sulfur amounts	94
Figure 3.25. Sulfate concentration profile for bioleaching with different sulfur amounts	95
Figure 3.26. Phosphorus dissolution profile for bioleaching with different sulfur amounts.....	95
Figure 3.27. pH and conductivity profiles for bioleaching in 2 L reactor	96
Figure 3.28. Sulfate concentration profile for bioleaching in 2 L reactor	97

Figure 3.29. Phosphorus dissolution profile for bioleaching in 2 L reactor	97
Figure 3.30. pH profile for electrodialysis realized with bioleaching solution and graphite electrodes	99
Figure 3.31. Conductivity profile for electrodialysis realized with bioleaching solution and graphite electrodes	100
Figure 3.32. Sulfate concentration profile for middle part	101
Figure 3.33. Phosphate concentration profiles for the middle and anode parts.....	101
Figure 3.34. Graphite electrode of the anode part after electrodialysis.....	102
Figure 3.35. Phosphate concentration profiles for the middle, anode and cathode parts	103
Figure 3.36. Phosphorus passage percentages to anode part	103
Figure 3.37. Mass balance for phosphate ion after electrodialysis.....	104
Figure 3.38. Distribution of phosphate species as a function of pH (Thanh and Liu, 2017).....	105
Figure 3.39. Phosphate species for different pH values	106
Figure 3.40. pH profile for electrodialysis realized with bioleaching solution and gold coated copper electrodes.....	107
Figure 3.41. Conductivity profile for the anode part.....	107
Figure 3.42. Phosphate concentrations for the middle part and anode part.....	108
Figure 3.43. Phosphorus passage percentages to anode part	108
Figure 3.44. Mass balance for phosphate ion after electrodialysis.....	109
Figure 3.45. Gold coated copper electrodes at the anode part before and after the electrodialysis (left side: before electrodialysis, right side: after electrodialysis).....	110

LIST OF TABLES

	PAGE
Table 1.1. Examples of phosphate containing applications (Gantner et al., 2014).....	9
Table 1.2. Elemental composition of waste bone ashes (Darwish et al., 2016a).....	15
Table 1.3. Elemental composition of CMIA (Kaikake et al., 2009).....	17
Table 1.4. Elemental yields after each precipitation (Kaikake et al., 2009).....	17
Table 1.5. The maximum phosphate adsorption capacity of commercial and natural agricultural waste/byproducts based biosorbents (Nguyen et al., 2014).....	19
Table 1.6. Properties of potential phosphorus recovery flows (Egle et al., 2015).....	21
Table 1.7. Phosphate removal efficiencies based on optimum $Mg^{2+}:PO_4^{3-}$ ratio in different type of wastewaters (Liu et al., 2013).....	24
Table 1.8. Different forms of crystallized calcium phosphates (Montastruc et al., 2003).....	26
Table 1.9. General information about processes for the phosphorus recovery from municipal wastewater (Ye et al., 2017).....	27
Table 1.10. Phosphorus recovery technologies from wastewater treatment plants (Egle et al., 2016).....	31
Table 1.11. Concentrations of toxic and non-toxic elements inside the sewage sludge ash (Lynn et al., 2015).....	44
Table 1.12. Physical-chemical characteristics of sewage sludge ash.....	45
Table 1.13. Acidophilic microorganisms used in bioleaching process with optimum and range of growth for pH and temperature (Schippers, 2007).....	46
Table 1.14. Factors affecting bioleaching process (Pradhan et al., 2008).....	48
Table 2.1. Experiments performed for the determination of optimum ash amount.....	63
Table 2.2. Experiments performed for the determination of optimum inocula volume	64
Table 2.3. Experiments performed for the determination of optimum sulfur amount...	64

Table 2.4. Conditions for 2 L batch bioleaching experiment	65
Table 2.5. Performed electro dialysis experiments	66
Table 2.6. Properties of the anion and cation exchange membranes	67
Table 3.1. Physico-chemical characteristics of the sewage sludge ash	70
Table 3.2. Phosphorus and heavy metals contents of the sewage sludge ashes used in other studies and this study.....	72
Table 3.3. Phosphorus dissolution percentages for trial with Iron oxidizing bacteria...	76
Table 3.4. Heavy metal dissolution percentages after bioleaching.....	98
Table 3.5. Content of the bioleaching solution	104
Table 3.6. Heavy metals, Ca and Mg passage percentages to the cathode part.....	111

1. INTRODUCTION

1.1. Aim and Scope of the Study

Phosphorus is an essential element for all living organisms and it can't be replaced by other substances in food production. However, phosphate rock is a limited source that takes approximately 10–15 million years to form (Havukainen et al., 2016). Also, phosphorus cannot be cycled through the atmosphere because it is not volatile and does not form any stable gaseous compounds, like nitrogen (Franz, 2008). Because of these reasons, phosphorus recovery strategies must be improved.

One of the most promising phosphorus recovery sources is the sewage sludge (Donatello and Cheeseman, 2013). However, sewage sludge cannot be used directly because it often contains heavy metals and organic contaminants (e.g., pharmaceuticals and personal care products). Removal of the organics inside the sewage sludge is possible by incineration and after incineration sewage sludge ash forms. Sewage sludge ash (SSA) has concentrated mineral fraction and it is a secondary resource for phosphorus (Herzel et al., 2016). SSA contains 10-25.7% phosphorus as P_2O_5 while commercially used phosphate minerals contain 5-40% of phosphorus as P_2O_5 by weight (Fang et al., 2018). Recovery of phosphorus from SSA can be realized by bioleaching, wet-chemical extraction, wet-chemical leaching, thermo-chemical, thermo-electric, thermo-reductive approaches (Egle et al., 2015). Most of these approaches rely on the addition of chemicals (e.g. acids, bases), temperatures above 1000°C or special reactors. However, bioleaching is a release technology that relies on the solubilization of nutrients and heavy metals from solid substrates either directly by the metabolism of leaching microorganisms or indirectly by the products of metabolism. Bioleaching realizing microorganisms include mesophiles such as *Acidithiobacillus thiooxidans* and *Acidithiobacillus ferrooxidans*; thermophiles such as *Sulfobacillus thermosulfidoxidans*; and heterotrophic microbes such as *Acetobacter* and *Acidophilum* (Mehta et al., 2015). After bioleaching, both phosphorus and heavy metals inside the sewage sludge ash are dissolved. Dissolved heavy metals and phosphorus should be separated from each other to use this phosphorus. There are a few methods to separate phosphorus from heavy

metals such as sequential precipitation, liquid-liquid extraction, ion exchange and electro dialysis (Petzet et al., 2012; Ottosen et al., 2014).

This study was mainly focused on the recovery of phosphorus from the sewage sludge ash that was obtained from the incineration of the dried sewage sludge. Bioleaching process was used to dissolve the phosphorus that sewage sludge ash contains. Bioleaching experiments were carried out to obtain maximum phosphorus solubilization from the sewage sludge ash. Lastly, electro dialysis process was used to separate the dissolved phosphorus and heavy metals to obtain phosphorus rich solution.

1.2. Phosphorus

Phosphorus (P) is an indispensable element for all living organisms because it is used in the molecules with energetic and genetic functions (Arnout and Nagels, 2016). It is non-substitutable element for the life because of the involvement of very important biological processes. It is used in the reproduction of cells as a part of DNA, used in energy supply as a part of ATP and also used in some structures like teeth and bones (van Dijk et al., 2016). For the plants, phosphorus is the second limiting macronutrient after nitrogen because it should be in bioavailable form which is orthophosphate ion and deficiency of this bioavailable phosphorus because of the sorption and complexation in the soil increases the demand for the fertilizer. Also, for the microbes, phosphorus is important for the cellular metabolism as a part of ATP (Udaeta et al., 2017).

The main source of the phosphorus is the phosphate rock, is non-renewable and after the year 2035, demand will be higher than its supply (He at al., 2016). Phosphate rock is a limited source and it forms approximately within 10-15 million years and it is consumed in one century (Havukainen et al., 2016). Rock phosphate is used in many areas like agriculture, production of animal feed and production of pharmaceuticals, oils, detergents and textile (Cieřlik and Konieczka, 2017). Although it is used for many areas, because its sources are limited, in 2014, European Commission listed the phosphate rock as one of the 20 critical raw materials and inside these phosphorus is the only one which mainly related to agriculture and food security (Zhou et al., 2017; George et al., 2016).

Phosphorus cannot be substituted by anything in the production of food, and world with a 9 million people by 2050, phosphorus will be very important for the food security (Cordell et al., 2011). Growth in population and changes in diet mainly affect the phosphorus demand for the agriculture. Countries that have not enough phosphorus sources are dependent to imports from other countries and affected by the fluctuations in price (Egle et al., 2015). Therefore, geographic location is also important for the phosphate supply. Because, phosphate rock is not equally distributed in the world and the main phosphate rock reserves are in Morocco, China, South Africa and United States (Cieřlik and Konieczka, 2017).

1.2.1. Phosphorus cycle

Phosphorus is not cycled in the atmosphere because it is a non-volatile and does not form any gaseous compounds. Inorganic compounds of phosphates flow to surface waters or groundwater from the soil and it is a one way flow (Franz, 2008). Figure 1.1 shows the aquatic phosphorus cycle with main reservoirs and fluxes. As it is seen from the Figure 1.1, main phosphorus fluxes are between ocean and aquatic biota and between soil and soil biota (Worsfold et al., 2016).

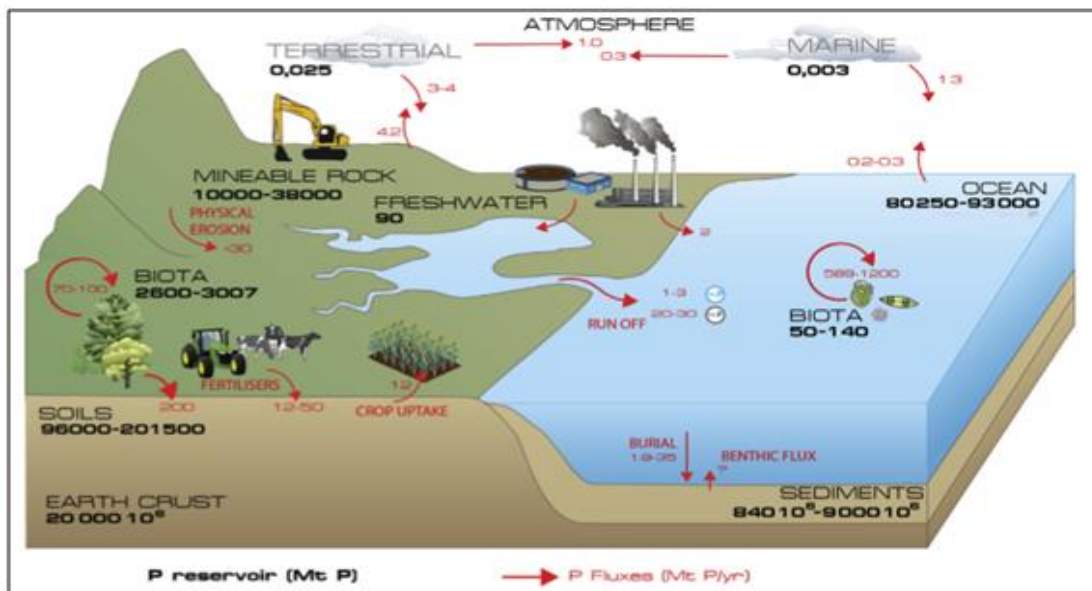


Figure 1.1. A schematic diagram of aquatic phosphorus cycle (Worsfold et al., 2016)

After the entrance of phosphorus to urban system as food, wood, detergents, chemicals and fertilizers, it is converted to wastewater or solid waste as it is shown in Figure 1.2. Forms of the generated wastes can be incinerated or landfilled solid waste or sewage sludge (Pearce, 2015).

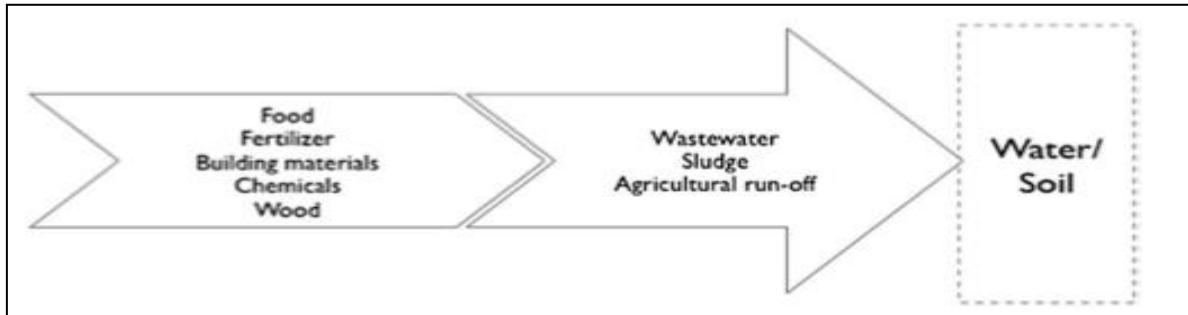


Figure 1.2. Phosphorus flow in urban areas (Pearce, 2015)

1.2.2. Phosphorus production

Growth of population requires more food production on existing agricultural area because significant increase in agricultural area is not possible. To increase the crop yield, addition of fertilizers that include enough phosphate must be increased (Franz, 2008). Thus, demand for phosphorus increases because of increasing population. As it is seen from the Figure 1.3, phosphorus production increases with time till it reaches its peak. However, the critical period is not the point where 100% of the rock phosphate reserves are consumed, but rather where the high grade and accessible reserves are consumed. After the depletion of high grade and highly accessible phosphate rock, mining and processing of remaining phosphate rock will not be economical. Thus, phosphorus production starts to decrease even though demand for phosphorus increases (Cordell et al., 2009).

Similar to phosphate rock reserves, global phosphate rock production is dominated by several countries as shown in Figure 1.4 and Figure 1.5. In the year 2016, totally 261 MT of rock phosphate was mined and China has the highest production percentage with 53% (United States Geological Survey, 2017).

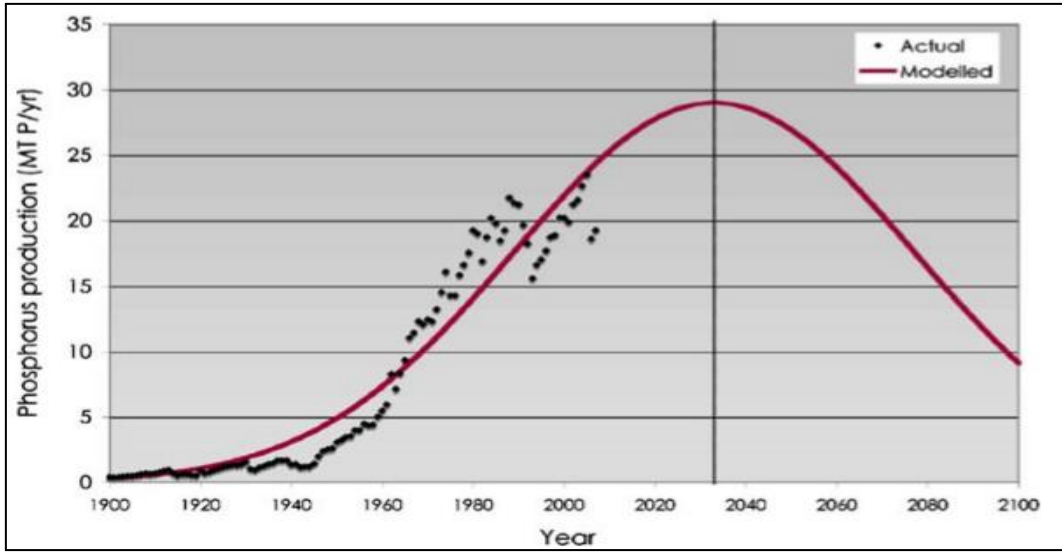


Figure 1.3. Phosphorus production curve (Cordell et al., 2009)

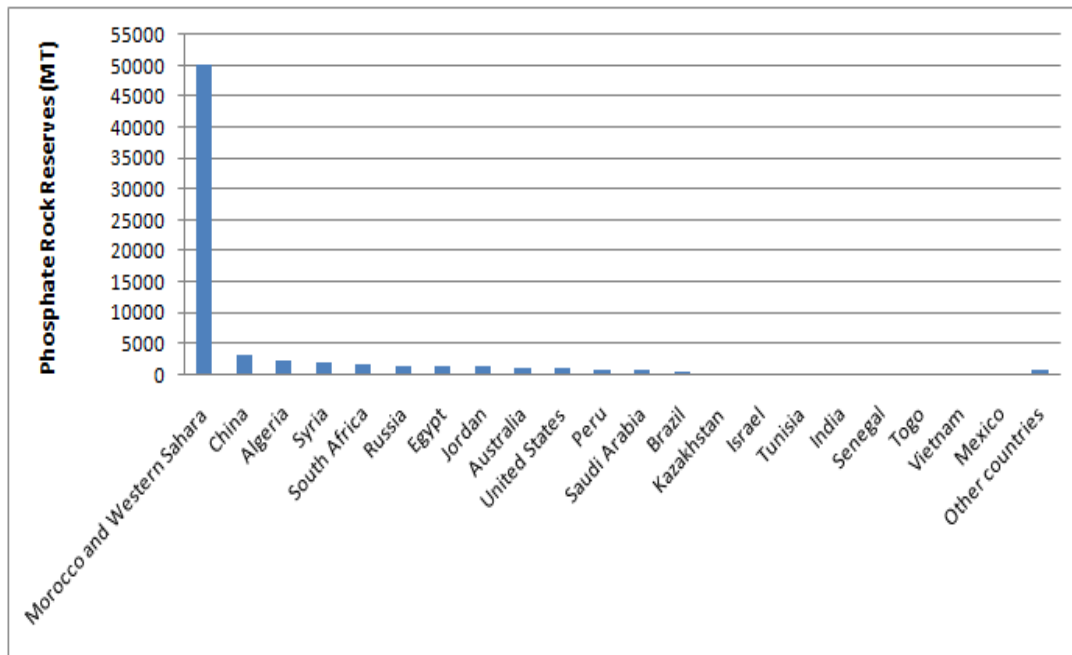


Figure 1.4. World phosphate rock reserves in 2016 (Data: United States Geological Survey, 2017)

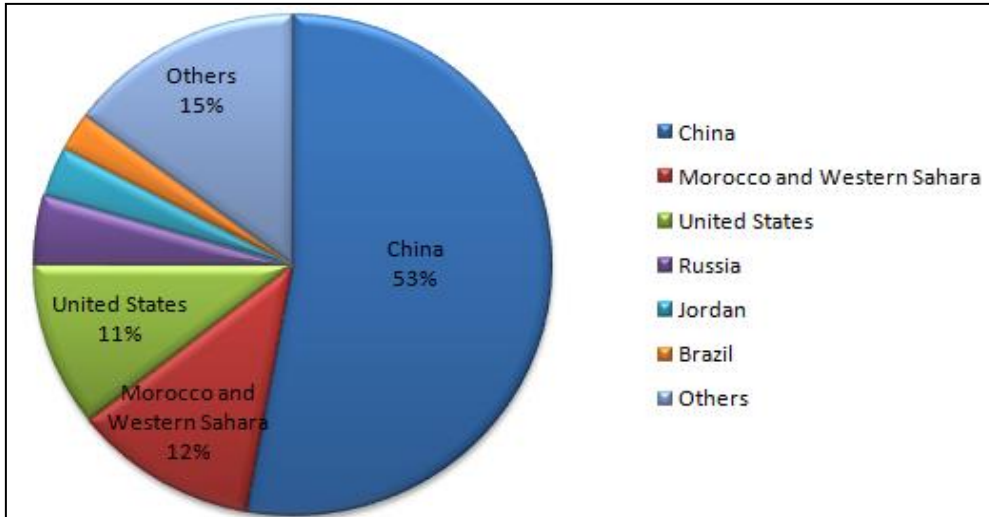


Figure 1.5. Share of world rock phosphate production in 2016 (Data: United States Geological Survey, 2017)

Main natural source of the phosphorus is the phosphate rock and phosphate rock is used to produce phosphate fertilizers and elemental phosphorus that is used in the production of chemicals and foods. Phosphate rock includes mainly insoluble calcium phosphate (apatite) and its chemical formula is $\text{Ca}_5(\text{PO}_4)_3(\text{Cl}, \text{F}, \text{OH})$. Apatite is named as chloro, fluoro or hydroxy apatite according to last functional group (Avdalović et al., 2015). Except a few phosphate rocks that classified as reactive, phosphorus rocks are insoluble and their usage are difficult for the plants. For this reason, approximately 96% of the rock phosphate is processed in a form which can be taken by the roots of plants to supply required phosphorus to them. More than 90% of phosphate rock is processed with wet chemical methods; between 72-78% is treated with sulfuric acid to produce phosphoric acid, between 10-14% is treated with sulfuric acid to produce single superphosphate and partially acidulated phosphate rock, between 2-4% is treated with nitric acid to produce nitrophosphates. Less than 5% of phosphate rock is processed with thermal methods to produce elemental phosphorus. Most of the non-fertilizer products of phosphorus and some part of the detergent production uses the elemental, white phosphorus (P_4) which is produced by thermal methods (Scholz et al., 2014; Gantner et al., 2014).

In wet chemical process, phosphate rock is reacted with sulphuric, nitric or hydrochloric acids. Most commonly used acid is the sulphuric acid (Villalba et al., 2008). Production

of phosphoric acid is shown in Figure 1.6. Produced phosphoric acid is used to produce phosphate fertilizers called as diammonium phosphate (DAP), monoammonium phosphate (MAP) and triple superphosphate (TSP). DAP that has 38% market share and MAP 27% market share are produced from the reaction of ammonia and phosphoric acid. TSP has market share of 7%. All of these fertilizers are soluble in water and they can be absorbed through the roots of the plants (Scholz et al., 2014).

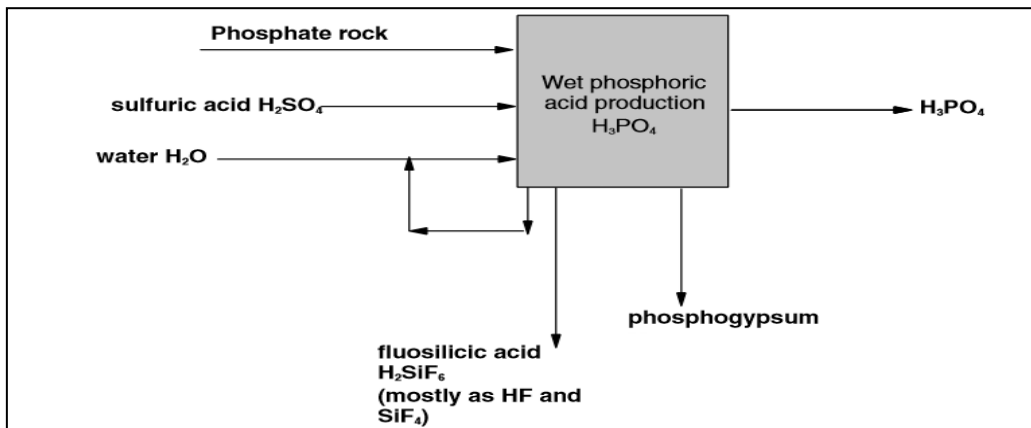


Figure 1.6. Production of phosphoric acid with wet chemical method (Villalba et al., 2008)

After the reaction of sulfuric acid with rock phosphate, by product of phosphogypsum (calcium sulfate) forms. Besides this, this chemical reaction also produces gaseous emissions in the form of silicon tetrafluoride (SiF₄) and hydrofluoric acid (HF) (Scholz et al., 2014).

In thermal phosphoric acid production, apatite is reduced electrothermally in an electric furnace at 1600°C with coke as reducing agent and gravel as slag former. Therefore, white phosphorus (P₄) is produced. In this way, phosphorus and carbon monoxide form as gases. Produced phosphorus is condensed, while carbon monoxide is used as fuel or burned as waste (Gantner et al., 2014; Villalba et al., 2008).

Thermally produced phosphoric acid is higher in quality than wet chemically produced phosphoric acid. Therefore, in food industry and industrial purposes thermally produced phosphoric acid is used. Wet chemically produced phosphoric acid is generally used as fertilizer (Villalba et al., 2008).

1.2.3. Usage areas of phosphorus

Phosphorus is used in many areas with different usage percentages as shown in Figure 1.7. Phosphorus is mainly used for fertilizer production with approximate percentage of 82%. Remaining part of the rock phosphate is used for different purposes: 7% is used for the production of animal feed, 11% is used for the production of detergents, broad set of cleaning and industrial products and some industries like lighting and electronic (Cieřlik and Konieczka, 2017; Scholz et al., 2014).

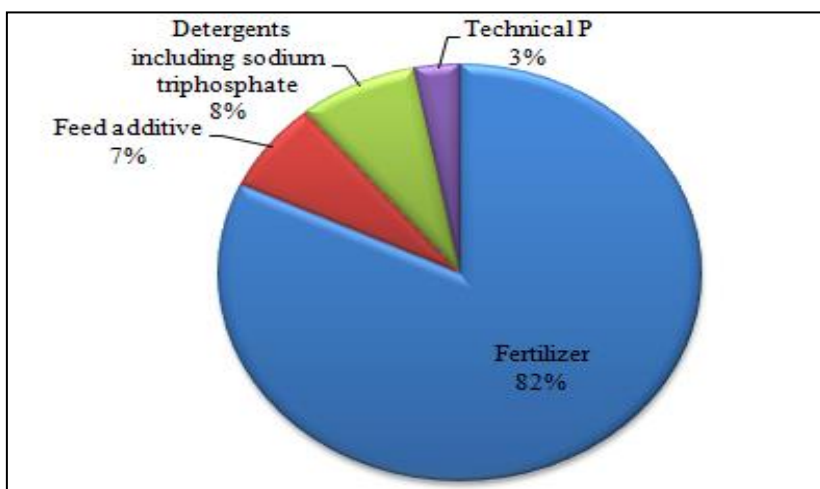


Figure 1.7. Share of phosphate rock use (Scholz et al., 2014)

White phosphorus produced electrothermally is used as the father compound of many different (organo)phosphorus compounds and these compounds are used for many different purposes in industry as shown in Figure 1.8 (Gangner et al., 2014).

Phosphate is also used in beverage, building and construction, cleaning agents, flame protection, flame retardants, food processing, glass and ceramic, lighting, medical engineering, pharmaceuticals, industrial phosphoric acid production. In Table 1.1, forms and the functions of phosphate addition are shown.

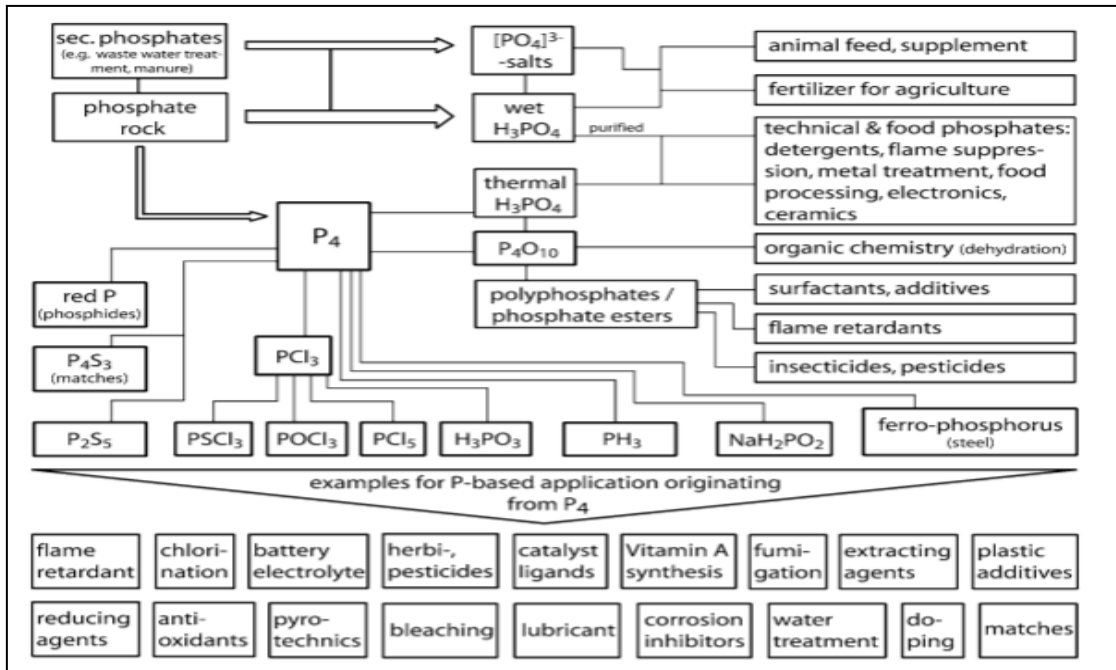


Figure 1.8. Technical use of phosphorus (Gantner et al., 2014)

Table 1.1. Examples of phosphate containing applications (Gantner et al., 2014)

Phosphate containing applications	Chosen examples for a finished product	Ingredients	Phosphate function
Beverage	Cola	Food grade phosphoric acid	Acidulant
Building/construction	Cement	Sodium tripolyphosphate, tetrasodium pyrophosphate, Sodium monofluorophosphate	Retarding agent for cement
Flame protection	Fire extinguisher	Mono- and diammonium phosphates	Fire retardants
Food processing	Dairy, Seafood, Meat	Polyphosphates (sodium tripolyphosphate, potassium tripolyphosphate, etc.)	Moisture retention, emulsifier, shelf life
Medical engineering	Dental cement	Magnesium phosphate, ammonium phosphate	Dental investment, binding agent

1.2.4. Phosphorus removal in wastewater treatment plants

Phosphorus is removed from the wastewater by biological and/or chemical processes to prevent eutrophication. Eutrophication is undesirable increase of living aquatic organisms in aquatic environments because it results in depletion of oxygen and it damages to aquatic ecosystem. Phosphorus losses from croplands, animal farms, industries, and domestic usages to environment. Industrial and domestic wastewater discharges are point sources, while agricultural losses and atmospheric deposition of water bodies are non-point sources for phosphorus (Egle et al., 2015; Liu et al., 2008).

1.2.4.1. Biological phosphorus removal

Biological phosphorus removal relies on the incorporation of phosphorus inside the influent wastewater into cell biomass and its finally removed from the process as excess sludge. This is achieved with the movement of biomass from an anaerobic to an aerobic reactors as shown in Figure 1.9. Phosphorus accumulating organisms (PAOs) are promoted to grow and remove phosphorus in a reactor configuration that gives advantage PAOs over other types of bacteria. PAOs have a capability of storing excess amounts of phosphorus as polyphosphates (Metcalf & Eddy, 2004; Davis, 2010).

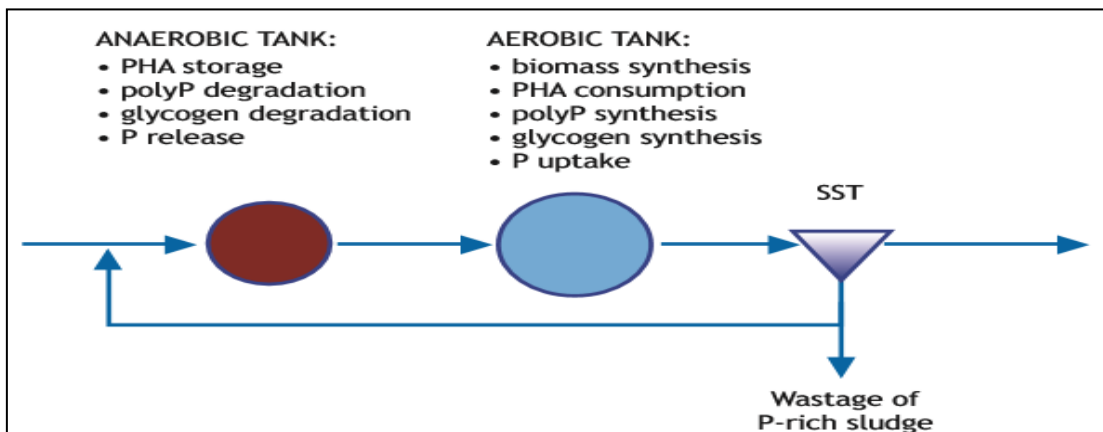


Figure 1.9. Biological phosphorus removal (Henze et al., 2008)

In anaerobic zone, with the fermentation of biodegradable soluble COD, acetate produces. PAOs use the energy that is supplied from stored polyphosphates, assimilate the acetate and intracellular polyhydroxybutyrate (PHB) products are produced. Also, some of the glycogen inside the cell is used. With the uptake of the acetate, release of

orthophosphate is actualized. Therefore, while PHB content of PAOs increases, the polyphosphate decreases (Metcalf & Eddy, 2004). Biochemical model for the PAOs under anaerobic conditions is shown in Figure 1.10.

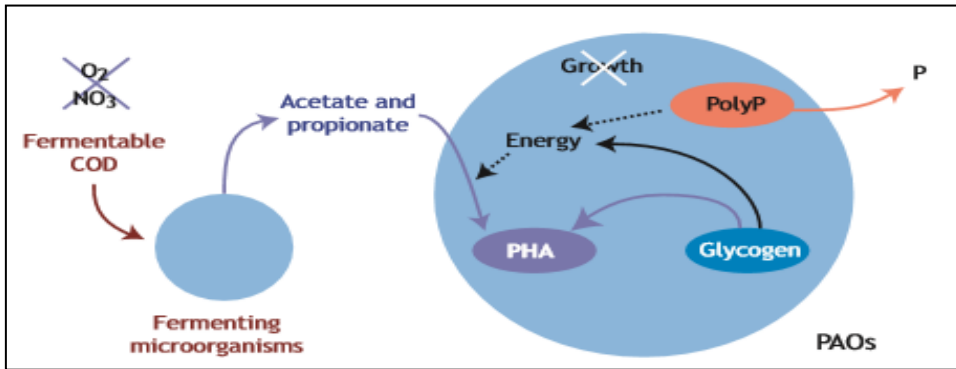


Figure 1.10. Biochemical model for PAOs under anaerobic conditions (Henze et al., 2008)

In the aerobic/anoxic zone, in the presence of oxygen (or nitrate under anoxic conditions) stored PHB is used to provide energy for the growth of the new cell. With the usage of PHB, some glycogen is produced. PHB oxidation releases energy that is used to form polyphosphate bonds in cell storage. Therefore, removal of soluble orthophosphate is actualized and it is taken into bacterial cell. Phosphorus inside the biomass is removed as sludge from the process (Metcalf & Eddy, 2004; Henze et al., 2008; Davis, 2010). Biochemical model for the PAOs under aerobic conditions is shown in Figure 1.11.

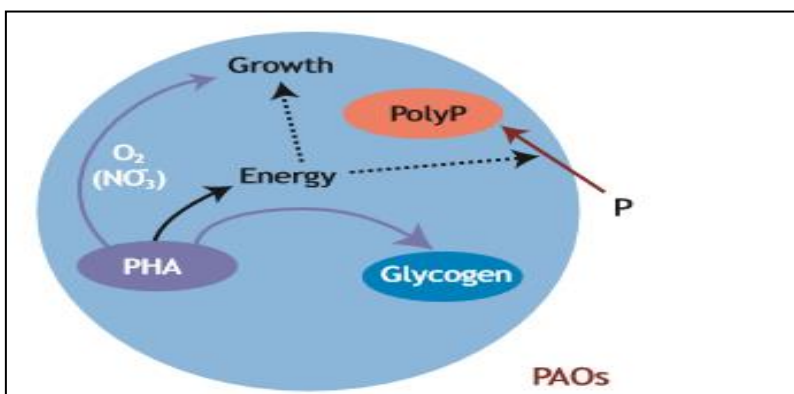


Figure 1.11. Biochemical model for PAOs under aerobic (or anoxic) conditions (Henze et al., 2008)

1.2.4.2. Chemical phosphorus removal

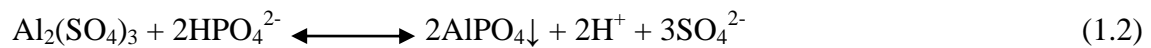
Chemical removal of phosphorus from wastewater involves the incorporation of phosphate into chemical precipitates. Addition of the multivalent metal ion salts forms sparingly soluble phosphate precipitates. Most frequently used multivalent metal ions are calcium (Ca^{2+}), aluminum (Al^{3+}) and iron (Fe^{3+}). As flocculant purpose, polymers can be used with alum and lime. Phosphate precipitation chemistry with calcium is different than the chemistry with aluminum and iron (Metcalf & Eddy, 2004).

Precipitation reactions for lime, aluminum sulfate and ferric chloride are as follows:

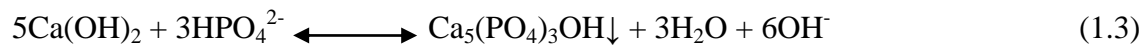
Ferric chloride:



Aluminum Sulfate:



Lime:



While addition of alum and ferric chloride reduces the pH, addition of lime increases. The effective pH range for alum and ferric chloride is between 5.5-7.0. In the case of deficiency of alkalinity, to buffer the system in this range, lime addition is necessary (Davis, 2010).

There are some factors affecting the selection of chemical to use for phosphorus removal. These are influent phosphorus level, wastewater suspended solids, alkalinity, chemical cost, reliability of chemical supply, sludge handling facilities, ultimate disposal methods and compatibility with other treatment processes (Metcalf & Eddy, 2004).

1.3. Phosphorus Recovery

Phosphorus demand is estimated to be grown at an annual rate of 1.9% globally, between the years 2013-2018 and while its consumption is stabilized in developed countries, demand is increasing in the world. For this reason, recovery of phosphorus from phosphorus rich sources such as manure, meat and bone meal, agricultural waste and sewage sludge is very important to sustain phosphorus included processes (Kataki et al., 2016; Atienza-Martinez et al., 2014). Phosphorus content (gram P/kg) by mass for some different materials with conventional inorganic fertilizer are shown in Figure 1.12.

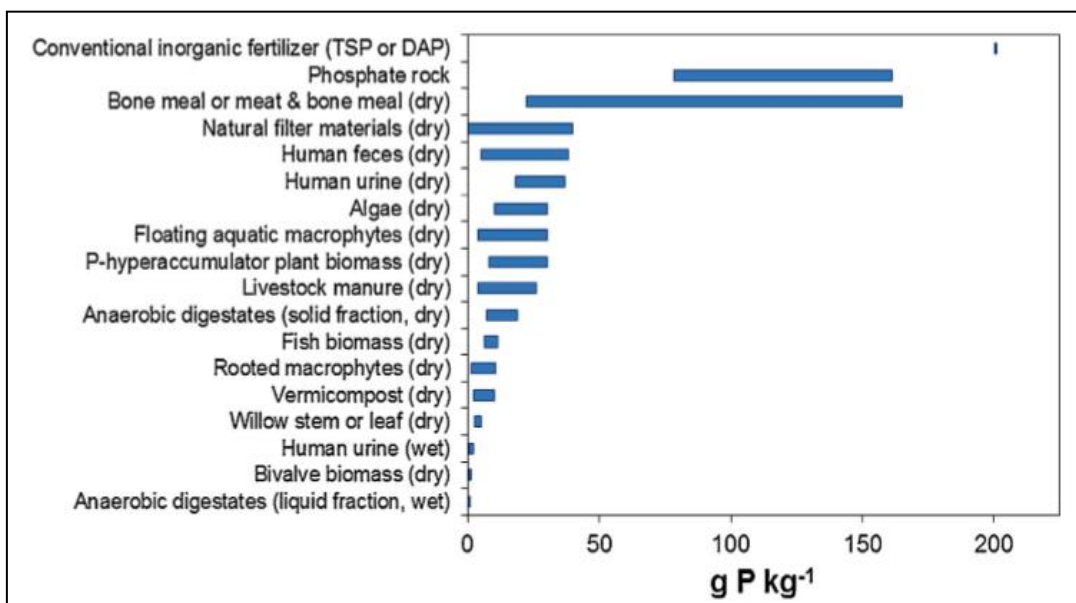


Figure 1.12. Phosphorus content for different materials (Roy, 2017)

1.3.1. Phosphorus recovery from meat and bone meal

Meat and bone meal (MBM) is the byproduct of meat industry. In Europe, since 2003, MBM is classified in 3 categories.

Category 1: Animals byproducts suspicious to infection by transmissible spongiform encephalopathy (TSE) and specified risk materials (SRM),

Category 2: Animals byproducts presenting a infection other than TSE,

Category 3: Animals byproduct that are formed from the production of human consuming products and non suspected to diseases transmissible to humans or animals.

Category 1 products have to be incinerated or rarely disposed of in approved landfill. Category 3 products have low risk and can be used in the pet food production. In the production of fertilizers, Category 2 and Category 3 products can be used (Coutand et al., 2008; Spångberg et al., 2011).

Incineration of MBM is one of the most proper methods to exterminate it, because it has a heating value ranging between 13-30 MJ/kg. Thermochemical methods that are used for MBM includes pyrolysis, combustion and gasification. Thermal treatment of MBM produces huge amounts (350,000-1,000,000 tons/year) of ash in Europe. This ash includes high amounts of phosphorus which make it suitable for fertilizer usage (Coutand et al., 2008; Toldrá et al., 2016).

In the study of Darwish et al. (2016a), they used fish, chicken and cow wasted bones from different sources. To obtain black residue, they incinerated the wastes at 600°C for 2 hour in a muffle furnace. They also mixed these black residues before another 2 hour of incineration. Thus, organic content was completely decomposed and clear ashes were formed. XRD analysis of the ashes showed that ashes were composed of calcium phosphate and carbonate compounds (apatite), mainly. Elemental composition of ashes are shown in Table 1.2. The highest phosphorus content was inside the fish ash with 17% (wt).

They have performed 3 sets of experiments with 2 different molar ratios of Mg:N:P as 1:1:1 and 1.3:1:1 for struvite precipitation. Reagent combinations were as follows: $\text{MgCl}_2 \cdot 6\text{H}_2\text{O}$ and $\text{Na}_2\text{HPO}_4 \cdot 12\text{H}_2\text{O}$, MgO and $\text{Na}_2\text{HPO}_4 \cdot 12\text{H}_2\text{O}$, MgO and P obtained from the H_2SO_4 leaching of ash. Experiments were carried out in 1.5 L of beakers with 1 L of samples. pH was adjusted to 9.0 ± 0.05 with 10 M NaOH.

Table 1.2. Elemental composition of waste bone ashes (Darwish et al., 2016a)

Element	Source of waste bone ash		
	Fish	Chicken	Beef
Concentration (mg/g)			
Ca	221.203	210.108	254.752
P	170	155	142
K	8.540	15.508	3.763
Mg	4.480	4.947	2.702
Fe	1.192	1.330	1.221
Concentration (µg/g)			
Zn	133.784	281.363	94.128
Cd	1.090	0.366	0.317
Ni	3.846	3.452	2.028
Cr	4.996	6.832	5.175
Cu	8.788	6.470	3.677
As	65.365	93.676	82.443
Al	113.693	81.642	89.412

Acidic leaching with 2 M H₂SO₄ and 1.25 kg H₂SO₄/kg ash was given the 95% phosphorus recovery from ash. Moreover, application of recovered phosphorus solution in struvite precipitation showed high efficiency of NH₄ removal.

1.3.2. Phosphorus recovery from manure

Animal feeding operations result in large amounts of manure. This manure causes the air pollution through volatilization of hydrogen sulfide (H₂S), ammonia (NH₃) and greenhouse gases (CO₂, CH₄, N₂O, etc.). Manures generally contain high levels of organic matters and nutrients such as phosphorus and nitrogen. Traditionally, manure was directly applied to farmland as fertilizer. However, this has a risk of environmental problems like eutrophication and water pollution. Therefore; physical, chemical and biological processes are investigated to recover nutrients like phosphorus from manures.

Evolution of dairy manure management is shown in Figure 1.13 (Szögi et al., 2015; Ekpo et al., 2016; Tao et al., 2016).

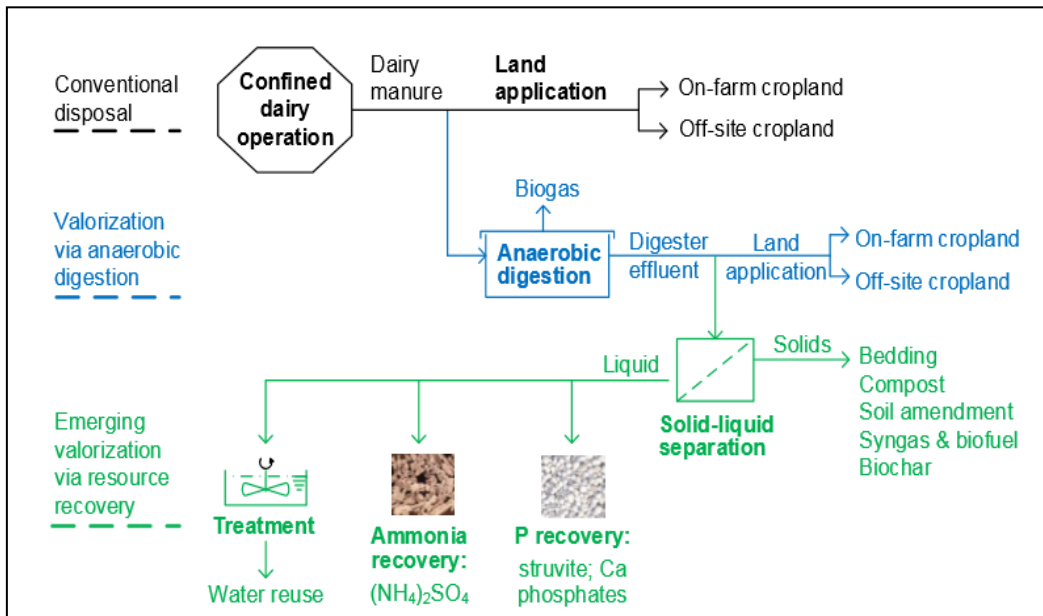


Figure 1.13. Evolution of dairy manure management (Tao et al., 2016)

In the study of Kaikake et al. (2009), they have investigated the recovery of phosphorus from chicken manure incinerated ash (CMIA) with procedure of acid dissolution-alkali precipitation. For this purpose, they have obtained CMIA from commercial incineration plant. XRD results of CMIA showed that, it included $Ca_5(PO_4)_3(OH)$, phosphorus structure in the ash was hydroxyapatite. Elemental composition of CMIA was shown in Table 1.3.

In this study, phosphorus recovery with the acid dissolution-alkali precipitation procedure was applied to CMIA. Hydrochloric acid was used to obtain phosphorus rich solution from CMIA and pH was gradually changed to 3.0, 4.0 and 8.0. Recovery of the elements during each precipitation stage was given in Table 1.4.

Table 1.3. Elemental composition of CMIA (Kaikake et al., 2009)

	Concentration (mg/kg)
P	84500
Mg	21600
Na	27000
K	120000
Ca	72000
Fe	4900
Cu	270
Zn	1600
Ni	76.0
Pb	8.00
Cr	26.0

Table 1. 4. Elemental yields after each precipitation (Kaikake et al., 2009)

	CMIA solution (pH 2.80)	First precipitation (pH 3.05)		Second precipitation (pH 4.03)		Final precipitation (pH 8.15)	
		Precipitant	Filtrate	Precipitant	Filtrate	Precipitant	Filtrate
P	100 [18300]	7.0 (7)	93.0 (93)	84.2 (91)	8.8 (9)	8.3 (94)	0.5 (6)
Ca	100 [9670]	5.4 (5)	94.6 (95)	71.9 (76)	22.7 (24)	8.6 (38)	14.1 (62)
Fe	100 [25.6]	97.5 (97)	2.5 (3)	0.7 (28)	1.8 (72)	0.6 (33)	1.2 (67)
Zn	100 [52.6]	14.3 (14)	85.7 (86)	26.5 (31)	59.2 (69)	59.1 (100)	>0.1 (0)
Cu	100 [26.1]	6.8 (7)	93.2 (93)	41.5 (45)	51.5 (55)	51.5 (100)	0.1 (0)

[]: concentration in phosphorus solution (mg/L).
(): yield in each precipitation in %.

In the first precipitation at pH 3.0, little amount of phosphorus was precipitated to remove iron. High amount of phosphorus (84% in the phosphorus rich solution) was recovered as $\text{CaHPO}_4 \cdot 2\text{H}_2\text{O}$ with 92% purity at pH 4.0. At pH 8.0, phosphorus could be recovered in 8% phosphorus rich solution as hydroxyapatite. Total recovery of phosphorus as $\text{CaHPO}_4 \cdot 2\text{H}_2\text{O}$ and hydroxyapatite was up to 92%.

In the study of Szögi et al. (2015); they have investigated the recovery of phosphorus from pig manure solids. For this reason they have applied quick wash process that is shown in Figure 1.14.

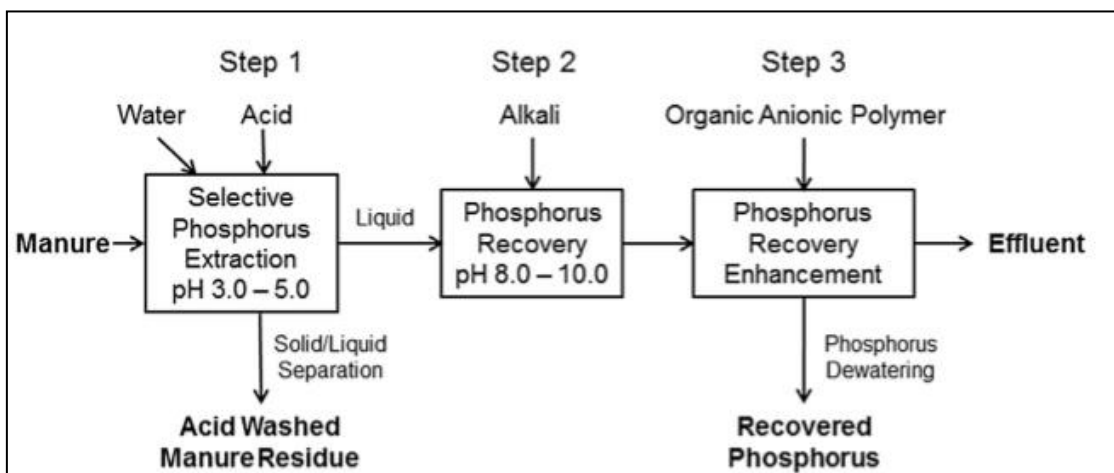


Figure 1.14. Schematic of quick wash process (Szögi et al., 2015)

Phosphorus inside the manure was extracted with citric or hydrochloric acid and phosphorus was precipitated at high pH with enhancement with anionic polyacrylamide as calcium containing phosphorus precipitate. Quick wash process resulted in total phosphorus recovery up to 90%.

1.3.3. Phosphorus recovery from agricultural waste

Agricultural wastes are clean, renewable and plentiful and they can be transferred into useful materials (Wu et al., 2017). For example, there is an increasing attention on agricultural waste/byproducts (AWBs) based biosorbents. These phosphate biosorbents are expected to be low cost, high effectiveness, high selectivity, high adaptability to different process parameters (Nguyen et al., 2014). The maximum phosphate adsorption capacity of commercial and natural AWBs based biosorbents were shown in Table 1.5.

Table 1.5. The maximum phosphate adsorption capacity of commercial and natural agricultural waste/byproducts based biosorbents (Nguyen et al., 2014)

Adsorbent	Maximum adsorption capacity (mg PO₄/g)
<u>Unmodified AWBs based biosorbents</u>	
Oyster shell	0
Giant reed	0.836
Sugarcane bagasse	1.10
Soybean milk residues (okara)	2.45
Coir pith	4.35
Date palm fibers	13.33
Scallop shells	23.00
Palm surface fibers	26.05
Granular date stones	26.66
<u>Commercially available adsorbents</u>	
Zr-MCM 41	3.36
Whatman QA-52	14.26
Zirconium ferrite	27.73
Duolite A-7	31.74
Amberlite IRA-400	32.24
Aluminium oxide	34.57
Zirconium ferrite	39.84
Dowex	40.23
Hydrotalcite	60.00
Zirconium loaded MUROMAC	131.77

Removal of phosphorus with conventional adsorbents and recovery of phosphorus as MAP or calcium phosphate are commonly used processes. However, there are less studies about the combination of adsorption and precipitation (Nguyen et al., 2014). In Figure 1.15, recovery of phosphorus with the combination of adsorption and precipitation processes is given.

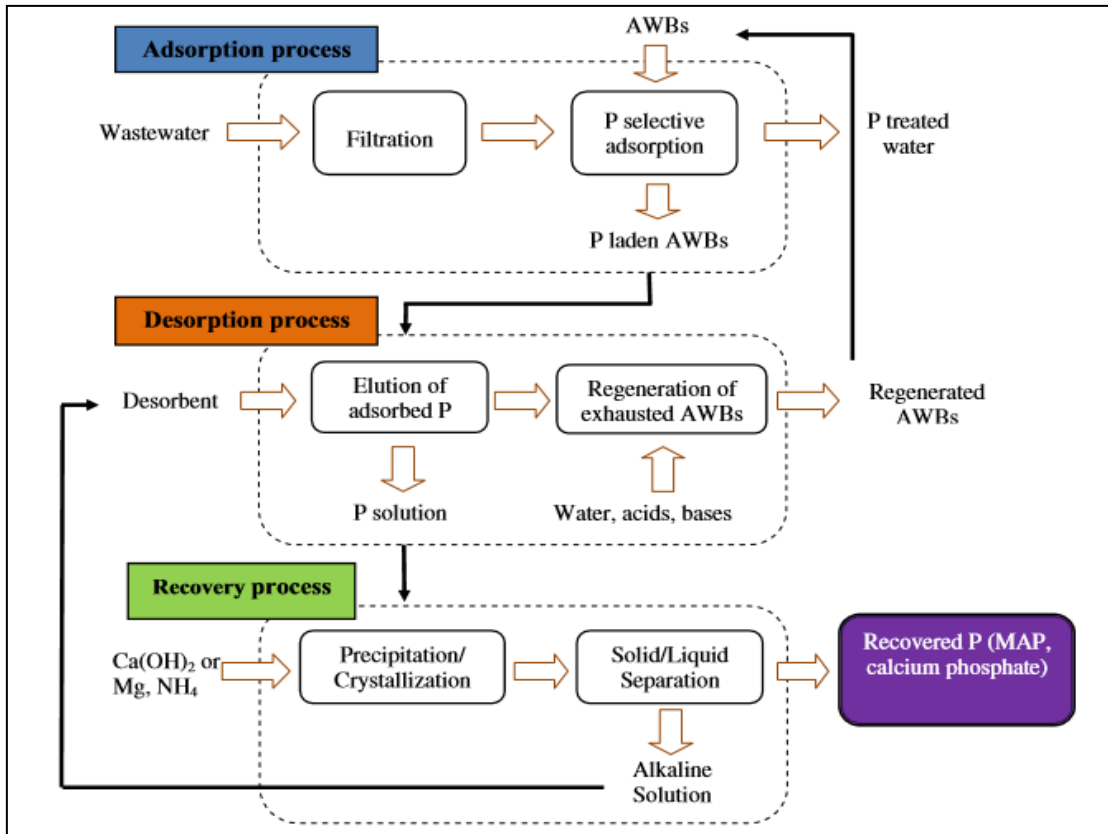


Figure 1.15. Schematic of AWBs based biosorbents usage for phosphorus removal and recovery from aqueous solutions (Nguyen et al., 2014)

1.3.4. Phosphorus recovery from wastewater treatment plants

Sewage is the one of the sources that has the highest potential of phosphorus recovery. Phosphorus can be recovered from the both liquid (e.g. supernatant of anaerobic digester) and solid phases (e.g. sewage sludge or sewage sludge ash) of wastewater treatment processes (Ye et al., 2016). Various points of the wastewater treatment plants for the phosphorus recovery are shown in Figure 1.16.

Phosphorus recovery from wastewater can be achieved from urine, effluent of secondary treatment, digester supernatant, sewage sludge and sewage sludge ash. However, their flows are different from each other in terms of volume, concentration of phosphorus, forms of phosphorus and theoretical phosphorus recovery potentials (Egle et al., 2015). Table 1.6 shows the different phosphorus recovery sources and its properties.

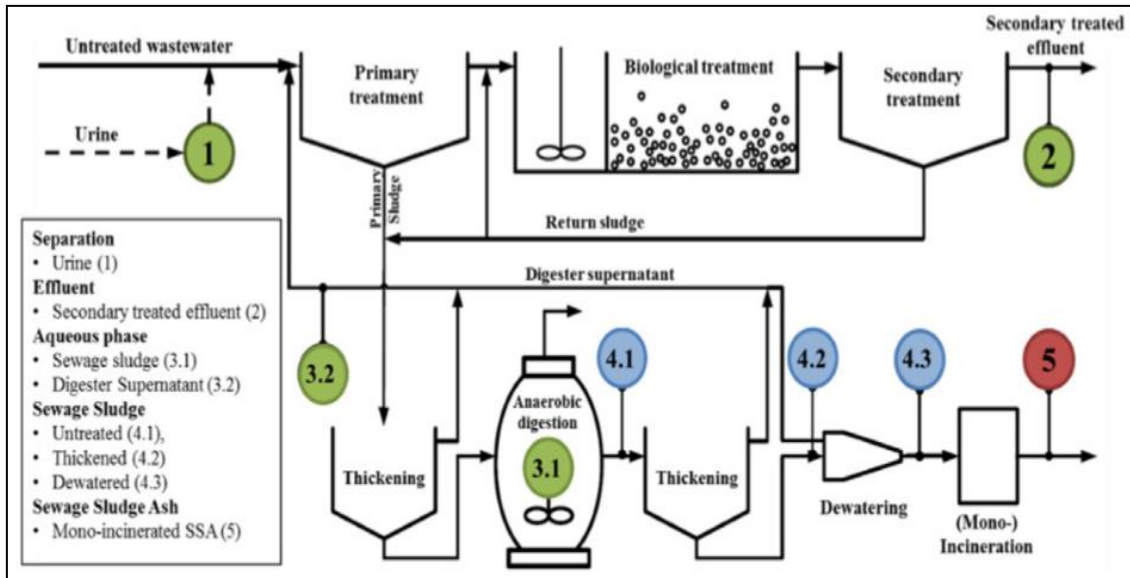


Figure 1.16. Possible phosphorus recovery points from wastewater treatment plants (Egle et al., 2016)

Table 1.6. Properties of potential phosphorus recovery flows (Egle et al., 2015)

Source	Mass flow	P/PO ₄ -P concentration	Form of P	P recovery potential (%)
Untreated wastewater	200 L/cap.day	~10 mg P/L	Bound/dissolved	100
(1) Urine	~1.5-2 L/cap.day	~150-250 mg PO ₄ -P/L	Dissolved	30-50
(2) Secondary treated effluent	200 L/cap.day	~5-10 mg PO ₄ -P/L	Dissolved	50-70
(3.1) Digested sewage sludge (SS) (~3.5% TS)	1.6 kg/cap.day	Dissolved part: 20-400 PO ₄ -P mg/L	Partly dissolved (10-30%)	10-30
(3.2) Digester supernatant	1-10 L/cap.day	20-400 PO ₄ -P mg/L	Dissolved	10-30
(4.1) Digested sewage sludge (~3.5% TS)	1.6 kg/cap.day	1.4 g P/kg sludge	Bound(bio/chem); partly dissolved	90
(4.2) SS thickened (10% TS)	0.6 kg/cap.day	4 g P/kg sludge	Bound (bio/chem)	90
(4.3) SS dewatered (30% TS)	0.2 kg/cap.day	12 g P/kg sludge	Bound (bio/chem)	90
(5) Sewage sludge ash	0.03 kg/cap.day	50-130 g P/kg TS	Bound (chem)	~90

Phosphorus recovery from aqueous phase of wastewater is achieved by precipitation/crystallization processes. For this purpose, calcium or magnesium salts are used to recover phosphate as calcium phosphate or struvite. Phosphorus recovery from sewage sludge or sewage sludge ash is achieved by wet chemical or thermal processes (Desmidt et al., 2015).

1.4. Final Products of Phosphorus Recovery Processes

Phosphorus recovery with crystallization process is generally either as calcium phosphates or as magnesium ammonium phosphate hexahydrate (struvite, $\text{MgNH}_4\text{PO}_4 \cdot 6\text{H}_2\text{O}$). Calcium phosphates are similar products to phosphate rocks, and magnesium ammonium phosphate hexahydrate is known as slow release fertilizer. Struvite can be in the form of K-struvite ($\text{KMgPO}_4 \cdot 6\text{H}_2\text{O}$) which has similar structure with struvite, the only difference is the replacement of NH_4^+ with K^+ ion. Phosphorus also can be recovered from sewage sludge and sewage sludge ash in the form of struvite or calcinated phosphate (Desmidt et al., 2015).

1.4.1. Struvite

Struvite contains magnesium, ammonium and phosphate in equal molar concentrations and it is also an orthophosphate. It is a crystalline mineral powder and the specific gravity of struvite is around 1.7. Struvite is generally white, however it can be yellow, brownish or light grey also, based on the crystallization media. It is sparingly soluble in alkaline or neutral media, but it is readily soluble in acidic media (Le Corre et al., 2009; Darwish et al., 2016b).

Struvite formation can be observed naturally in wastewater treatment plants either as magnesium or potassium form. Because it forms spontaneously at high pH levels ($\text{pH} > 8.0$) and equal molar concentrations of magnesium, phosphate and either magnesium or potassium, in highly turbulent systems (e.g. elbows, valves, propellers and pipe joints). Scale problem related with the struvite formation occurs frequently in anaerobic digestion units, digester supernatant discharge line, heat exchangers and centrifuge dewatering units (Le Corre et al., 2009; Sengupta et al., 2015; Kataki et al., 2016).

Struvite precipitates in a 1:1:1 molar ratio and general equation for struvite formation is as follows:



MAP precipitation decreases the pH of the solution, because of the crystallization of soluble $\text{PO}_4\text{-P}$ and this means the dominant form of phosphorus in MAP formation reaction is HPO_4^{2-} or H_2PO_4^- rather than PO_4^{3-} . Thus, MAP formation reaction realizes according to reactions shown below (Liu et al., 2013):



The occurrence and development of MAP crystals are realized in two chemical steps as shown in Figure 1.17.

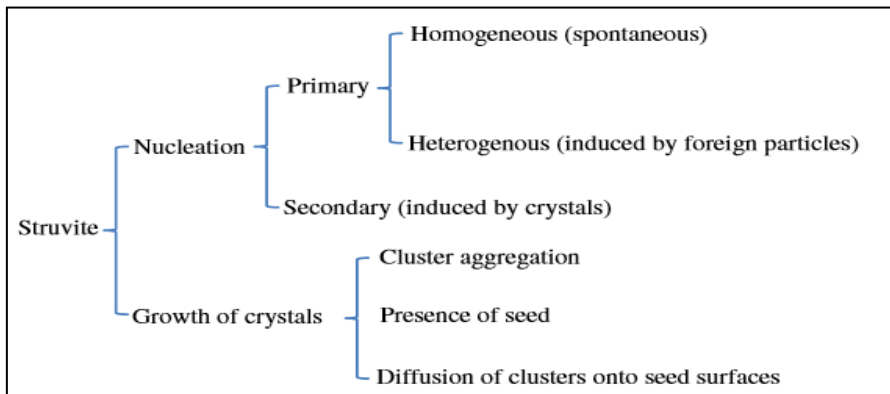


Figure 1.17. Occurrence and development of MAP crystals (Liu et al., 2013)

The first step for struvite formation is nucleation (birth of crystal) and the second step is growth of crystals. In nucleation stage, crystal embryos are formed by the combination of ions. Homogeneous primary nucleation occurs in highly purified or highly supersaturated solutions, that does not exist practically. Heterogeneous nucleation occurs in the presence of foreign particles and these particles act as nuclei for heterogeneous nucleation. Because wastewaters contain high impurities, struvite crystal formation is generally realized by heterogeneous nucleation. Secondary nucleation occurs when there are parent crystals which provide local interactions of present

crystals. The time required for nucleation is called as induction time and it is influenced by pH, mixing energy, supersaturation and presence of foreign ions.

In the growth stage of struvite formation, the size of embryo crystals increase and they reach a detectable size. This is actualized by mechanisms of mass transfer and surface integration (Le Corre et al., 2009; Liu et al., 2013).

The process of struvite formation is influenced by solution supersaturation, pH, molar ratio of Mg:N:P, type of reagents, reaction time, temperature, presence of foreign ions and mixing. Supersaturation is the main driving factor and it causes nucleation of crystals. At supersaturation state of a solution, solute concentration is higher than the equilibrium value. Moreover, pH is very important for crystallization process because it affects solubilization and supersaturation. Moreover, although theoretically Mg:N:P molar ratio is 1:1:1, in practice it is not the actual optimum ratio because of the presence of other species that forms by products. Thus optimum molar ratio should be defined specifically (Darwish et al., 2016b; Le Corre et al., 2009). Some examples of optimum Mg:P molar ratios for different wastewaters are given in Table 1.7.

Table 1.7. Phosphate removal efficiencies based on optimum $Mg^{2+}:PO_4^{3-}$ ratio in different type of wastewaters (Liu et al., 2013)

Type of wastewater	Mg source	Optimum $Mg^{2+}:PO_4^{3-}$ ratios	P removal (%)
Synthetic swine wastewater	MgCl ₂ /NaOH	1.4:1	97.0
Swine wastewater	MgCl ₂ /Air Stripping	0.8-1.0:1	87-93
Anaerobic swine lagoon liquid	MgCl ₂ /NaOH	1.6:1	96.0
Sewage sludge anaerobic digester	MgCl ₂ /H ₃ PO ₄ /NaOH	1.5:1	95.0
Synthetic wastewater	-	1.3-1.5:1	89-92
Synthetic urine	MgO/MgCl ₂	4.2:1	97.5
Semiconductor wastewater	MgCl ₂	3.0:1	92.1
Landfill leachate	MgCl ₂ ·6H ₂ O/Na ₂ HPO ₄ ·12H ₂ O	1:1	92.0
Sewage	MgCl ₂	1.05:1	95.0

Another important factor that affects struvite formation is pH. In the pH range of 8-10, struvite can be formed. There are different ways to increase pH to required levels such as chemical dosing and air stripping. In the case of chemical dosing, $\text{Mg}(\text{OH})_2$, $\text{Ca}(\text{OH})_2$, lime or NaOH can be used to increase pH. Application of air stripping strips CO_2 and provides very gentle pH increase. However; when pH is increased to values higher than 10, struvite formation can be inhibited due to other reactions that form $\text{Mg}_3(\text{PO}_4)_2$, $\text{Mg}(\text{OH})_2$ and $\text{Ca}_{10}(\text{PO}_4)_6(\text{OH})_2$. Also, NH_4^+ is converted to NH_3 at $\text{pH} > 10$ (Darwish et al., 2016b; Le Corre et al., 2009; Liu et al., 2013).

Although temperature is one of the factor that affects struvite formation, its impact is lower when compared with pH or supersaturation. Temperature affects solubility of struvite and crystal morphology. At low temperatures, between 5-20°C, struvite solubility decreases, it increases the supersaturation and this results in smaller particle size. Moreover, high temperatures affect struvite formation significantly. Because, when temperature increases, solubility of struvite increases (Darwish et al., 2016b; Le Corre et al., 2009).

1.4.2. Calcium phosphate

Phosphorus can be recovered as calcium phosphate via precipitation process and depending on the pH and ionic composition, several forms of calcium phosphate can be obtained. In Table 1.8, these different forms of calcium phosphates are shown. However, thermodynamically the most stable form of calcium phosphate is the hydroxyapatite ($\text{Ca}_5(\text{PO}_4)_3\text{OH}$) (Metcalf & Eddy, 2014).

To recover phosphorus as calcium phosphate pretreatment is applied to prevent calcium carbonate precipitation. For this purpose, influent is acidified to pH less than 5 with strong inorganic acid and then CO_2 stripping is applied. After this pretreatment, calcium hydroxide is added to precipitate calcium phosphate (Metcalf & Eddy, 2014). Flow diagram for the calcium phosphate precipitation is shown in Figure 1.18.

Table 1.8. Different forms of crystallized calcium phosphates (Montastruc et al., 2003)

Name	Formula
Dicalcium phosphate dihydrate (DCPD)	$\text{CaHPO}_4 \cdot 2\text{H}_2\text{O}$
Dicalcium phosphate anhydrate (DCPA)	CaHPO_4
Octocalcium phosphate (OCP)	$\text{Ca}_8\text{H}(\text{PO}_4)_6 \cdot 2.5\text{H}_2\text{O}$
Tricalcium phosphate (TCP)	$\text{Ca}_3(\text{PO}_4)_2$
Amorphous calcium phosphate (ACP)	$\text{Ca}_3(\text{PO}_4)_2$
Hydroxyapatite (HAP)	$\text{Ca}_{10}(\text{PO}_4)_6(\text{OH})_2$

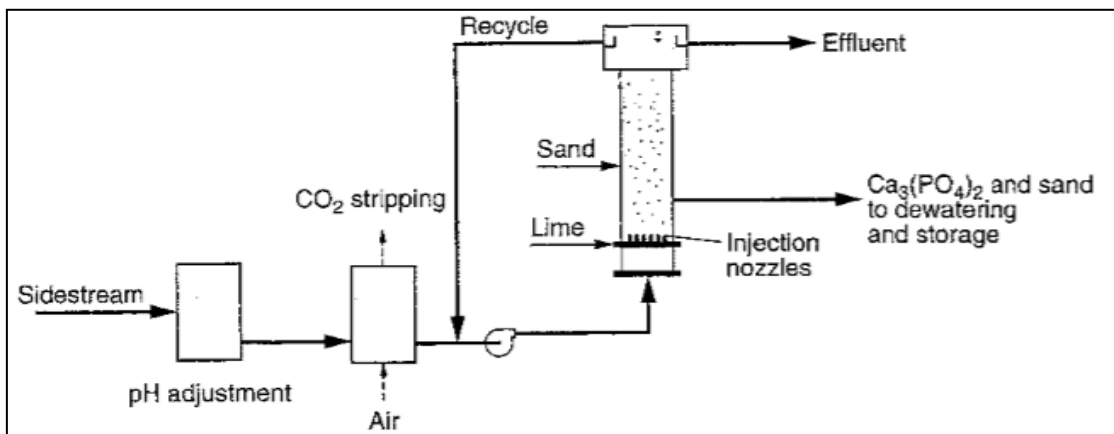


Figure 1.18. Calcium phosphate precipitation for phosphorus recovery (Metcalf & Eddy, 2014)

Calcium phosphate precipitation is a complex process because it is affected from many parameters. These parameters are concentrations of calcium and phosphate ions, supersaturation, temperature, pH, time (solid-solid transformation) (Montastruc et al., 2003).

pH should be between 8-9 for the calcium phosphate precipitation. Typically, quick lime (CaO) is used as calcium source for the precipitation and also to increase the pH from 5 or less to 8-9 (Metcalf & Eddy, 2014).

The form of the precipitated calcium phosphate mainly depends on pH and kinetics. At acidic pHs around 5, the phase is predicted as dicalcium phosphate dihydrate (DCPD, $\text{CaHPO}_4 \cdot 2\text{H}_2\text{O}$). At pH around 6, the phase is predicted as octacalcium phosphate (OCP, $\text{Ca}_8\text{H}(\text{PO}_4)_6 \cdot 5\text{H}_2\text{O}$). At pH 7 and above, hydroxyapatite (HAP, $\text{Ca}_5(\text{PO}_4)_3\text{OH}$) precipitation is realized (Desmidt et al., 2015).

1.5. Main Phosphorus Recovery Processes from Municipal Wastewater

Phosphorus can be recovered from municipal wastewater with the application of crystallization & precipitation method, wet chemical process, adsorption and thermochemical process. While chemical precipitation and adsorption methods are used for the liquid phase, wet chemical process and thermochemical process are used for the sludge phase. In Table 1.9, general information about these methods is given.

Table 1.9. General information about processes for the phosphorus recovery from municipal wastewater (Ye et al., 2017)

Technology	Recovery spot	Main chemicals	P recovery
Chemical precipitation	Liquid phase	Mg/Ca materials	Over 80%
Adsorption	Liquid phase	Metal-based adsorbents	Over 90%
Wet-chemical process	Sludge phase	Acid/alkaline solution	Over 60%

1.5.1. Chemical precipitation

Chemical precipitation is generally used for the recovery of phosphorus from liquid phase. In this process, proper precipitants are added, generally calcium (Ca^{2+}) or magnesium (Mg^{2+}), and dissolved phosphorus is recovered. Application of chemical precipitation process results in formation of magnesium ammonium phosphate or calcium phosphate as it is mentioned in Section 1.4.

There are some factors that affect precipitation of phosphorus. These are molar ratio of phosphorus and precipitating agent, concentration of ions, pH and temperature. For the struvite formation, required Mg:N:P ratio is 1:1:1 and for the hydroxyapatite formation

required Ca:P ratio is 1.7:1. However, to start precipitation reactions, higher Mg or Ca ratios are needed. The pH should be higher than 8.0 for the precipitation of both struvite and hydroxyapatite. However, when pH is higher than 10, phosphorus recovery efficiency can decrease because ammonia is converted to gaseous ammonia and Ca and Mg hydroxides can form at these high pH levels. For the pH adjustment, generally caustic soda (NaOH) is used or CO₂ is stripped out with aeration (Ye et al., 2017; Egle et al., 2015).

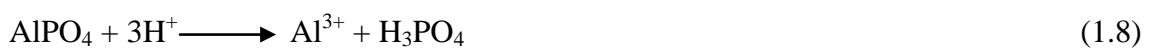
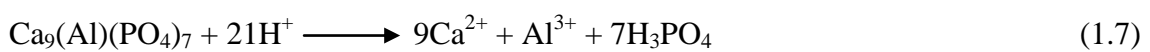
1.5.2. Adsorption

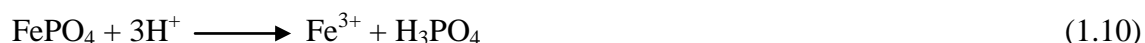
Phosphorus recovery with adsorption process has some advantages like low cost and simple operation. Adsorption process happens in two steps: adsorption of phosphate and desorption of phosphate loaded adsorbent. Recovered phosphorus is enriched from the desorption solution and it is can be used for land application (Ye et al., 2017).

1.5.3. Wet chemical process

In wet chemical leaching method, pH and thus solubility of phosphorus is changed with the addition of strong acids (e.g. HCl or H₂SO₄) or bases (e.g. NaOH), and phosphorus is converted from a solid bound form to a dissolved form. With the application of wet chemical leaching method, 90% of phosphorus can be dissolved (Egle et al., 2015).

Phosphorus recovery with acidic wet chemical methods are realized at pH levels below 2 and over 80% of phosphorus can be dissolved from sewage sludge or sewage sludge ash. For this process, approximately 0.3-0.68 kg strong acids are used for 1 gram of sewage sludge ash and phosphorus dissolution between 66.5-99.4% is achieved (Ye et al., 2017). Amount of the dissolved metals is dependent to the sewage sludge ash characteristics (whether it is rich in Fe or Al) and the acid that is used for dissolution (HCl or H₂SO₄). Mostly phosphorus inside the sewage sludge ash is in the form of calcium phosphates (Ca-P), aluminum phosphates (Al-P) or iron phosphates (Fe-P) and reactions for the phosphorus dissolution from these type of ashes are as follows:





In equations (1.7), (1.8), (1.9) and (1.10) theoretical chemical demand for complete acidic dissolution of different phosphorus compounds are given and these equations show that for each phosphorus compounds the required acid amount is 3 mol H⁺/mol P. On the other hand, more acid is needed in practice because of the presence of other acid soluble components such as MgO, K₂O, CaO, CaCO₃, Ca(OH)₂ (Petzet et al., 2012).

Besides high phosphorus dissolution percentages, unavoidably metals or their compounds are also dissolved with acidic wet chemical leaching methods. Therefore, further separation step must be applied for the phosphorus-heavy metal separation and there are several methods to achieve this separation. These are ion exchange, sequential precipitation, nanofiltration and liquid-liquid extraction (Ye et al., 2017; Petzet et al., 2012).

Phosphorus can also be recovered with alkaline leaching because cells inside the sludge are disintegrated at pH levels above 11 and it provides release of phosphorus to the liquid phase. The demand for the NaOH is about 0.12 kg/kg ash. Moreover, heavy metal removal is not necessary after application of this method, because under alkaline conditions dissolution of heavy metals is barely (Ye et al., 2017; Egle et al., 2015).

1.5.4. Thermochemical process

Thermochemical process is based on the heavy metals removal from the sewage sludge ash in the presence of chlorine donor (e.g. MgCl₂, CaCl₂) at the temperatures of 800-1000°C. In this process, volatile heavy metal chlorides are removed from the sewage sludge ash. Moreover with the application of this process, phosphorus is converted into bio-available mineral phases that is available for plants (Adam et al., 2009). Schematic of thermochemical phosphorus recovery is shown in Figure 1.19.

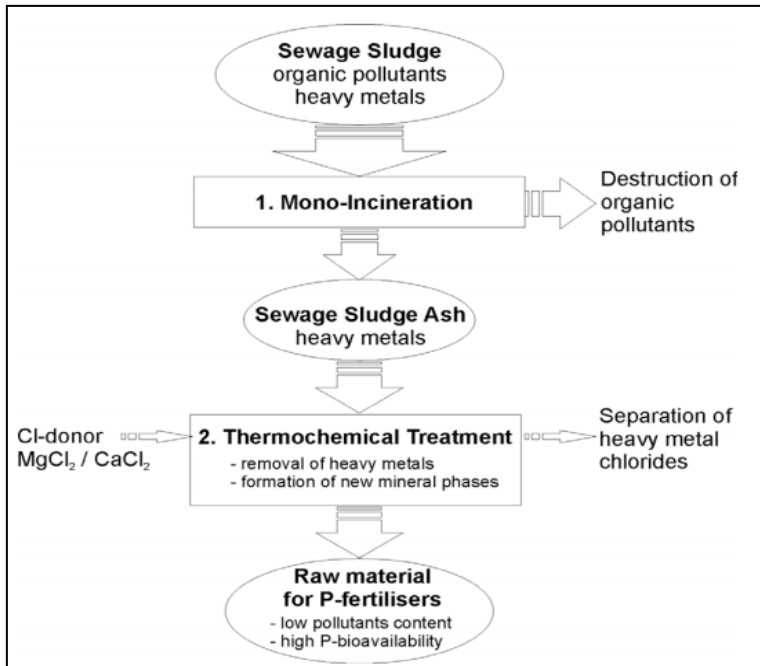


Figure 1.19. Schematic of the phosphorus recovery from sewage sludge ash by thermochemical process (Adam et al., 2009)

Major aim of thermochemical processes is the evaporation of heavy metals as heavy metal chlorides. In Figure 1.20, gaseous fractions of some heavy metal chlorides and oxides as a function of temperature are given. Nearly all of the heavy metal chlorides are in the vapor phase except copper. This means that thermochemical treatment is theoretically possible for these heavy metals (Vogel et al., 2011).

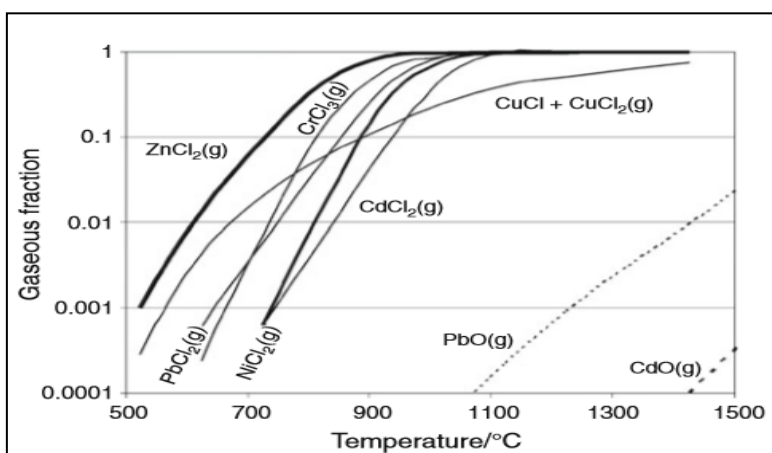


Figure 1.20. Gaseous fractions of some heavy metal chlorides (Vapor pressure of some heavy metals oxides are lower by several orders of magnitude. Thus, only PbO and CdO are visible in the graph) (Vogel et al., 2011)

1.6. Phosphorus Recovery from Municipal Wastewater

As it is mentioned in Section 1.3.4, there are some possible points for phosphorus recovery in wastewater treatment plants. These are secondary treated effluent, sewage sludge, digester supernatant and sewage sludge ash. There are special phosphorus recovery technologies from wastewater treatment plants and they are shown in Table 1.10.

Table 1.10. Phosphorus recovery technologies from wastewater treatment plants (Egle et al., 2016)

Aqueous phase	Sewage Sludge (SS)	Sewage Sludge Ash (SSA)
REM-NUT [®] (ion exchange, precipitation)	Gifhorn process (wet-chemical leaching)	AshDec [®] depollution (thermo-chemical)
AirPrex [®] (precipitation/crystallization)	PHOXNAN (wet-oxidation)	LEACHPHOS [®] (acidic wet-chemical, leaching)
Ostara Pearl Rector [®] (crystallization)	Aqua Reci [®] (super critical water oxidation)	EcoPhos [®] (acidic wet chemical, leaching)
DHV Crystalactor [®] (crystallization)	MEPHREC (metallurgic melt-gassing)	RecoPhos [®] (acidic wet-chemical, extraction)
P-RoC [®] (crystallization)		Thermphos (P ₄) (thermo-electrical)
PRISA (precipitation/crystallization)		

1.6.1. Phosphorus recovery from aqueous phase

Secondary treated effluent, anaerobic sludge and digester supernatant can be categorized as phosphorus recovery points of aqueous phase and there are some technologies to recover phosphorus from aqueous phase. These are REM-NUT[®] process, AirPrex[®] process, Ostara Pearl Reactor[®], DHV Crystalactor[®] process, P-RoC[®] process, PRISA process and NuReSys[®] process.

Secondary treated effluent contains approximately 5-10 mg PO₄-P/L and its volume is high (approximately 200 L/capita.day). Thus secondary treated effluent can be a

phosphorus recovery source. For this purpose, selective ion exchangers can be used and ion exchangers remove nutrients (NH_4^+ , K^+ , HPO_4^{2-}) from wastewater. REM-NUT[®] process relies on this principle and it achieves recovery of phosphorus as struvite by adding Mg^{2+} to nutrients at controlled pH (Egle et al., 2015; Liberti et al., 2001). Schematic figure of this process is shown in Figure 1.21.

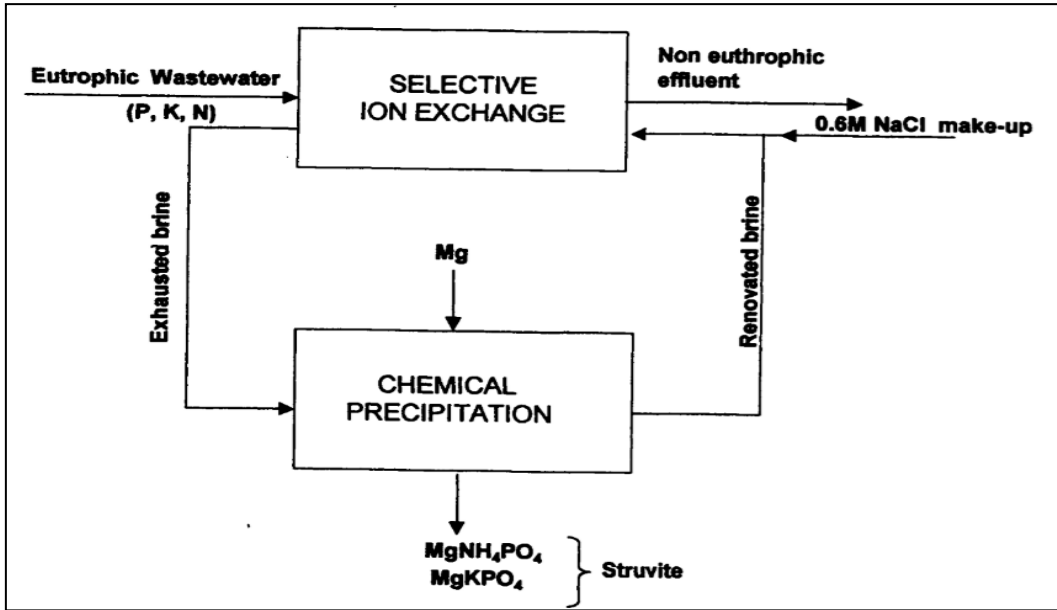


Figure 1.21. Schematic of REM-NUT[®] process (Liberti et al., 2001)

After anaerobic digestion process, phosphorus releases from the sludge and this sludge contains about 200-400 mg $\text{PO}_4\text{-P/L}$. This value can be higher if additional sludge treatment and disintegration methods like acidification of thermal treatment are applied. There are some approaches to recover phosphorus from anaerobic sludge or digester supernatant.

AirPrex[®] process is developed for the prevention of undesired struvite formation after digestion. In this process, pH is increased by CO_2 stripping with intensive aeration and MgCl_2 solution is used as Mg source to recover phosphorus as struvite in an airlift reactor. Average chemical demand is 14.5 kg MgCl_2/kg recovered P and molar Mg:dissolved P ratio is 2.1. Struvite crystals are harvested at the bottom of the reactor, and because struvite is formed in wet sludge it can contain some impurities. To improve quality of struvite washing and drying processes are also applied (AirPrex[®], 2015). Schematic of AirPrex[®] is shown in Figure 1.22.

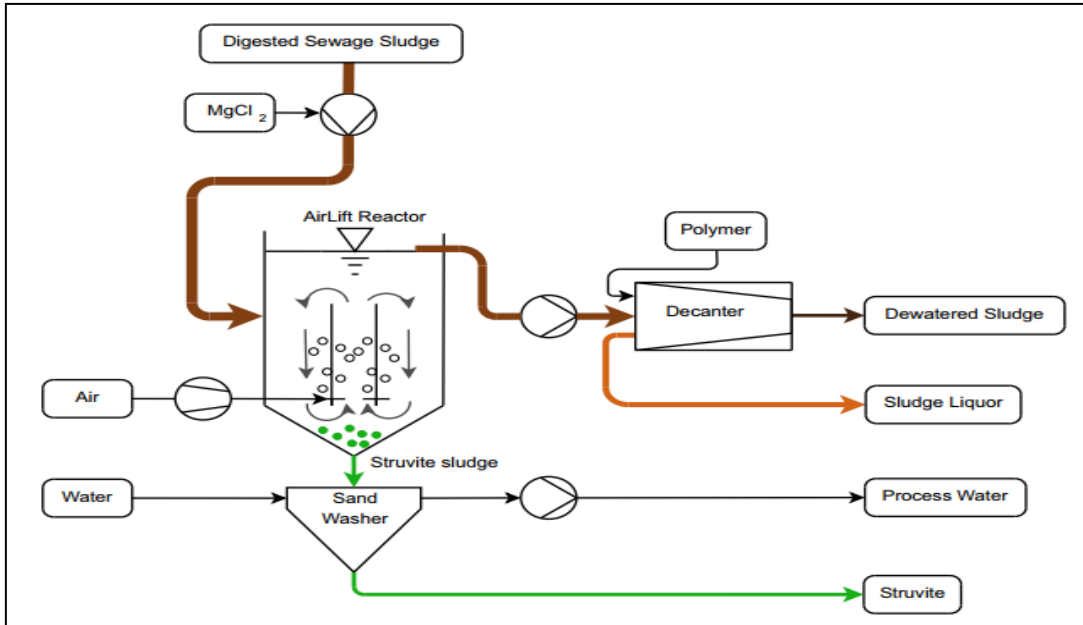


Figure 1.22. Schematic of AirPrex[®] process (AirPrex[®], 2015)

Ostara Pearl[®] process is another process that recovers phosphorus from sludge liquor of anaerobic digesters in a wastewater treatment plant that has a biological phosphorus removal process. With this process, phosphorus is recovered as struvite in an upflow fluidized bed reactor that has multiple reactive zones of increasing diameters to control chemical crystallization as shown in Figure 1.23. $MgCl_2$ is used as a Mg source and for pH adjustment, $NaOH$ is used. Typical phosphorus removal is about 85-90% in this process. Moreover, the Ostara Pearl[®] process has an advantage of allowing large struvite pellets that have a diameter of 1.5 to 4.5 mm (Desmidt et al., 2015).

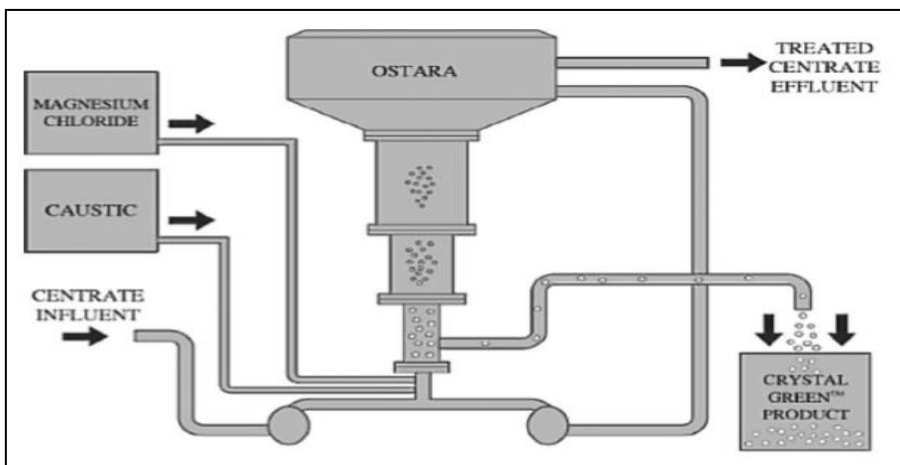


Figure 1.23. Schematic of Ostara Pearl[®] process (Desmidt et al., 2015)

In DHV Crystalactor[®] process, side stream of the sludge is fed to the fluidized bed reactor and phosphorus is recovered as calcium phosphate. To prevent carbonate inhibition of calcium phosphate precipitation, removal is achieved in cascade stripper before the entrance of the reactor. pH is adjusted to 3.5 with H₂SO₄ to strip carbonates. As shown in Figure 1.24, in DHV Crystalactor[®] process, cylindrical fluidized bed reactor and filter sand are used. Initially quartz sand is used as seed to accelerate precipitation and pellets settle to the bottom of the reactor. Because calcium phosphate crystallization requires pH of 9, Ca(OH)₂ solution is fed to the reactor (Desmidt et al., 2015; Melia et al., 2017).

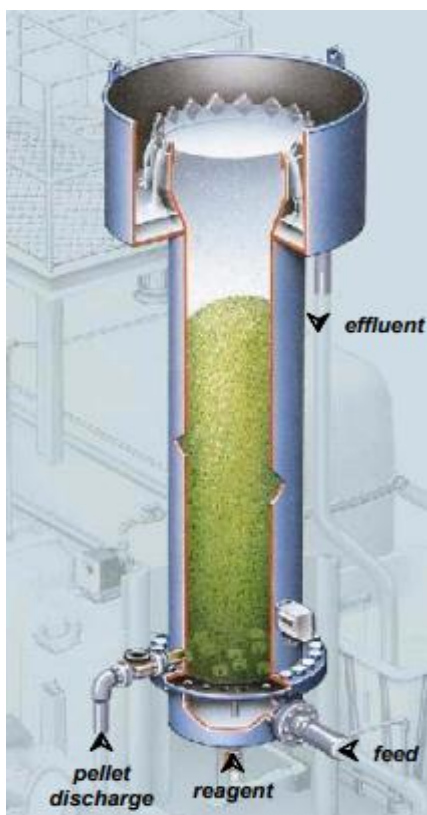


Figure 1.24. Schematic of Crystalactor[®] process (Giesen et al., 2009)

In P-RoC[®] (Phosphorus Recovery from wastewater by Crystallization of calcium phosphate compounds) process, phosphorus recovery is achieved similar to Crystalactor[®] process however complex pretreatment steps like pH adjustment or CO₂ stripping can be avoided. In this process, phosphorus is recovered again as calcium phosphate and to realize this process, calcium silicate hydrate (CSH) compounds or synthesized tobermorite pellets are used as seed materials. Moreover, product of this

process has a phosphorus content of 11-13% which is comparable to phosphate rock (Berg et al., 2005; Melia et al., 2017). Schematic of P-RoC[®] process is given in Figure 1.25.

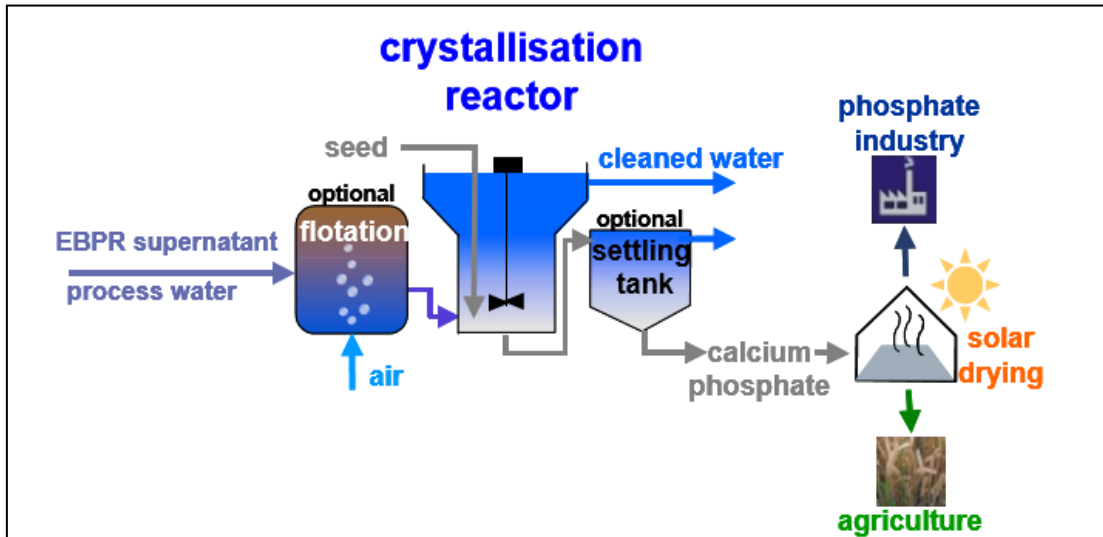


Figure 1.25. Schematic of In P-RoC[®] process (Berg et al., 2005)

In NuReSys[®] process mixed tanks are used for the phosphorus recovery from wide range of wastewaters like manure treatment and dairy industry, digested sewage sludge. In Figure 1.26 struvite formation from anaerobic digestion supernatant by NuReSys[®] process is given.

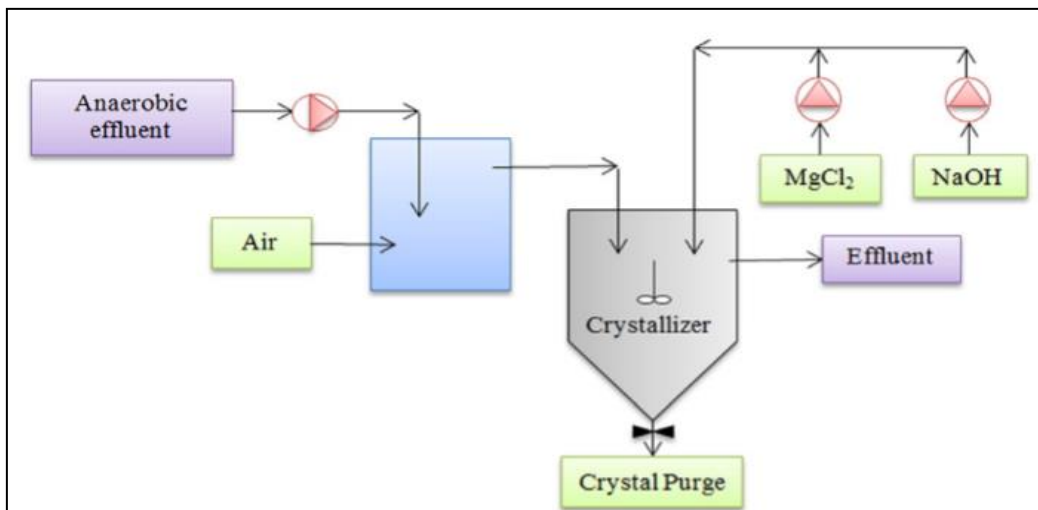


Figure 1.26. Schematic of NuReSys[®] process for phosphorus recovery (Ye et al., 2017)

In NuReSys[®] process, to be able to increase pH, air stripping is applied and MgCl₂ is used as magnesium source. Also NaOH is used to increase pH of the solution. The optimum pH is between 8-8.5 for this process. With NuReSys[®] process, 80-85% of phosphorus recovery is achieved (Ye et al., 2017).

1.6.2. Phosphorus recovery from sewage sludge

Sewage sludge is heterogeneous, semi-solid residue obtained from wastewater treatment processes and it contains essential nutrients for plants like phosphorus, potassium, magnesium, nitrogen. However it also contains heavy metals, pharmaceuticals, endocrine disrupting compounds and pathogens which makes generally it unusable for agricultural usage. Therefore some processes are developed to recover phosphorus from sewage sludge. These processes are Gifhorn process, PHOXNAN[®] process, Aqua Reci[®] process and MEPHREC[®] process.

Gifhorn is based on acidic leaching process. In this process, phosphorus inside the solid phase of the digested sludge is extracted with the addition of H₂SO₄ at pH 4.5. Because acidic leaching causes dissolution of heavy metals, as a second step with the addition of Na₂S dissolved heavy metals are precipitated at pH 5.6 which is adjusted with NaOH. Then, solid-liquid separation is achieved with a decanter and mixture of struvite & calcium phosphate precipitation is initialized with the addition of Mg(OH)₂ at pH:9 that is adjusted with NaOH. Lastly, phosphorus product is harvested by a second solid-liquid separation step (Gifhorn, 2015).

In PHOXNAN[®] process, there is a combination of low pressure wet oxidation with two membrane filtration steps. Sludge oxidation with pure oxygen is realized at high temperature and pressure at acidic conditions that is provided by the addition of H₂SO₄. Organic pollutants are oxidized and phosphorus is recovered mainly as H₃PO₄ and H₂PO₄²⁻ because of the low pH. For the separation of solids, ultrafiltration is used and for the elimination of metal ions nanofiltration is used (Melia et al., 2017).

Aqua Reci[®] process is used supercritical water oxidation (SWO) which is an innovative and effective organic destruction method for sewage sludge. SWO destroys organic matters with the use of water in its supercritical state. Water enters a supercritical phase

at temperatures above 375°C and pressure of 220 bar. Addition of technical oxygen results in destruction of organic matters in one minute with 99.99%. After application of SWO process to sewage sludge, inorganic ash and liquid phase are obtained. This inorganic ash contains majority of phosphorus and heavy metals. To recover phosphorus, extraction is applied whether with acid (HCl) or base (NaOH). With the alkaline leaching high percentages up to 90% of the phosphorus is dissolved and it is precipitated as hydroxyapatite (Egle et al., 2015; Stendahl and Jäfverström, 2004).

MEPHREC[®] process is developed for the recovery of phosphorus from sewage sludge or ash. In MEPHREC[®] process dewatered sewage sludge is pressed into briquettes. These briquettes are thermally treated in a shaft furnace at temperatures above 1450°C. At these conditions heavy metals are reduced into their elemental form and the volatile ones like Cd, Hg, Pb, Zn are evaporated. Non-volatile heavy metals are separated from the slag in a liquid metal phase. The phosphate which is initially inside the sewage sludge is transformed into silicophosphates (Mephrec[®], 2015).

1.6.3. Phosphorus recovery from sewage sludge ash

Sewage sludge ash is obtained from the thermal treatment of the sewage sludge and organic matters inside the sewage sludge is almost completely oxidized with thermal treatment (800-900°C). 97-99.9% of the phosphorus inside the sewage sludge accumulates in the sewage sludge ash. However it also contains heavy metals (Egle et al., 2015). Therefore phosphorus recovery technologies from sewage sludge ash are developed. These are AshDec[®] process, LEACHPHOS[®] process, EcoPhos[®] process, RecoPhos[®] process and Thermphos (P₄) process.

In AshDec[®] process, sewage sludge ash is thermochemically treated in a rotary kiln. In this rotary kiln, sewage sludge ash is reacted with Na₂SO₄ (AshDec[®] Rhenania) at 900-1000°C with a minimum retention time of 20 minute to obtain bio-available NaCaPO₄. As a reducing agent, dry sewage sludge is used. Volatile heavy metals like As, Cd, Hg, Pb, Zn evaporate and removed via gas phase. The hot off-gas at the exit of the kiln can be used to heat ash, Na₂SO₄, and kiln air. There is an alternative AshDec[®] process (AshDec[®] depollution) that uses MgCl₂ in treatment. In this process, heavy metals are removed again in gas phase in the form of chlorides and oxichlorides, phosphorus is

recovered as magnesium ammonium phosphate (AshDec[®], 2015; Egle et al., 2016). Schematic of AshDec[®] process is given in Figure 1.27.

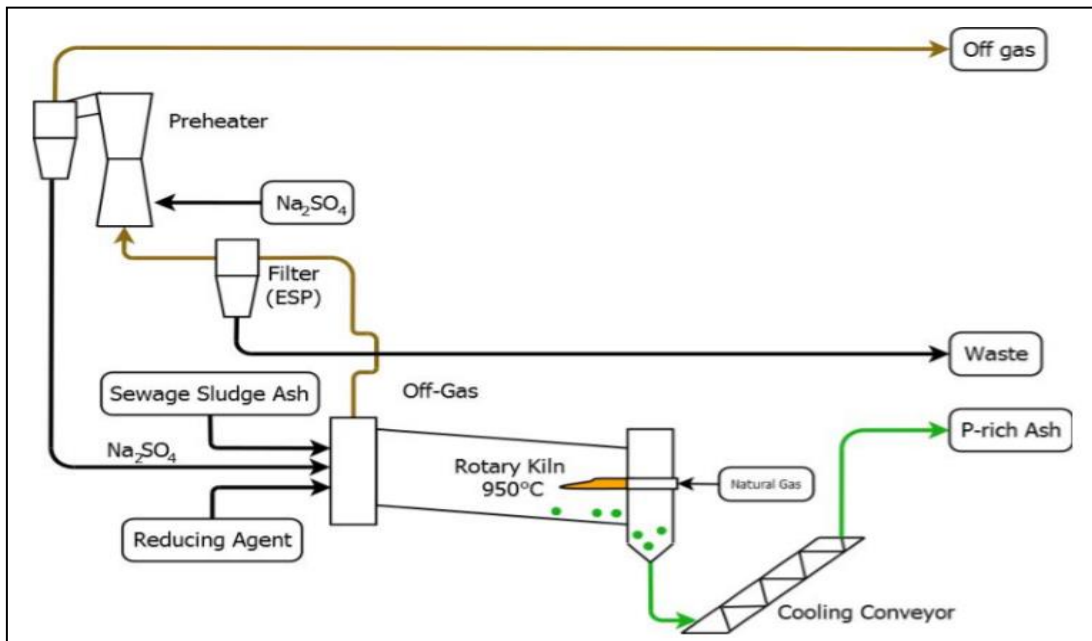


Figure 1.27. Schematic of AshDec[®] process (AshDec[®], 2015)

LEACHPHOS[®] process uses diluted sulfuric acid to extract phosphorus from sewage sludge ash. By this method, 80-95% of the phosphorus inside the sewage sludge ash is transferred into leachate. Then, pH is increased by the addition of sodium hydroxide or lime till the targeted recovery is obtained. Heavy metals like Cu, Zn, Cd are dissolved partially and precipitated. Mixture of aluminum phosphate, ferric phosphate and calcium phosphate is separated with filtration and remaining heavy metals are separated for disposal after precipitated at pH>9 with a precipitating agent. Phosphorus recovery as calcium phosphates or as struvite is targeted (LEACHPHOS[®], 2015). Schematic of LEACHPHOS[®] process is given in Figure 1.28.

EcoPhos[®] is another process that recovers phosphorus from sewage sludge ash with the application of acidic leaching. HCl or H₂SO₄ is used to extract phosphorus inside the ash. This process also includes the treatment of obtained slurry for the removal of impurities and solid residues. Products of this process are dicalcium phosphate or phosphoric acid (Melia et al., 2017).

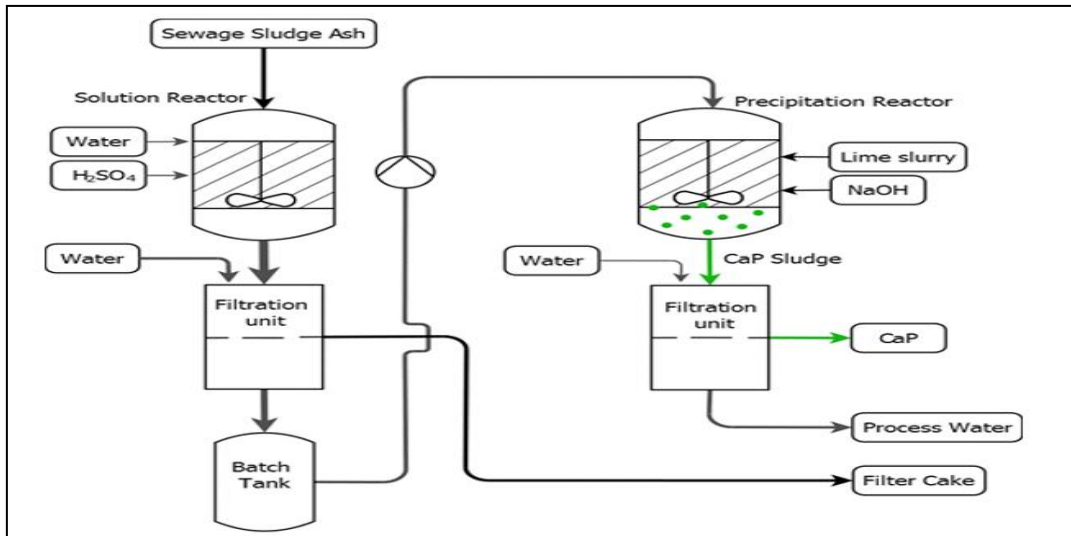


Figure 1.28. Schematic of LEACHPHOS[®] process (LEACHPHOS[®], 2015)

In RecoPhos[®] process, sewage sludge ash is reacted with phosphoric acid to increase plant available phosphate fraction. Industrial grade phosphoric acid (~52% H₃PO₄) is mixed with sewage sludge ash in rotary kiln. After the reaction with phosphoric acid, primary minerals inside the ash are transferred into soluble calcium and magnesium dihydrogen phosphate that is the primary component of the RecoPhos[®] P 38 fertilizer. Demand for the phosphoric acid for this process depends on phosphorus content of sewage sludge ash and for a sewage sludge ash that has phosphorus content of 8.5%, approximately 0.65 kg H₃PO₄/kg ash is required (Weigand et al., 2013; Egle et al., 2015).

1.7. Sewage Sludge Management

Processing of municipal wastewater in wastewater treatment plants causes production of huge amounts of sewage sludge. In Europe, each year approximately 11.6 million tons of dry sewage sludge is produced (Kleemann et al., 2017). In Turkey, 1.126 million tons of waste dry solid material (526,000 tons from wastewater sludge; 600,000 tons from industrial wastewater sludge) was produced in the year 2012 (Abuşoğlu et al., 2017). Whether sewage sludge is thought as precious or problematic is dependent to quality of sewage sludge, sludge handling options and local politics. Generally, sewage sludge contains high amounts of phosphorus, nitrogen, organic matters and some micronutrients. At the past, presence of this valuable ingredients made sewage sludge

cheap fertilizer and it was used in agriculture. On the other hand, presence of heavy metals, pathogens, emerging organic contaminants and xenobiotics like fragrances, antibiotics, antiseptics, hormones make sewage sludge unsuitable for land applications. Therefore, sewage sludge management becomes to be an important issue (Thomsen et al., 2017a).

There are some methods for the management of sewage sludge. These are, use of sewage sludge in agriculture and soil reclamation, thermal processes, use of processed sewage sludge in construction industry, use of sewage sludge in raw materials recovery. Usage of sewage sludge for agricultural purposes has some disadvantages because of the hazardous ingredients as mentioned before. Thermal processes are the most widely used sewage sludge management methods. Because inside all of the management methods, incineration has the advantages of volume reduction, stabilization and harmlessness. Usage of processed sewage sludge like ash in construction or in raw materials recovery also can be other options (Cieřlik et al., 2015; Zhu et al., 2015).

Thermal sewage sludge management can be applied by pyrolysis, thermal gasification and incineration methods. All these methods applied for thermal conversion of sewage sludge produces one or more ash and/or char fractions. The quality and quantity of these products depend on the processed sewage sludge characteristics and process conditions (Thomsen et al., 2017b).

Pyrolysis is a thermal organic matter decomposition in the lack of oxygen or in the presence of significantly lower oxygen than needed for complete combustion. Pyrolysis is generally realized at temperature range of 300-900°C. In this process, sewage sludge is heated in an inert atmosphere and organic matters release. After pyrolysis process, gas mixture that is rich in hydrocarbon, a liquid similar to oil and solid residue that is rich in carbon produce. In other words, products of pyrolysis are volatile fraction that consists of gasses, vapors and tar components; and carbon rich residue. This solid residue is proper for the usage as adsorbent because it has a porous structure and appropriate surface area. Gaseous fraction of the pyrolysis products include mainly hydrogen, methane, carbon monoxide, carbon dioxide and some other gases in smaller concentrations. The liquid fraction, tar and/or oil, includes substances like acetic acid, acetone and methanol. The proportions of the products depend on the conditions like

temperature, reactor residence time, pressure (Demirbas, 2009; Jindarom et al., 2007; Fytili and Zabaniotou, 2008).

Gasification is thermal decomposition of organic matters in oxygen deficiency to produce synthesis gas. This process is the combination of pyrolysis and combustion processes. In gasification process, series of complex sequential chemical and thermal sub-processes are realized. The total process is sustainable by itself and in steady conditions generally energy input is not necessary. After pyrolysis of sewage sludge, produced condensable and non-condensable vapors and char are subjected to gasification process. In this process, concurrently oxidation and reduction to permanent gases take place, solid or liquid carbon containing materials are partially oxidized to fuel gases (synthesis gas, producer gas) like CO, H₂, CH₄ and lighter hydrocarbons in association with CO₂ and N₂. This gas can be burnt to produce process heat or steam, or can be used in the production of electricity by gas turbines. Solid products mostly ash, sometimes char coal, produces during the solidification of mineral substances. Liquid products called as tar form as a result of condensation of the contaminants that are inside the gas. Drawbacks of gasification process are the tar formation that makes this process complex and costly; and the accumulation of the heavy metals that are inside processed sewage sludge in final residue (Demirbas, 2009; Töre and Kar, 2017; Murakami et al., 2009; Fytili and Zabaniotou, 2008). Schematic example of gasification process is given in Figure 1.29.

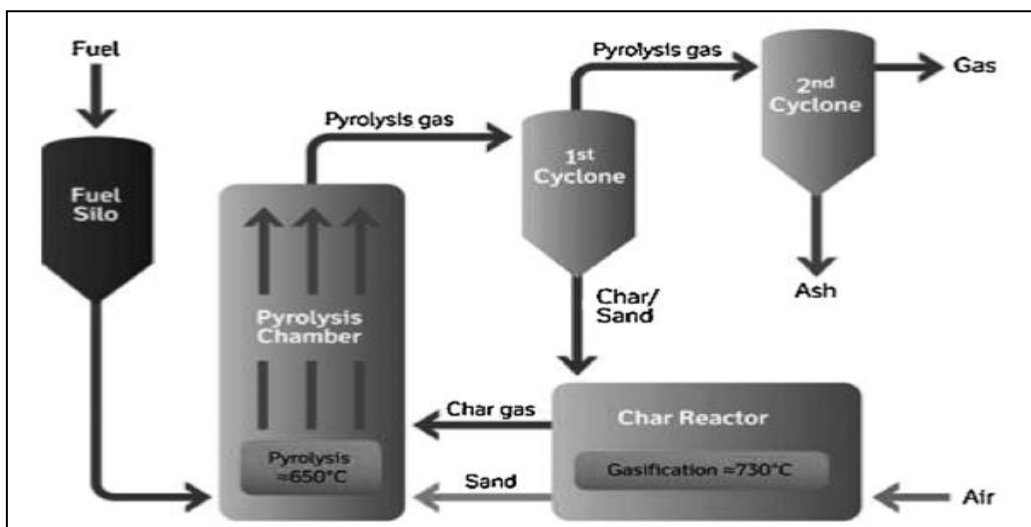


Figure 1.29. Schematic example of gasification process (Viader et al., 2015)

Incineration process reduces the volume and mass of the sewage sludge by approximately 70% and 90%, respectively and produces sewage sludge ash. Significant volume reduction achieved by incineration process makes this process one of the most convenient processes for the produced sewage sludge. 10 Mt dry mass sewage sludge is produced annually in 28 European countries and 22% of this sludge is incinerated. While Netherlands and Switzerland incinerate their all sewage sludge, Germany incinerates 55% of their sewage sludge (Lynn et al., 2015; Herzel et al., 2016).

The major difference between the incineration and pyrolysis is the presence and absence of oxygen. In incineration process, there is a combustion with excess amounts of oxygen at high temperatures and there is a recovery of heat usually that is used for different purposes. However, pyrolysis is realized in oxygen limited conditions and lower temperatures (500°C) compared with incineration which provides lower heavy metal concentrations in pyrolysis gas (Kleemann et al., 2017).

In incineration process organic matter is combusted, CO₂ and other trace gases form. Sewage sludge incineration produces inorganic sewage sludge ash. This ash is removed from produced gases and further managed (Donatello and Cheeseman, 2013). Modern fluidized bed reactors are widely used for the incineration of sewage sludge. In Figure 1.30, schematic of typical fluidized bed sewage sludge incineration process is shown.

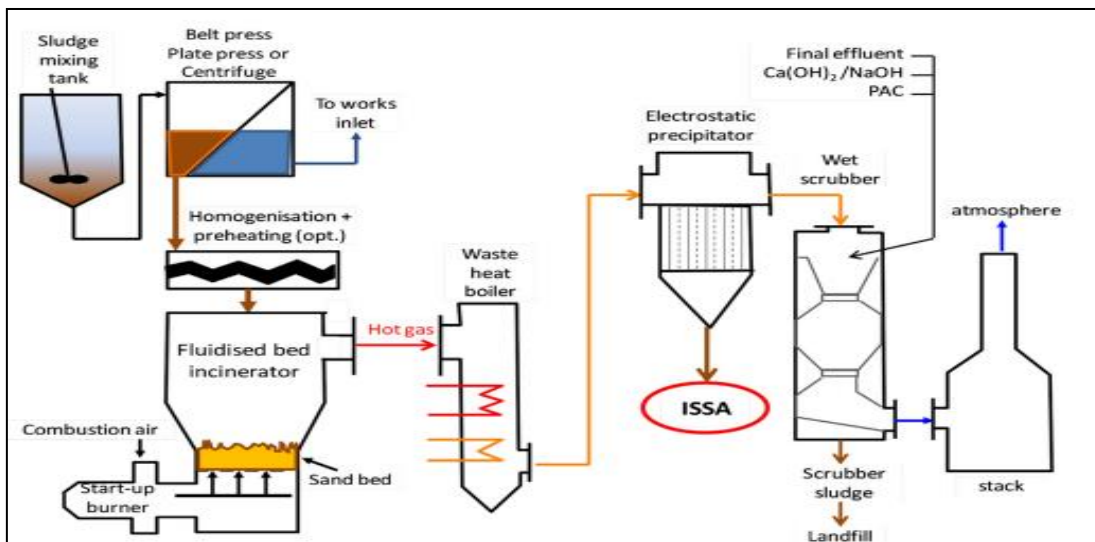


Figure 1.30. Schematic of sewage sludge incineration in fluidized bed reactor (Donatello and Cheeseman, 2013)

In incineration process, sewage sludge and hot compressed air (500-600°C) are given to the combustion chamber. The temperature at the sand bed is typically 750°C and the temperature at the overhead freeboard zone is 800-900°C. Control of the temperature can be achieved by injection of water or liquefied gas oil. The sand bed stabilizes the fluctuations in temperature. The residence time of the particles at the combustion chamber is around 1-2 second and during this residence water evaporates, volatile metals vaporize and organic materials combust completely to gases. The ash produced after incineration is usually passed through a heat exchanger and removed by bag filters, electrostatic precipitators or cyclones. The flue gas is treated with acid, alkali and activated carbon dosing to meet emission limits (Donatello and Cheeseman, 2013).

Advantages of the incineration process are large reduction in volume of the sewage sludge, thermal destruction of pathogens, minimization of odors, recovery of renewable energy. Besides these advantages, drawback of the incineration process is the presence of heavy metals inside; because ash is potential hazardous waste and further processes are needed for the disposal (Samolada and Zabaniotou, 2014).

1.8. Sewage Sludge Ash

Sewage sludge incineration is well approved technology and there are hundreds of incineration plants in the worldwide; annual sewage sludge ash production reaches to 1.7 million tons in the world (Ottosen et al., 2016). Although this amount can be significantly lower than municipal solid waste production, it is still considerable at a local levels and its treatment can be necessary according to environmentally acceptable levels. Also, sewage sludge ash can be used sustainably as secondary materials. For this purpose, sewage sludge ash is used in construction industry and recovery of some metals and phosphorus (Lynn et al., 2015; Cieřlik et al., 2015).

1.8.1. Sewage sludge ash characteristics

Analysis of sewage sludge ash shows that quartz (SiO_2) and hematite (Fe_2O_3) are the most abundant minerals inside the ash. Also, it contains many other iron oxides, iron phosphates, aluminum phosphates and calcium phosphates in lower amounts. When it is analyzed elementally; Si, Ca, Fe, Al and P are the most plentiful elements inside the

ash. Contents of the Fe and Al are mostly dependent on the presence of chemical phosphorus removal that is based on usage of iron and aluminum salts. Besides these elements, ash also contains some toxic trace elements like Cu, Cr, Cd, Ni, Pb and Zn (Lynn et al., 2015; Donatello and Cheeseman, 2013). Table 1.11 shows the mean concentrations and standard deviations (S.D.) of toxic and non-toxic elements.

Table 1.11. Concentrations of toxic and non-toxic elements inside the sewage sludge ash (Lynn et al., 2015)

Element	Sample number	Mean (mg/kg)	S.D. (mg/kg)
<u>Toxic</u>			
Fe	23	68454	52037
Al	22	44885	27053
Zn	54	3355	4360
Cu	56	2260	3701
Ba	8	1997	725
Cr	47	750	1292
Sr	5	435	171
Pb	52	373	502
Ni	39	290	420
V	7	251	228
Co	8	200	227
Se	6	96	208
Sb	5	51	23
As	14	38	68
Cd	42	24	77
Hg	15	3	3
<u>Non-toxic</u>			
Si	8	113368	69872
P	21	60697	42802
Ca	15	54493	24451
Na	11	17126	26002
Mg	12	13894	6097
K	9	9756	3694
Ti	7	3344	3592
Mn	17	1404	831
Cl	19	434	533
Zr	7	378	296
Sn	7	182	187
Ag	9	166	129

Table 1.12 shows the physical-chemical characteristics of the sewage sludge ash from the literature. Investigations about the sewage sludge ash have shown that pH of the sewage sludge ash is alkaline. Also, loss on ignition values which are the measure of the unburned carbon content are generally below 3% and this shows the effective combustion of the sewage sludge (Donatello and Cheeseman, 2013).

Table 1.12. Physical-chemical characteristics of sewage sludge ash

pH	Conductivity (mS/cm)	Water Content (%)	Loss on Ignition (550°C, %)	Reference
12.44±0.01	3.23±0.51	0.10±0.18	0.15±0.05	Guedes et al., 2014
8.85±0.03	4.81±0.13	16±0.38	0.92±0.08	Guedes et al., 2014
9.6±0.1	2.8±0.2	-	0.5±0.05	Ottosen et al., 2016
12.4±0.1	10.3±0.1	-	3.0±0.12	Ottosen et al., 2016
10.0±0.02	32.4±1.1	-	5.7±0.06	Ottosen et al., 2014
10.3±0.3	1.69±0.04	-	0.19±0.02	Ottosen et al., 2014
9.1	2.54	-	-	Ebbers et al., 2015a

1.9. Bioleaching

Process of the biological conversion of insoluble metal compounds into water soluble forms is called as bioleaching (Schippers, 2007). This process is used for the extraction of metals from the minerals like low grade ores. Moreover its application is not restricted with the extraction of metals, it is also used for the non-metallic elements such as recovery of arsenic from medicinal realgar and solubilization of phosphorus from rock phosphate. When bioleaching of rock phosphate is compared with the chemical leaching with sulfuric acid, bioleaching has advantage of being ecologically safe and low cost (Li et al., 2016).

Bioleaching process is carried out by aerobic, acidophilic ferrous (Fe^{2+}) and/or sulfur oxidizing Bacteria or Archaea (Schippers, 2007). Most widely used organisms are the *Acidithiobacillus ferrooxidans* and *Acidithiobacillus thiooxidans* (Wen et al., 2013).

1.9.1. Microorganisms in bioleaching

Microorganisms used in bioleaching process are the mesophilic and moderately thermophilic Bacteria and extremely thermophilic Archaea. Acidophilic microorganisms used in bioleaching process are given in Table 1.13.

Table 1.13. Acidophilic microorganisms used in bioleaching process with optimum and range of growth for pH and temperature (Schipper, 2007)

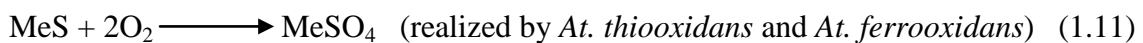
Species	Optimum pH	pH Range	Optimum Temperature (°C)	Temperature Range (°C)
Mesophilic and moderately thermophilic Bacteria				
<i>Acidimicrobium ferrooxidans</i>	~2	na	45-50	<30-55
<i>Acidithiobacillus albertensis</i>	3.5-4.0	2.0-4.5	25-30	na
<i>Acidithiobacillus caldus</i>	2.0-2.5	1.0-3.5	45	32-52
<i>Acidithiobacillus ferrooxidans</i>	2.5	1.3-4.5	30-35	10-37
<i>Acidithiobacillus thiooxidans</i>	2.0-3.0	0.5-5.5	28-30	10-37
<i>Alicyclobacillus disulfidooxidans</i>	1.5-2.5	0.5-6.0	35	4-40
<i>Ferrimicrobium acidiphilum</i>	2-2.5	1.3-4.8	37	<10-45
<i>Leptospirillum ferriphilum</i>	1.3-1.8	na	30-37	na-45
<i>Leptospirillum ferrooxidans</i>	1.5-3.0	1.3-4.0	28-30	na
<i>Sulfobacillus acidophilus</i>	~2	na	45-50	<30-55
<i>Sulfobacillus sibiricus</i>	2.2-2.5	1.1-3.5	55	17-60
<i>Sulfobacillus thermosulfidooxidans</i>	~2	1.5-5.5	45-48	20-60
<i>Sulfobacillus thermotolerans</i>	2-2.5	1.2-5	40	20-60
<i>Thiobacillus plumbophilus</i>	na	4.0-6.5	27	9-41
<i>Thiobacillus prosperus</i>	~2	1.0-4.5	33-37	23-41
<i>Thiomonas cuprina</i>	3.5-4	1.5-7.2	30-36	20-45
Mesophilic and moderately Thermophilic Archaea				
<i>Ferroplasma acidarmanus</i>	1.2	<0-1.5	42	23-46
<i>Ferroplasma acidiphilum</i>	1.7	1.3-2.2	35	15-45
<i>Ferroplasma cupricumulans</i>	1-1.2	0.4-1.8	54	22-63
Extremely thermophilic Archaea				
<i>Acidianus infernus</i>	~2	1-5.5	~90	65-96
<i>Metallosphaera prunae</i>	2-3	1-4.5	~75	55-80
<i>Sulfolobus metallicus</i>	2-3	1-4.5	65	50-75
<i>Sulfurococcus mirabilis</i>	2-2.6	1-5.8	70-75	50-86
<i>Sulfurococcus yellowstonensis</i>	2-2.6	1-5.5	60	40-80
na: data not available.				

Acidithiobacillus species can make the conversion of insoluble metal sulfides from the solid materials like minerals, ores, wastes to soluble metal sulfates. They can realize this conversion by oxidation reaction and production of sulfuric acid. All of the acidophilic metal sulfide oxidizing microorganisms oxidize ferrous and/or sulfur compounds and most of these organisms are chemolithoautotrophic (Schippers, 2007; Fang and Zhou, 2006).

As it is mentioned before most important bioleaching microorganisms are the *Acidithiobacillus ferrooxidans* and *Acidithiobacillus thiooxidans*. Both of these bacteria are gram negative chemolithoautotrophs and their carbon source is CO₂. *Acidithiobacillus ferrooxidans* derive the energy from the oxidation of ferrous ions, several sulfur compounds like elemental sulfur, thiosulfate, trihionate, sulfide. *Acidithiobacillus thiooxidans* derive the energy from the sulfur compounds like elemental sulfur, thiosulfate and tetrathionate (Schippers, 2007; Fang and Zhou, 2006).

1.9.2. Mechanisms of bioleaching

Mechanisms of bioleaching process have been distinguished as ‘direct’ and ‘indirect’ bioleaching. In the case of ‘direct’ bioleaching, there is a direct contact between the bacteria and the metallic sulfide, thus metallic sulfide is directly oxidized to soluble metal sulfate by the bioleaching bacteria. Reactions for the direct mechanism for *Acidithiobacillus thiooxidans* and *Acidithiobacillus ferrooxidans* are as follows:

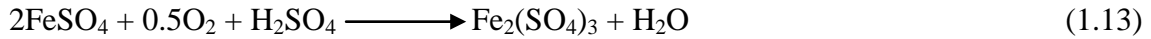


where Me is the metal.

In the case of indirect bioleaching, bacteria does not need to be in contact with the mineral surface. While in indirect bioleaching by *Acidithiobacillus thiooxidans* realize oxidation of elemental sulfur or reduced sulfur compounds to sulfuric acid; indirect bioleaching by *Acidithiobacillus ferrooxidans* realize oxidation of ferrous to ferric ion and ferric ion goes into a chemical reaction. Reaction for the indirect mechanism for *Acidithiobacillus thiooxidans* is as follows:



Reactions for the indirect mechanism for *Acidithiobacillus ferrooxidans* are as follows:



where MeS is the metal sulfide and Me^{2+} is soluble metallic ion.

In reactions (1.12) and (1.13), *Acidithiobacillus* take active part. However, reaction (1.14) realizes chemically without any involvement of bacteria. Sulfuric acid production decreases the pH and metal solubilization increases (Pathak et al., 2009).

Similar to other processes that include living constituents, bioleaching process is affected from physical-chemical, environmental and biological factors. These factors are given in Table 1.14.

Table 1.14. Factors affecting bioleaching process (Pradhan et al., 2008)

Factor	Parameters affecting bioleaching
Physical and chemical parameters	Temperature, pH, redox potential, CO ₂ and O ₂ content, nutrient availability, homogenous mass transfer, Fe(III) concentration, presence of inhibitors, etc.
Biological parameters	Microbial diversity, population density, microbial activities, metal tolerance, spatial distribution of microorganisms, attachment to ore particles, adaptation abilities of microorganisms and inoculum
Ore characteristics	Composition, mineral type, acid consumption, grain size, mineral dissemination, surface area, porosity, hydrophobic galvanic interactions and formation of secondary minerals

Temperature is the one of the factors that affects bioleaching process, because microorganisms need their optimum temperature to work actively. At the temperatures below the optimum, bacteria become to be inactive and at the temperatures above the optimum, bacteria destroy. Another important factor for the bioleaching is the pH

because pH affects both the growth of the microorganisms and solubilization. Aeration is also important for bioleaching. Because bioleaching bacteria are mostly chemolithotrophic and aerobic, aeration supply both O₂ and CO₂ to bioleaching systems. Carbon dioxide inside the air is the carbon source of the bioleaching bacteria for biomass generation (Pradhan et al., 2008; Pathak et al., 2009).

1.9.3. Studies about bioleaching

Bioleaching is a process that is used for different purposes like phosphorus leaching from phosphate rock, heavy metal removal from sewage sludge and copper leaching from chalcopyrite (CuFeS₂). Some example studies about these are as follows:

In the study of Priha et al. (2014), they have evaluated the bioleaching of phosphorus from fluorapatites with using iron and sulfur oxidizing bacteria. For this purpose, they have performed batch experiments in erlenmeyer flasks at 30°C, 140 rpm in shaker for 21 days. At the end of this experiment they have obtained 97% phosphorus leaching from low grade fluorapatite ore.

In the study of Xiao et al. (2011), they studied the solubilization of phosphorus from rock phosphate with using moderately thermophilic and mesophilic sulfur oxidizing bacteria (*Acidithiobacillus caldus* and *Acidithiobacillus thiooxidans*). Batch experiments were performed in flasks at pH 2.5 and flasks were shaken under 160 rpm at 30°C and 45°C for *A. thiooxidans* and *A. caldus*, respectively. At the end of the 20 days of bioleaching experiments, they have seen that solubilization of phosphorus with thermophiles was more effective than with mesophiles and while *A. caldus* achieved phosphorus solubilizing rate of 27.6%, *A. thiooxidans* achieved phosphorus solubilizing rate of 25.2%.

In the study of Chi et al. (2006), they have studied the bioleaching of phosphorus from rock phosphate by *Acidithiobacillus ferrooxidans* and they have investigated the effects of dosage of rock phosphate, dosage of pyrite, culture temperature and time on the phosphorus leaching. After the bioleaching experiments, they have concluded that when dosage of rock phosphate is increased, fraction of the leached phosphorus decreases sharply. Increase in pyrite dosage from 0 to 30 g/L showed positive effect on

phosphorus leaching because pyrite supplied energy for *A. ferrooxidans*. However, further increase of pyrite from 30 g/L to 50 g/L affected phosphorus leaching in a negative way. Because excess pyrite decreases the contact between the solvent and the rock phosphate. They have also investigated the effect of temperature on bioleaching process with changing temperature between 5 to 44°C and they have concluded that optimum temperature is 30°C and further increase after 30°C decreases the phosphorus leaching. Lastly, they have reported that when culture time was increased, leached phosphorus fraction increased also.

In the study of Li et al. (2016), they have investigated the effects of energy source and leaching method on bioleaching of rock phosphate. For this purpose, they have used *Acidithiobacillus ferrooxidans*. As energy source, they have used ferrous iron and/or sulfur. Experiments were performed in 250 mL flasks in a rotary shaker at 150 rpm, 30°C. After 20 days of incubation, lowest pH was obtained as 0.99 from the experiments at which both ferrous iron and sulfur were used for energy source. While experiments realized with ferrous iron reached the lowest pH of 1.19, experiments with sulfur reached the pH of 1.14. In this study, they have also investigated the effect of pre-cultivation on rock phosphate bioleaching. In the experiments with pre-cultivation, rock phosphate was added to cultures that was incubated 20 days, however in the experiments without pre-cultivation, rock phosphate was added to inocula initially. The highest recovery percentage of phosphorus was achieved with the pre-cultivated ferrous and sulfur fed culture as 76.75% after 4 days of leaching. Therefore, they have concluded that usage of mixed energy source enhances the phosphorus solubilization and also pre-cultivation has positive effect on it. Because unfavorable impacts of the some elements inside the mineral on activity of bacteria can be lowered with pre-cultivation.

In the study of Wen et al. (2013), their aim was to investigate bioleaching of some heavy metals (Cr, Pb, Zn, Cu) from sewage sludge. For this purpose, they have used iron oxidizing microorganisms. Experiments were performed in a gyratory incubator at 30°C, 150 rpm. After 12 days of bioleaching with 2% solid concentration, 20 g/L $\text{FeSO}_4 \cdot 7\text{H}_2\text{O}$ and 10% inocula concentration; they have obtained the removal of 88.5%, 79.9%, 33.2% and 50.1% for Zn, Cu, Pb and Cr, respectively.

In the study of Feng et al. (2012), they have studied the bioleaching of chalcopyrite. For this purpose, firstly they have isolated the mesophilic, extremely acidophilic sulfur oxidizing bacteria from industrial bioleaching heap and they have performed experiments with pure cultures and mixed cultures. After 31 days of bioleaching, they have obtained copper recovery of 60.1%.

In the study of Zimmermann and Dott (2009), they have studied the recovery of phosphorus from sewage sludge ash by sequenced bioleaching and bioaccumulation process. For this purpose, they have used newly developed bacteria population named as AEDS (*Acidithiobacillus sp.* enriched digested sludge). In this study, they have used *Acidithiobacillus sp.* to release the phosphorus inside the sewage sludge ash and used poly-P-accumulating organisms (PAOs) to recover released phosphorus and separate from heavy metals by the accumulation inside the bacteria. AEDS population enrichment was achieved by the incubation of the digested sewage sludge with elemental sulfur for 15 days at 22°C. Lab-scale bioleaching reactor was used to realize the experiments. They have used 25 mL/min constant flow of the media, 500 mL of medium volume, 20 L/min ambient air aeration and ash amount of 2 g. Bioleaching experiments were lasted 11 days. They have achieved, 66% of phosphorus release from sewage sludge ash with AEDS population and this population was accumulated 66% of the released phosphorus. Thus, phosphorus was recovered and separated from heavy metals. They have also obtained 93% of phosphorus release with mixed culture of *Acidithiobacillus ferrooxidans* and *Acidithiobacillus thiooxidans*. Metal extraction percentages for mixed culture for Fe, Al, Cu, Zn, Cr and Co were 16, 61, 41, 20, 13 and 34%, respectively.

1.10. Electrodialysis

Electrodialysis is an electrochemical separation process in which application of electric current causes transfer of ions through ion exchange membranes. Electrochemical processes are applied for many purposes in separation and reuse like obtaining drinking water, salt removal from sea water, acid separation and concentration, metal salts recovery from industrial wastewater and phosphorus recovery from sewage sludge and sewage sludge ash (Valero et al., 2011; Altin et al., 2017; Ebberts et al., 2015b; Ottosen et al., 2014).

In electro dialysis process there are at least 4 components. These are direct current supply, electrodes, ion exchange membranes, and electrolytes. Direct current supply maintains the reinforcement for the ion transport. Moreover, by adjusting the current density, transportation rate of the ions can be controlled. Electrodes are used to conduct direct current to the system. Ion exchange membranes are used for the separation of the ions. Electrolytes are the carriers for the current between the anode and the cathode compartments (Huang et al., 2007). Figure 1.31 shows the principle of electro dialysis process.

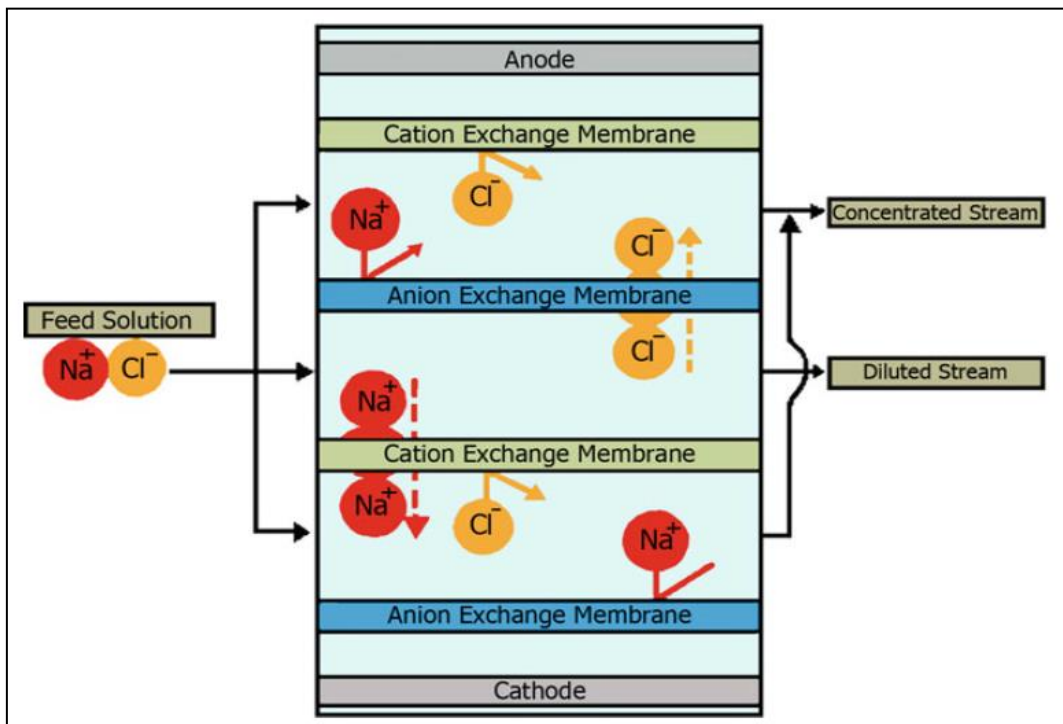


Figure 1.31. Principle of electro dialysis process (Bernardes et al., 2014)

As it is seen from the Figure 1.31, there are concentrate and dilute sections in an electro dialysis process. Application of electric current causes transportation of cations that pass through cation exchange membrane to cathode and transportation of anions that pass through anion exchange membrane to anode. Therefore, while the solution between the membranes loses its ions, solutions of anode and cathode become concentrated (Altin et al., 2017).

Applied electrical potential between the anode and cathode is the driving force for the transportation of ions. Application of an electric field to electrodes causes anode to be

positively charged and anode to be negatively charged. Then, when electric field is applied cations move to cathode, anions move to anode. Through this transportation, cations pass through cation exchange membranes but cannot pass through anion exchange membrane and vice versa for anions (Bernardes et al., 2014).

Transport rate of the ions is dependent to electric current between the electrodes. Therefore, working with high current density is desired. Ohm's Law describes the relationship between applied voltage (U) and the electric current (I).

$$U = IR \quad (1.15)$$

where R is the sum of the partial resistances. Total electrical resistance includes resistances of electrodes, membranes and solutions (Káňanová et al., 2014; Bernardes et al., 2014).

1.10.1. Ion exchange membranes

Three types of ion exchange membranes are used in electro dialysis process. These are anion exchange membranes, cation exchange membranes and bipolar membranes. These membranes can be used in electro dialysis either separately or in combination (Huang et al., 2007).

Anion exchange membranes are conductive electrically and they allow only the passage of negatively charged ions. Cation exchange membranes also have similar properties and they allow only the passage of positively charged ions. Both anion and cation exchange membranes have similar properties like low electrical resistance, being insoluble in aqueous solutions, being semi-rigid for easy assembling of stack, being resistant to changes in pH from 1 to 10, being resistant to high temperatures (Valero et al., 2011).

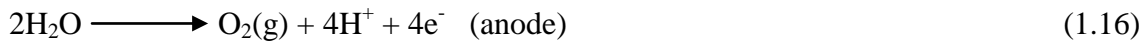
Bipolar membranes are composed of cation selective layer and anion selective layer. For this reason, it can be thought as combination of anion exchange and cation exchange membranes. The difference of the bipolar membranes from the monopolar membranes is the ability of the dissociation of solvent molecules under the reverse potential (Huang et al., 2007).

1.10.2. Electrodes and electrode reactions

Metal electrodes placed to the each end of the membrane stack to conduct the direct current to stack. Carbon, platinum or titanium electrodes are used as electrodes because they are inert and usage of these materials avoids interferences in electrode reactions. Generally platinum coated titanium electrodes are used because anode compartment has the corrosive nature (Valero et al., 2011; Gonçalves, 2015). Another reason for the plating titanium with precious metals or their oxides is the formation of non conductive oxide film especially at anode side. Because this film is non conductive, when it is used without coating, the anodic current is interrupted and even at high voltages anode is passivated (Bewer et al., 1982).

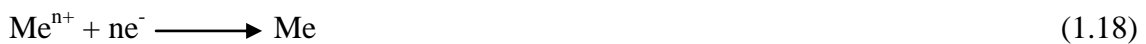
Driving force for the ion migration is maintained from the oxidation and reduction reactions that take place at the anode and cathode because these reactions actualize transformation from ionic conduction to electron conduction (Huang et al., 2007).

The main reaction that takes place with the application of electric current is the electrolysis of water. Reactions for anode and cathode are as follows:



As it is seen from Equations (1.16) and (1.17), while anode reactions produce acid, cathode reactions produce base.

If concentrations of metals increase in cathode solutions, metals can precipitate on the electrode surface:



where Me is a metal.

If chlorides are present in anolyte solution, production of chlorine gas can be realized, therefore precautions should be taken.



Solutions are circulated near the electrodes to prevent formation of concentration gradients and to remove gasses produced because of the electrode reactions. Electrode reactions also cause change in pH (Magro, 2014; Gonçalves, 2015).

1.10.3. Transport mechanisms

Transport mechanisms under the impact of electrical field are electromigration (ion transportation in the solution), electroosmosis (fluid transportation through the pores), electrophoresis (transportation of charged particles) and diffusion (Pedersen et al., 2016). Schematic presentation of these mechanisms is given in Figure 1.32.

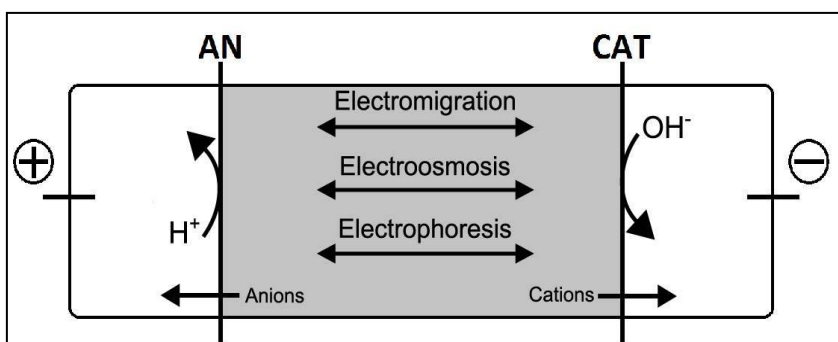


Figure 1.32. Schematic presentation of transport mechanisms in electro dialysis (AN: Anion exchange membrane, CAT: Cation exchange membrane) (Gonçalves, 2015)

Electromigration is the movement of ions and ion complexes to the electrodes of opposite charge under the applied electric field and this is the most important mechanism for the transportation of charged species. Electromigration causes movement of anions to anode and cations to cathode.

Electroosmosis is the movement of the ionic solution under the applied electric field. Application of electric field causes transportation of ions to the electrode of opposite charge and during this transportation, ions carry their water of hydrogen.

Electrophoresis is the transportation of charged particles (like colloids, clay particles, organic particles) under the applied electric field. Electrophoresis realizes rarely.

Diffusion is the movement of the ions because of the concentration gradient that forms because of the mass transfer caused by electric field. Diffusion realizes where concentration gradient is high (Sun, 2013; Gonçalves, 2015).

1.10.4. Studies about electrodialysis

In the study of Guedes et al. (2014), they have evaluated the possibility of recovery of phosphorus from 2 different sewage sludge ashes and separation from heavy metals with the application of electrodialysis process. For this purpose, they have used 3-compartment electrodialysis cell that was shown in Figure 1.33. Platinum coated electrodes and a power supply that maintains constant current of 50 mA were used. For the extraction purpose, 0.08 M H_2SO_4 was used in the ratio of 1:10 (mass:volume).

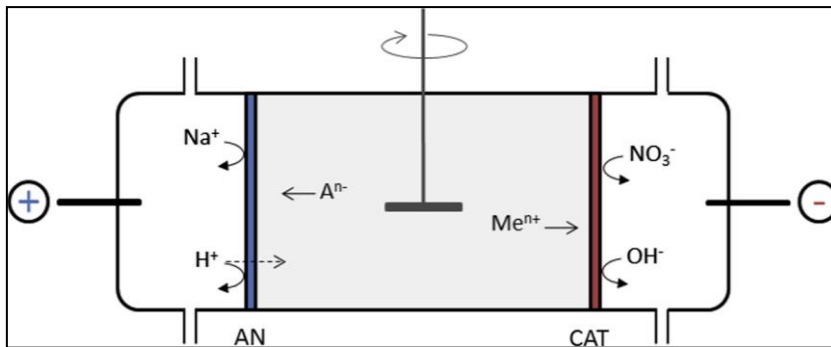


Figure 1.33. 3-compartment electrodialysis cell (Guedes et al., 2014)

During the experiments of electrodialysis, they have seen decrease in pH in central compartment which increases the solubilization. This pH decrease was caused by water splitting at the anion exchange membrane which supplies H^+ ions to the central compartment. Moreover, dissolution of ash particles caused increase in conductivity.

After 7 days, phosphorus passage to anode side was 20%. However, after 14 days, it increased to 59% and 69% for two different sewage sludge ashes. Moreover, they have also seen passage of phosphorus to cathode side with the percentages of 17% and 12%. This was because of the reaction of phosphorus with some species and formation of positively charged compounds. Also, they have obtained highest heavy metal removal efficiency for Cu (79% and 82%). While removal percentages of Zn, Al and Cd were

approximately 50%, removal efficiencies for Fe and Pb were approximately 6% which shows the presence of strong bond between these metals and less soluble particles.

In the study of Ebbbers et al. (2015a), they have studied the recovery of phosphorus from sewage sludge ash with electro dialysis. For this purpose, they have used 2-compartment and 3-compartment electro dialysis cells and have compared them. Figure 1.34 shows the 3-compartment and 2-compartment electro dialysis cells. The difference between the 3-compartment and 2-compartment electro dialysis cells was the exclusion of anion exchange membrane and the placement of anode to the direct contact with the suspension. To extract phosphorus from sewage sludge ash, 0.19 M H_2SO_4 was used with the liquid to solid ratio of 10. Experiments were lasted 14 days and 50 mA direct current was used throughout the experiments.

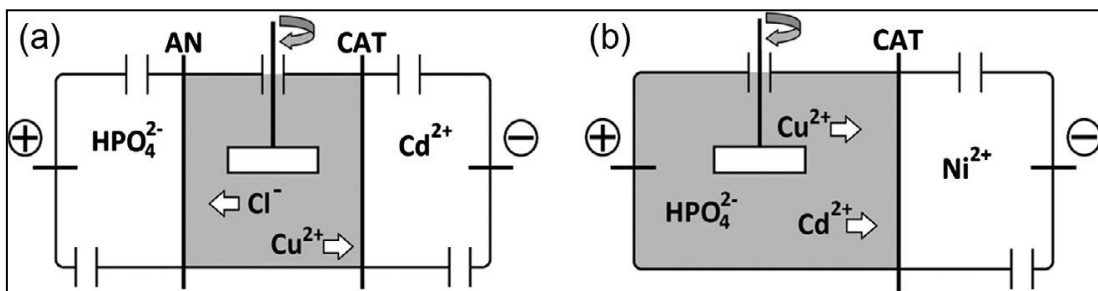


Figure 1.34. Schematic of (a) 3-compartment and (b) 2-compartment electro dialysis cells (Ebbbers et al., 2015a)

After the experiments, they have seen that pH decrease in 2-compartment electro dialysis cell is faster than 3-compartment cell. This is because of the reaction that takes place at the anode compartment. Dissolution of phosphorus from sewage sludge ash in the 2-compartment cell was 93% and 96% after 7 and 14 days, respectively. In 3-compartment cell, this was 90% and 95% after 7 and 14 days, respectively. In 3-compartment cell, percentage of phosphorus at the anode was 49% and 50% after 7 and 14 days, respectively. Moreover, 7% of the total phosphorus was found at the cathode side because of the positively charged phosphorus complexes like $\text{CrH}_2\text{PO}_4^{2+}$ and $\text{NiH}_2\text{PO}_4^+$. When dissolution of metals is considered, it was seen that dissolution was faster in 2-compartment cell.

2. MATERIAL AND METHOD

The major aim of this study was the recovery of the phosphorus from sewage sludge ash. For this purpose, bioleaching process was used to obtain phosphorus rich solution from sewage sludge ash. After this step, separation of the heavy metals from phosphorus rich solution was realized with electro dialysis.

In the scope of this MSc Thesis, recovery of phosphorus from sewage sludge ash was achieved by following these steps:

- Incineration of dried sewage sludge ash to obtain sewage sludge ash
- Isolation and enrichment of bioleaching bacteria from sewage sludge
- Batch bioleaching experiments
- Electro dialysis experiments.

2.1. Sewage Sludge Ash

Sewage sludge ash was obtained from the incineration of dried sewage sludge that is taken from Ambarlı Advanced Biological Wastewater Treatment Plant, at 850°C for 15 minutes and 550°C for 30 minutes. Figure 2.1 shows the photographs of dried sewage sludge and incinerated sewage sludge ash.

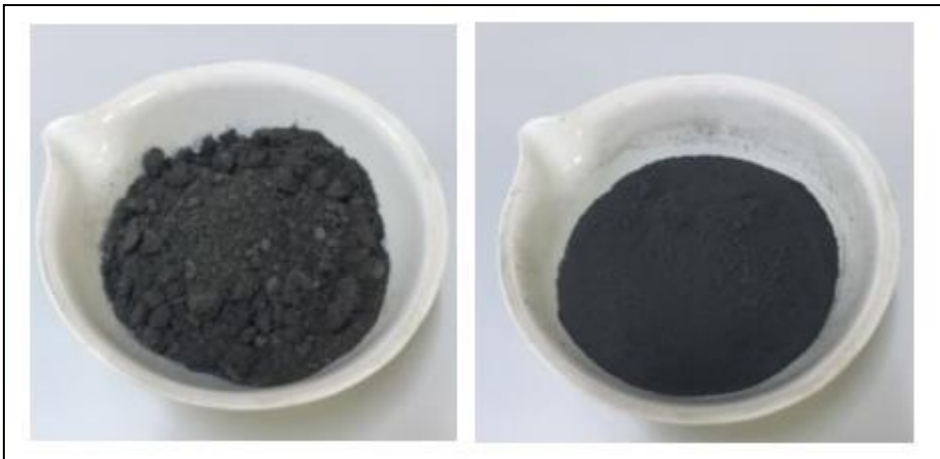


Figure 2.1. Dried sewage sludge and incinerated sewage sludge ash (from left to right)

2.1.1. Characterization of sewage sludge ash

Physical and chemical characterization of sewage sludge ash was investigated according to Guedes et al. (2014) and Ottosen et al. (2014). In this scope; pH, conductivity, loss on ignition (LoI) and water content of the sewage sludge ash were measured.

pH and conductivity of the sewage sludge ash were measured in the suspension that has been prepared in the ratio of 1:2.5 (mass of ash:volume of de-ionized water) after 1 hour of mixing. After 1 hour of mixing, pH and conductivity were measured using pH and conductivity probes. For the determination of water content, ash was waited in 105°C oven for 24 hours. From the weight loss (difference between the initial and final weights of the ash), water content of sewage sludge ash was calculated. Loss on ignition value was determined from the weight loss after 30 minutes at 550°C oven and it was calculated similar to water content.

Heavy metal and phosphorus content of sewage sludge ash were determined after acidic digestion according to USEPA METHOD 3051A (Microwave Assisted Acid Digestion of Sediments, Sludges, Soils and Oils). For this purpose, CEM Microwave-Accelerated Reaction System (MARS) equipment was used. After extraction, heavy metals were measured with Inductively Coupled Plasma- Optical Emission Spectrometry (ICP-OES) and phosphorus was measured with HACH DR2500 Spectrophotometer according to Amino Acid Method (Method 8178).

2.2. Isolation and Enrichment of Bioleaching Bacteria

Iron oxidizing and Sulfur oxidizing bacteria were isolated and enriched from waste activated sludge taken from Ambarlı Advanced Biological Wastewater Treatment Plant.

2.2.1. Isolation and enrichment of Iron oxidizing bacteria

Isolation and enrichment of Iron oxidizing bacteria were achieved according to Peng et al. (2011). 200 mL of sludge was taken into erlenmeyer flask and 20 g/L of $\text{FeSO}_4 \cdot 7\text{H}_2\text{O}$ was added as energy source. Then flask was incubated in incubator shaker (IKA KS 4000) at 28°C, 200 rpm. pH was monitored and when it dropped to 2.5, 10% (volume:volume) of the inocula was transferred to Leathen medium that contains 20 g/L $\text{FeSO}_4 \cdot 7\text{H}_2\text{O}$. The composition of Leathen medium was as follows:

- 0.45 g/L $(\text{NH}_4)_2\text{SO}_4$,
- 0.15 g/L K_2HPO_4 ,
- 0.05 g/L KCl,
- 0.5 g/L $\text{MgSO}_4 \cdot 7\text{H}_2\text{O}$,
- 0.01 g/L $\text{Ca}(\text{NO}_3)_2 \cdot 2\text{H}_2\text{O}$.

pH of the erlenmeyer flask was monitored and incubation was continued till the pH dropped to 2.5. When pH dropped to 2.5, re-inoculation was done again taking 10% of inocula to Leathen medium that contains 20 g/L $\text{FeSO}_4 \cdot 7\text{H}_2\text{O}$. Re-inoculation was repeated 4 times. Color of the solution turned to dark reddish-brown and this is the indicator of presence of Iron oxidizing bacteria. Figure 2.2 shows the photographs of enriched Iron oxidizing bacteria.



Figure 2.2. Iron oxidizing bacteria

2.2.2. Isolation and enrichment of Sulfur oxidizing bacteria

Isolation and enrichment of Sulfur oxidizing bacteria were achieved according to Zhang et al. (2009). 150 mL of sludge was taken into an erlenmeyer flask and 10 g/L elemental sulfur (S^0) was added as energy source. Then, erlenmeyer flask was incubated in incubator shaker (IKA KS 4000) at 28°C, 180 rpm till the pH dropped to below 2. When pH dropped to below 2, 7.5 mL of acidified sludge was mixed with 150 mL of fresh sewage sludge and same procedure (re-inoculation) was repeated 3 times.

After the isolation of sulfur oxidizing bacteria, Waksman liquid medium used in the study of Wen et al. (2012) was used for the enrichment of the Sulfur oxidizing bacteria.

The composition of Waksman liquid medium was as follows:

- 0.2 g/L $(\text{NH}_4)_2\text{SO}_4$,
- 3.0 g/L K_2HPO_4 ,
- 0.5 g/L $\text{MgSO}_4 \cdot 7\text{H}_2\text{O}$,
- 0.25 g/L $\text{CaCl}_2 \cdot 2\text{H}_2\text{O}$,
- 10 g/L S^0 as an energy source.

Figure 2.3 shows the photographs of enriched Sulfur oxidizing bacteria.



Figure 2.3. Sulfur oxidizing bacteria

2.3. Bioleaching Experiments

Bioleaching experiments were performed in 250 mL erlenmeyer flasks in incubator shaker (IKA KS 4000) at 30°C, 180 rpm to optimize the conditions (ash amount, inocula volume, sulfur amount) for bioleaching and to obtain maximum phosphorus leaching from sewage sludge ash. Figure 2.4 shows the bioleaching experiments performed in incubator shaker.

During all these bioleaching experiments; pH and conductivity of the samples were measured using pH and conductivity probes. Also, concentrations of sulfate and phosphate were measured using spectrophotometer with proper dilutions. Bioleaching experiments were realized in the order that was shown in Figure 2.5.



Figure 2.4. Bioleaching experiments performed in incubator shaker

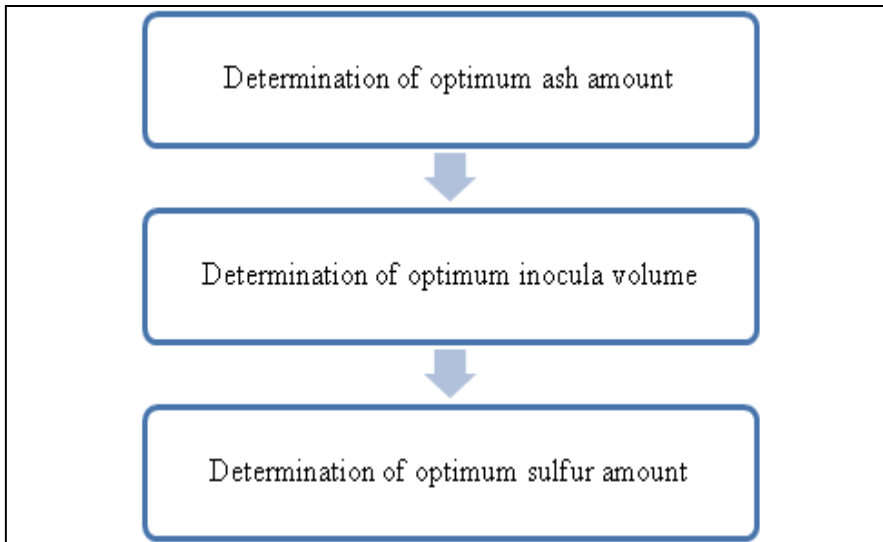


Figure 2.5. Performed bioleaching experiments

Bioleaching experiments were performed with only Sulfur oxidizing bacteria, with only Iron oxidizing bacteria and with the mixture of Sulfur and Iron oxidizing bacteria. In some of the bioleaching experiments, pH was adjusted to initialize the bioleaching at the pH that is optimum for the bacteria. pH adjustment for the trial realized with only Iron oxidizing bacteria was done with 1M HCl while for the trials realized with Sulfur oxidizing bacteria and mixture of Sulfur&Iron oxidizing bacteria pH adjustments were done with 1M H₂SO₄.

Besides the bioleaching experiments realized with the bacteria, control experiments were also conducted to see the effects of the presence of the bacteria. In the control

group experiments, the only difference was the absence of the bacteria; all of the other parameters were same with the others.

For the first trial of bioleaching experiment sequence of the steps was as follows:

- Addition of medium and bacteria
- pH adjustment
- Addition of ash.

For the other bioleaching trials sequence of the steps was as follows:

- Addition of medium and bacteria
- Addition of ash
- pH adjustment (if applied).

Table 2.1 shows the performed bioleaching experiments to determine optimum ash amount and the other information about these experiments.

Table 2.1. Experiments performed for the determination of optimum ash amount

	Trial with Iron Oxidizing Bacteria	Trial with Sulfur Oxidizing Bacteria	Trial with Mixture of Sulfur&Iron Oxidizing Bacteria
Ash Amount (g)	2, 4, 6, 8, 10	2, 4, 8	2, 4, 8
Initial pH	2.5	7	2.5
Inocula Volume (%)	10	20	20
Inocula Volume (mL)	20	40	40
Total Volume (mL)	200	200	200
Temperature (°C)	30	30	30
Shaking Speed (rpm)	180	180	180
Duration (days)	48	29	29
Control Ash Amount (g)	2, 4, 6, 8, 10	2	2
Energy Source	FeSO ₄ ·7H ₂ O	S ⁰	FeSO ₄ ·7H ₂ O and S ⁰
Energy Source Amount (g/L)	20	10	20 and 10

After the determination of optimum ash amount, experiments were performed to find the optimum inocula volume. For this purpose, experiments that were shown in Table 2.2 were realized with the ash amount that was found from previous experiments.

Table 2.2. Experiments performed for the determination of optimum inocula volume

	Trial with Sulfur Oxidizing Bacteria	Trial with Mixture of Sulfur&Iron Oxidizing Bacteria
Inocula Volume (%)	25, 30, 35, 40	25, 30, 35, 40
Inocula Volume (mL)	50, 60, 70, 80	50, 60, 70, 80
Ash Amount (g)	2	2
Initial pH	not adjusted	not adjusted
Total Volume (mL)	200	200
Temperature (°C)	30	30
Shaking Speed (rpm)	180	180
Duration (days)	29	29
Energy Source	S ⁰	FeSO ₄ ·7H ₂ O and S ⁰
Energy Source Amount (g/L)	10	20 and 10

After the determination of optimum inocula volume, experiments were performed to find the optimum amount of sulfur for Sulfur oxidizing bacteria. For this purpose, experiments that were shown in Table 2.3 were realized with the inocula volume that was found from previous experiments.

Table 2.3. Experiments performed for the determination of optimum sulfur amount

Trial with Sulfur Oxidizing Bacteria	
Sulfur amount (g/L)	10, 15, 20, 25
Inocula Volume (%)	40
Inocula Volume (mL)	80
Ash Amount (g)	2
Initial pH	not adjusted
Total Volume (mL)	200
Temperature (°C)	30
Shaking Speed (rpm)	180
Duration (days)	29

After these trials performed in erlenmeyer flasks, 1 trial of bioleaching experiment was realized in 2 L reactor at the optimum conditions obtained from the previous experiments. This trial was actualized with Sulfur oxidizing bacteria. Conditions for this experiment are given in Table 2.4.

Table 2.4. Conditions for 2 L batch bioleaching experiment

Trial with Sulfur Oxidizing Bacteria	
Sulfur amount (g)	20
Inocula Volume (%)	40
Inocula Volume (mL)	80
Ash Amount (g)	20
Initial pH	not adjusted
Total Volume (mL)	2000
Temperature (°C)	30
Mixer speed (rpm)	180
Duration (days)	30

2.4. Electrodialysis Experiments

For the separation of dissolved heavy metals from the dissolved phosphorus after bioleaching process, electrodialysis process was applied. These experiments were performed with a synthetic solution that contained phosphate (2000 mg/L K_2HPO_4 solution) and with solutions that were obtained from bioleaching of sewage sludge ash. The bioleaching solution was filtered from 1 μm filter paper prior to electrodialysis experiments to remove solid particles and to prevent membrane fouling.

Electrodialysis studies were realized in 3-compartment glass electrodialysis reactor. The diameter of the reactor was 10.5 cm and the length of the reactor was 20 cm. Lengths of the electrode compartments were 5 cm. Figure 2.6 shows the electrodialysis reactor and the system. 0.01M $NaNO_3$ solution was used as anolyte and catholyte solutions after its pH was adjusted to below 2 (Ebbbers et al., 2015a; Guedes et al., 2014; Ottosen et al., 2014). During the operation of the electrodialysis system, pH of the anolyte and catholyte were also measured and adjusted to 2 especially for the catholyte to prevent precipitation. The volumes of the anolyte and catholyte were 1000 mL and they were circulated via Watson-Marlow SCI 323 peristaltic pump with flow rate of 20 mL/minute. The reasons for the circulation of the electrolyte solutions were the removal of the gases produce at the electrodes and also prevention of the high concentration profiles close to membranes (Ebbbers et al., 2015a). Moreover, Heidolph RZR 2020 mechanical mixer was used to mix the middle part of the electrodialysis reactor and the rotational velocity of the mixer was 60 rpm.

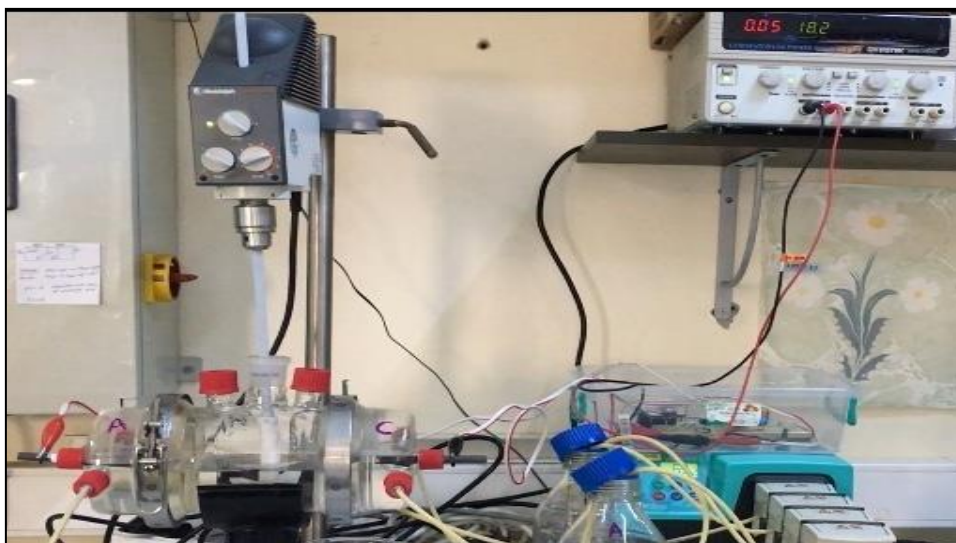


Figure 2.6. Electro dialysis reactor and system

Summary table for the performed electro dialysis experiments were given in Table 2.5.

Table 2.5. Performed electro dialysis experiments

Middle part solution	Electrodes	Volume of electrolyte solutions (mL)	Volume of middle part solution (mL)
Synthetic phosphate containing solution	Gold coated copper	1000	600
Bioleaching solution	Gold coated copper	1000	600
Bioleaching solution	Graphite	1000	600

At the end of the electro dialysis experiments, mass balances were done for the phosphorus to see the distributions on the different parts of the electro dialysis reactor. For this purpose, membranes and mechanical mixer were waited in 1 M HNO₃, solutions of the anode, cathode and middle parts were waited in 5 M HNO₃ for 1 day. After 1 day, phosphorus contents were measured and used in mass balance.

2.4.1. Electrodes

Graphite and gold coated copper electrodes were used in electro dialysis experiments. Electrodes were in rod shape with a diameter of 8 mm. Figure 2.7 shows the graphite and gold coated copper electrodes.



Figure 2.7. Graphite and gold coated copper electrodes (from left to right)

2.4.2. Anion and cation exchange membranes

Anion and cation exchange membranes used in this study were supplied from FUMATECH GmbH (fumasep[®] FKB-PK-130 and FAB-PK-130). Properties of the membranes are given in Table 2.6.

Table 2.6. Properties of the anion and cation exchange membranes

	FKB-PK-130	FAB-PK-130
Membrane type	cation exchange membrane	anion exchange membrane
Appearance/color	brown	brown
Thickness (dry) (μm)	110-140	110-130
Weight per unit area (mg/cm^2)	10-13	10-13
Ion exchange capacity (meq/g)	0.8-1.0 (as sodium form)	0.7-1.0 (as chloride form)

2.4.3. Power supply

Laboratory DC power supply from GW Instek (GPS-3303) was used to maintain 50 mA constant current from the electric circuit. Figure 2.8 shows the power supply. Voltage of this power supply ranges between 0 to 30 V, and current of it ranges between 0 to 3 A.



Figure 2.8. Power supply used in this study

2.5. Analytical Methods

2.5.1. pH and conductivity

pH of the samples were measured with benchtop pH meter (HACH-Sension 4). Conductivity of the samples were measured with a portable multi meter (HACH-HQ40D) and conductivity probe (HACH-CDC401). Also calibration of pH and conductivity probes were done periodically with standard solutions of HACH.

2.5.2. Phosphate

Phosphate concentrations of the samples were measured with spectrophotometer (HACH DR 2500) after filtering the sample from 0.45 μm syringe filter according to Amino Acid Method (Method 8178).

2.5.3. Sulfate

Sulfate concentrations of the samples were measured with spectrophotometer (HACH DR 2500) after filtering the sample from 0.45 μm syringe filter according to SulfaVer 4 Method (Method 8051).

2.5.4. Heavy metals

Heavy metals (Al, Fe, Zn, Cu, Ni, Cr, Pb, Cd) content of the sewage sludge ash, bioleaching solutions and electro dialysis solutions were determined with ICP-OES after filtering samples from 0.45 μm syringe filter. Measurements were done at Middle East Technical University Central Laboratory.

2.5.5. Calcium and Magnesium

Calcium and magnesium contents of the solutions were again determined with ICP-OES after filtering samples from 0.45 μm syringe filter. Measurements were done at Middle East Technical University Central Laboratory.

2.6. Calculations

All of the calculations were done on mass basis. The percentages of the phosphorus dissolution were calculated by dividing the mass of the soluble phosphorus after bioleaching process to mass of phosphorus inside the ash and multiplying with 100. Equation (2.1) shows the calculation of the phosphorus dissolution percentage.

$$\text{Phosphorus dissolution (\%)} = \frac{\text{mg P after bioleaching process}}{\text{mg P inside the ash}} \times 100 \quad (2.1)$$

Percentages of the phosphorus passage to the anode part were calculated from the ratio between phosphorus mass at the anode part and initial phosphorus mass at the middle part. Equation (2.2) shows the calculation of the phosphorus passage percentage to the anode part.

$$\text{Phosphorus passage to anode part (\%)} = \frac{\text{mg P at the anode part}}{\text{mg P at the middle part at day 0}} \times 100 \quad (2.2)$$

Dissolution of the heavy metals after bioleaching and also heavy metals passage to the cathode part were calculated similar to calculations done for phosphorus.

3. RESULTS AND DISCUSSION

3.1. Characterization of Sewage Sludge Ash

3.1.1. Physical-chemical characterization of sewage sludge ash

Characterization of the sewage sludge ash that was used in this study was realized. In order to characterize sewage sludge ash; pH, conductivity, water content and loss on ignition at 550°C were measured. Table 3.1 shows the pH, conductivity, water content and loss on ignition values of sewage sludge ash.

Table 3.1. Physico-chemical characteristics of the sewage sludge ash

pH	11.6±0.3
Conductivity (mS/cm)	2.04
Water Content (%)	0
Loss on Ignition (550°C, %)	0.49

pH of the sewage sludge ash was 11.6±0.3 which is alkaline and similar to pH values of sewage sludge ashes that were used in literature. For example, pH of the sewage sludge ashes used in the study of Ottosen et al. (2016) were 9.6±0.1 and 12.4±0.1; pH of the sewage sludge ashes used in the study of Guedes et al. (2014) were 12.44±0.01 and 8.85±0.03.

Conductivity of the sewage sludge ash was 2.04 mS/cm. This result was also similar to conductivity values of the sewage sludge ashes used in other studies. For example, conductivity values of the sewage sludge ashes used in the study of Guedes et al. (2014) were 3.23±0.51 mS/cm and 4.81±0.13 mS/cm.

Water content of the sewage sludge ash was found as zero, because sewage sludge ash used in this study was incinerated two times, first incineration was at 850°C for 15 minutes and the second incineration was at 550°C for 30 minutes, to be able to decrease the organic matter concentration as much as possible. Water contents of the sewage sludge ashes used in the study of Guedes et al. (2014) were 0.10±0.18% and 16±0.38%. The reason for this difference in conductivity levels might be because of the differences in the sampling. Because the value of 0.10±0.18% belonged to the ash that was sampled

immediately after incineration and the value of $16\pm 0.38\%$ belonged to the ash that was sampled from the deposit.

Loss on ignition value of the sewage sludge ash was 0.49% at 550°C . This parameter shows the unburned carbon content of the sewage sludge ash and this is generally below 3% (Donatello and Cheeseman, 2013). In the literature, there are both higher and lower values from the ash that was used in this study. For example, in the study of Ottosen et al. (2014), the loss on ignition values of the ashes were 5.7 ± 0.06 and 0.19 ± 0.02 .

The X-Ray diffraction pattern of the sewage sludge ash was shown in Figure 3.1. According to this diffractogram, ash contains quartz (SiO_2), calcium iron phosphate ($\text{Ca}_9\text{Fe}(\text{PO}_4)_7$), calcium azide ($\text{Ca}(\text{N}_3)_2$), calcium silicate hydrate ($\text{Ca}_{1.5}\text{SiO}_{3.5}\cdot x\text{H}_2\text{O}$). These are similar to results reported in the literature. Quartz, whitlockite ($\text{Ca}_3(\text{PO}_4)_2$), hematite (Fe_2O_3) were the common components of the sewage sludge ash (Donatello and Cheeseman, 2013). Also, Franz (2008) reported the hematite, calcium oxide (CaO), quartz, hydroxyapatite ($\text{Ca}_5(\text{PO}_4)_3(\text{OH})$) and iron oxide phosphate ($\text{Fe}_4(\text{PO}_4)_2\text{O}$) as the components of the sewage sludge ash. Moreover, calcium silicates are the possible components that forms after combustion.

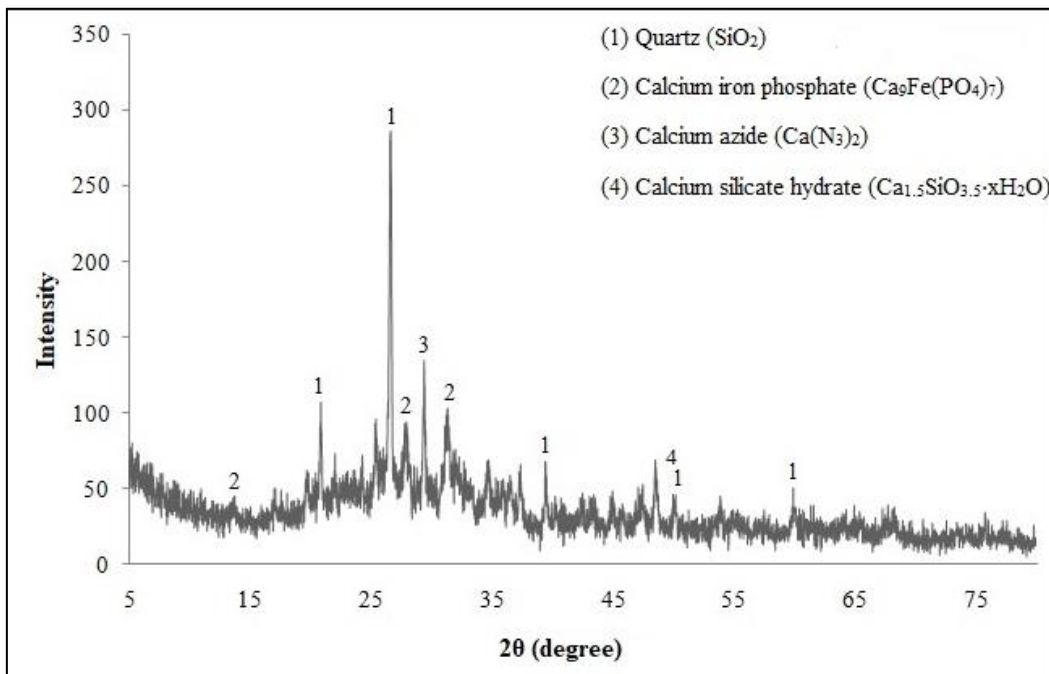


Figure 3.1. X-Ray diffractogram of the sewage sludge ash

Kleemann et al. (2017) reported the whitlockite-like compounds ($\text{Ca}_9\text{X}(\text{PO}_4)_7$) (X can be Fe, Cu, H, Al, Ni or Sr), quartz, calcite (CaCO_3) and anhydrite (CaSO_4) were the components of the sewage sludge ash. Moreover, presence of whitlockite is helpful for the phosphorus dissolution from the ash, because phosphorus easily dissolves from whitlockite under the acidic conditions (Kleemann et al., 2017).

3.1.2. Phosphorus and heavy metal content of sewage sludge ash

Phosphorus and heavy metals contents of the sewage sludge ash was given in Table 3.2 with the values from other studies for comparison. As it is seen from the Table 3.2, concentrations of the Fe and Al were higher because they are used in the chemical phosphorus removal processes. Moreover, phosphorus content of the ash used in this study was similar to ashes used in other studies.

Table 3.2. Phosphorus and heavy metals contents of the sewage sludge ashes used in other studies and this study

	Guedes et al., 2014 (mg/kg)	Lee and Kim, 2017 (mg/kg)	Kleemann et al., 2017 (mg/kg)	Petz et al., 2012 (mg/kg)	This study (mg/kg)		
P	134000	107400	57140	48770	80000	79000	82000
Zn	3335	429.7	-	-	1790	3810	2698
Fe	60000	41500	45208	42869	24000	130000	22786
Al	22600	111820	37020	30131	109000	45000	36478
Pb	293	823.9	641	704	137	239	46
Cu	758	837	1771	1416	1050	844	650
Ni	54.6	86.9	113	122	46	95	460
Cd	3.25	12.5	4	4	5	5	0
Cr	45.5	86.8	119	111	56	254	590
Ca	163000	79280	99316	103205	103000	98000	80352
Mg	-	25560	14090	13309	11000	12000	10394

3.2. Isolation and Enrichment of the Bioleaching Bacteria

Isolation and enrichment of the both Iron and Sulfur oxidizing bacteria were achieved as they were described in Section 2.2.1 and 2.2.2. During the isolation and enrichment of the both bacteria, change in pH was observed. Because these bacteria are acidophilic and produce sulfuric acid, pH decrease was observed as it should be.

pH changes for Iron oxidizing bacteria were given in Figure 3.2. Initial pH of the sludge was 6.7 and during incubation pH decreased. During the enrichment of the Iron oxidizing bacteria, start and the end of the re-inoculation periods were decided by pH decrease to 2.5. In the first inoculation period, pH reached to 2.5 after 5 days and then re-inoculation was started. The initial pH for this re-inoculation was 3 and it decreased to 2.5 after 4 days. Another re-inoculation was started. The starting pH for this re-inoculation was 3.3 and its decrease to 2.5 realized after 3 days from the start. Then last re-inoculation period was started with pH 3.2 and it lasted 3 days till pH decreased to 2.5. Total enrichment time for the Iron oxidizing bacteria was 18 days.

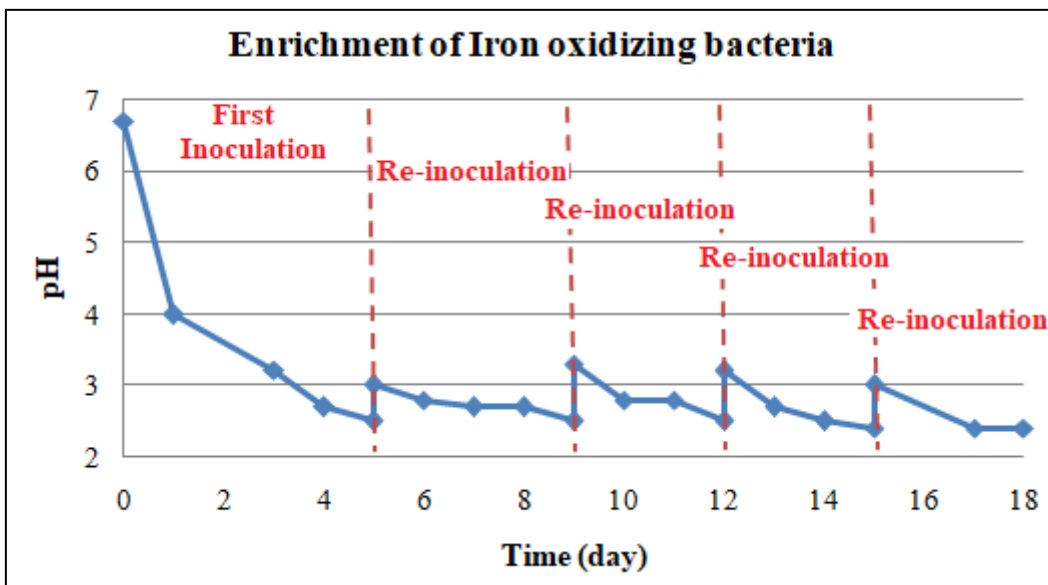


Figure 3.2. pH change during enrichment of Iron oxidizing bacteria

pH changes for Sulfur oxidizing bacteria were given in Figure 3.3. Initial pH of the sludge was 8.2 and during incubation period decrease in pH was observed. During the enrichment of the Sulfur oxidizing bacteria, start and the end of the re-inoculation periods were decided by pH decrease to 2. First inoculation period lasted 8 days and at this day pH was 1.7. Then re-inoculation period was started with pH 6.7 and this period lasted till pH level below 2 was obtained. After 6 days of incubation, pH decreased to 1.7 and another re-inoculation period was started. Initial pH for this re-inoculation period was 6.6 and after 3 days pH decreased to 1.9. Last re-inoculation period was started with pH 6.2 and after 4 days pH was 1.9. Total enrichment time for Sulfur oxidizing bacteria was 21 days.

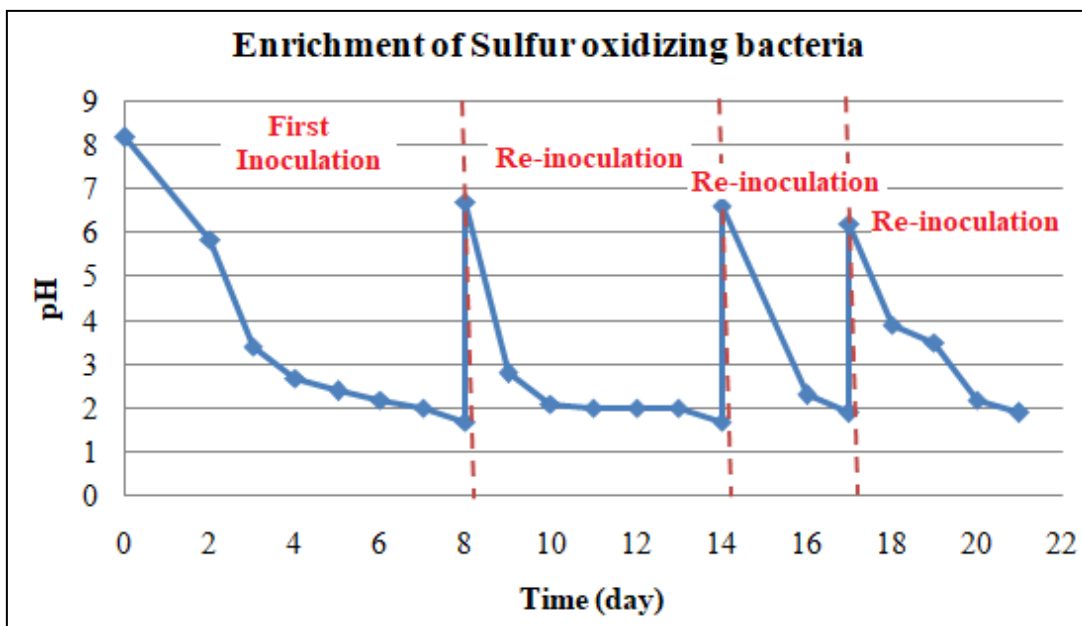


Figure 3.3. pH change during enrichment of Sulfur oxidizing bacteria

3.3. Bioleaching Studies

The important parameters for the bioleaching process are the ash amount, initial pH, inocula volume, energy source and temperature. Thus, to increase and optimize the dissolution of phosphorus from sewage sludge ash by bioleaching process, effects of these parameters were evaluated during this study. Evaluation of the parameters were achieved by monitoring pH, conductivity and also $\text{PO}_4^{3-}\text{-P}$ and SO_4^{2-} concentration because changes in these parameters give an information about the evolution of the bioleaching process.

3.3.1. Determination of optimum ash amount

Optimum ash amount was determined by 3 sets of experiments and the conditions for these experiments were given in Table 2.1. These 3 sets were performed with Iron oxidizing bacteria, Sulfur oxidizing bacteria and mixture of Sulfur&Iron oxidizing bacteria.

3.3.1.1. Bioleaching with Iron oxidizing bacteria

This trial was performed with Iron oxidizing bacteria with inocula volume of 10% and 2, 4, 6, 8, 10 grams of ash. This bioleaching experiments were lasted 48 days. The pH and conductivity profiles of this trial were given in Figure 3.4 and Figure 3.5.

The initial pH of the batches were different from each other because pHs were adjusted to 2.5 after the addition of medium and inocula before the addition of ash. Because ashes were added in different amounts, starting pHs were different. The higher initial pHs were seen in batches that had higher amounts of ash because of the strongly alkaline pH of the ash. For example, initial pH for the batch that had 2 g of ash was 3.99 while it was 6.02 for the batch that had 10 g of ash. After starting of bioleaching experiments, decreases in pH were seen almost for all of the batches. However, in some of the batches (8 g ash, 8 g ash control, 10 g ash and 10 g ash control) increase in pH were seen after 5 days which might be because of the dissolution of the ash. This situation was mostly seen in batches that had higher ash amounts, because the acid produced by bacteria and ferrous oxidation became not enough to decrease the pH increased by ash dissolution. The lowest pHs were obtained from the batches that had 2 g of ash. After 19 days of bioleaching, because pH was not at the desired levels (<2) for phosphorus dissolution (Tan and Lagerkvist, 2011; Egle et al., 2015), additional 20 g/L of $\text{FeSO}_4 \cdot 7\text{H}_2\text{O}$ as energy source was added to all batches. As it is seen from Figure 3.4, there were sharp decreases in pH levels for all the batches except for 2 g ash samples that were already around 2. After this point, there were slight fluctuations in pH, however there were no sharp changes. Thus, it was not meaningful to sustain the experiments after this point.

When conductivity profiles of the batches were investigated, it was seen that starting conductivity of the batches were similar unlike pH profiles. Initial conductivities of the samples ranged between 8.07 and 8.53 mS/cm. After 1 day later, there were decrease in conductivities which was an unexpected situation. Because there should be an increase in conductivity by dissolution of ions from the ash when bioleaching process works properly. The decrease of conductivity might be because of the precipitation of ions or oxidation of ferrous ion. Between the days 8 and 18, there were almost no change in conductivity levels. However, with the addition of 20 g/L of $\text{FeSO}_4 \cdot 7\text{H}_2\text{O}$, sharp

increases were seen. Addition of $\text{FeSO}_4 \cdot 7\text{H}_2\text{O}$ increased the conductivities to levels which were not seen before, however this was again not long lasted and they started to decrease again and between the days 26 and 48 almost there were no changes.

After 48 days of bioleaching, to evaluate the process in terms of phosphorus leaching, $\text{PO}_4^{3-}\text{-P}$ concentrations of batches were measured and dissolution percentages were calculated. Table 3.3 shows the dissolution percentages. As it is seen from the Table 3.3, the highest dissolution was obtained with batches realized with 2 g of ash with 14.93%. Moreover, results were similar with control experiments in all of the batches because there were pH decreases in all of the batches. The reason for this situation might be the hydrolysis of the ferric ion that formed by the oxidation of the ferrous ion. Hydrolysis reaction was shown in Equation (3.1) (Hem and Cropper, 1962).



As it is seen from the Equation (3.1), this reaction produces H^+ , thus decreases the pH.

Table 3.3. Phosphorus dissolution percentages for trial with Iron oxidizing bacteria

Batch name	Phosphorus Dissolution (%)
2 g Ash	14.93
2 g Ash Control	14.75
4 g Ash	2.49
4 g Ash Control	2.42
6 g Ash	0.95
6 g Ash Control	0.96
8 g Ash	0.91
8 g Ash Control	0.90
10 g Ash	0.85
10 g Ash Control	0.61

The reason for these low phosphorus dissolution percentages might be the phosphorus-iron chemistry. One of the possible reactions that can realize between iron(III) and phosphate ions is the complexation reactions and products of these reactions can be $\text{Fe}(\text{HPO}_4)_2^-$, $\text{Fe}(\text{H}_2\text{PO}_4)_4^-$, $\text{Fe}(\text{OH})\text{PO}_4^-$, $\text{Fe}(\text{HPO}_4)_3^{3-}$, $\text{Fe}(\text{PO}_4)_2^{3-}$ (Wilhelmy et al., 1985). Besides these complexes, adsorption of ortho-phosphates to iron (ferrous and ferric iron) oxides produces the adsorption complexes. Another possible reactions that can realize between the ortho-phosphates and iron oxides is the surface precipitation and this can form a solid phase (Wilfert et al., 2015).

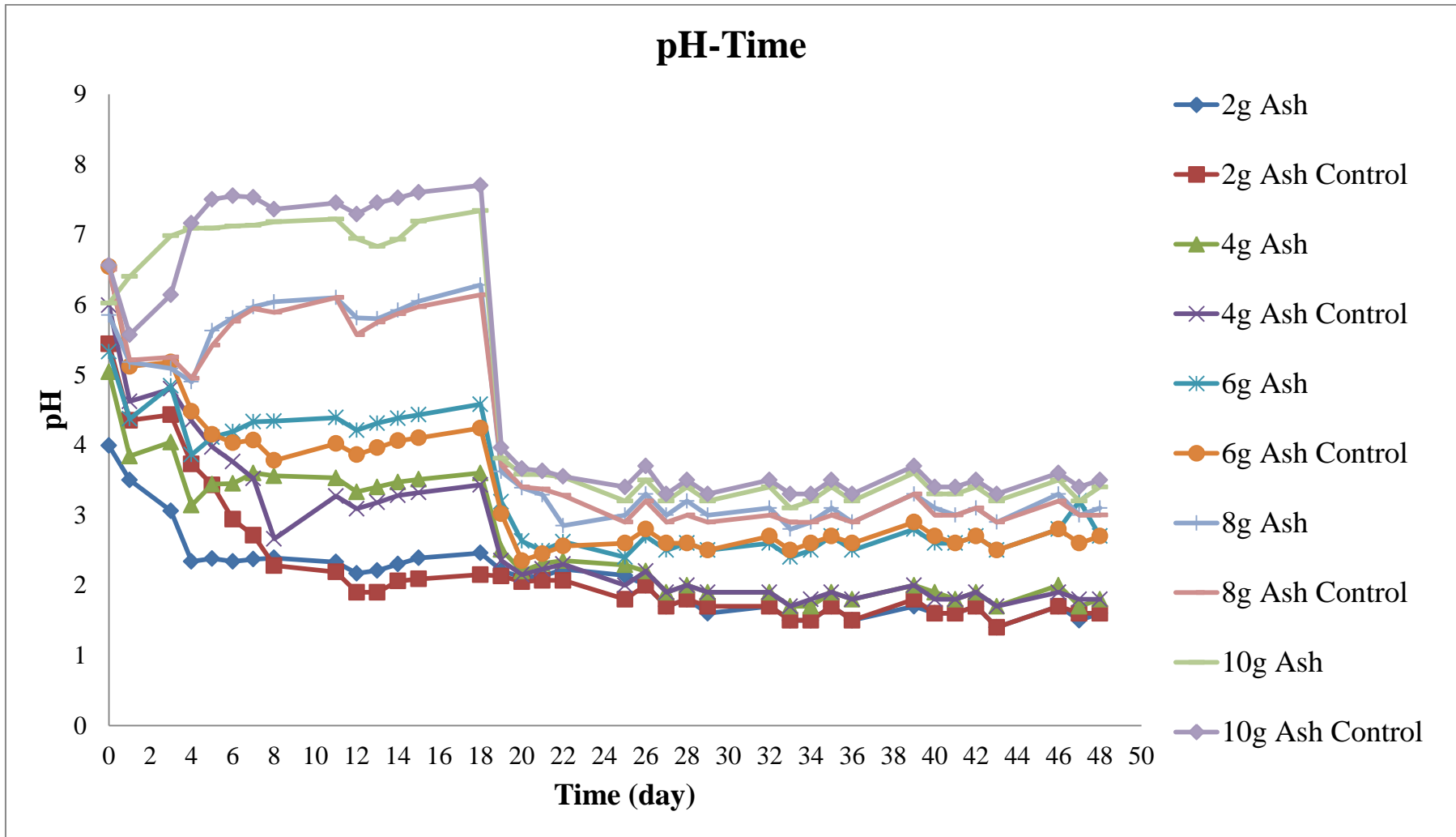


Figure 3.4. pH profile of trial with Iron oxidizing bacteria

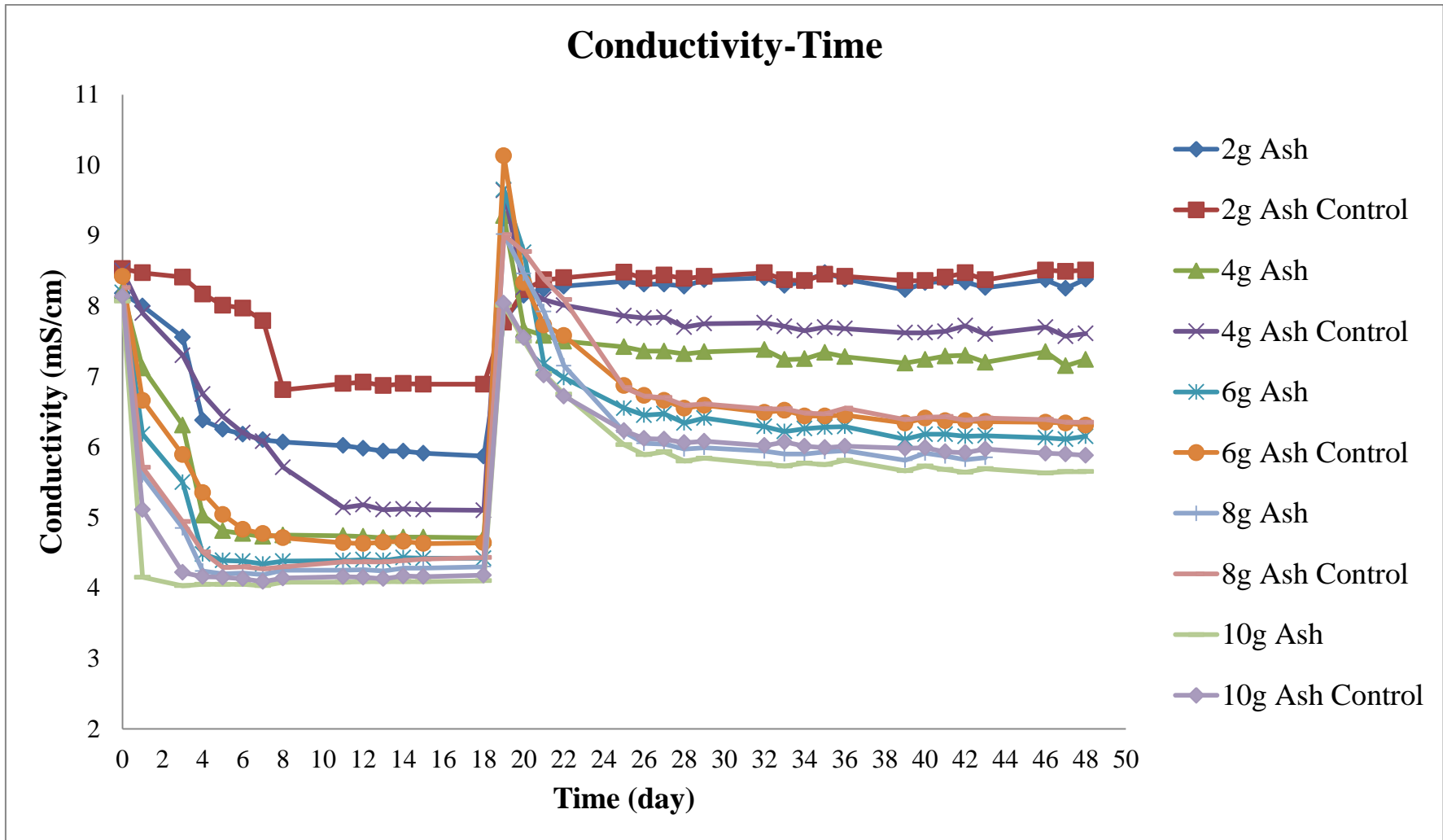
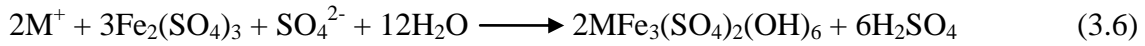
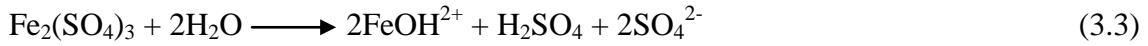
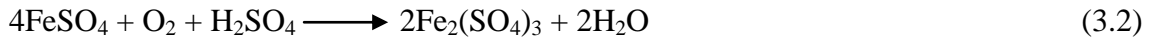


Figure 3.5. Conductivity profile of trial with Iron oxidizing bacteria

The X-Ray diffraction pattern of the residue obtained after the bioleaching of the sewage sludge ash with Iron oxidizing bacteria was shown in Figure 3.6. As it is seen from this diffractogram; ammoniojarosite ((NH₄)Fe₃(SO₄)₂(OH)₆), gypsum (CaSO₄·2H₂O), iron phosphate (Fe₃PO₇) and phosphorus oxide (P₂O₅) were the main components. Jarosite (hydroxysulfate precipitates) formation is seen during the oxidation of the ferrous ion by bacteria because Fe³⁺ ions form a sulfate complex (Díaz-Tena et al., 2016). Formation reactions of the jarosite are as follows (Li et al., 2016):



(M may be H₃O⁺, K⁺, Na⁺ or NH₄⁺).

Formation reaction for the gypsum is also given in Equation (3.7) (Wang et al., 2010).

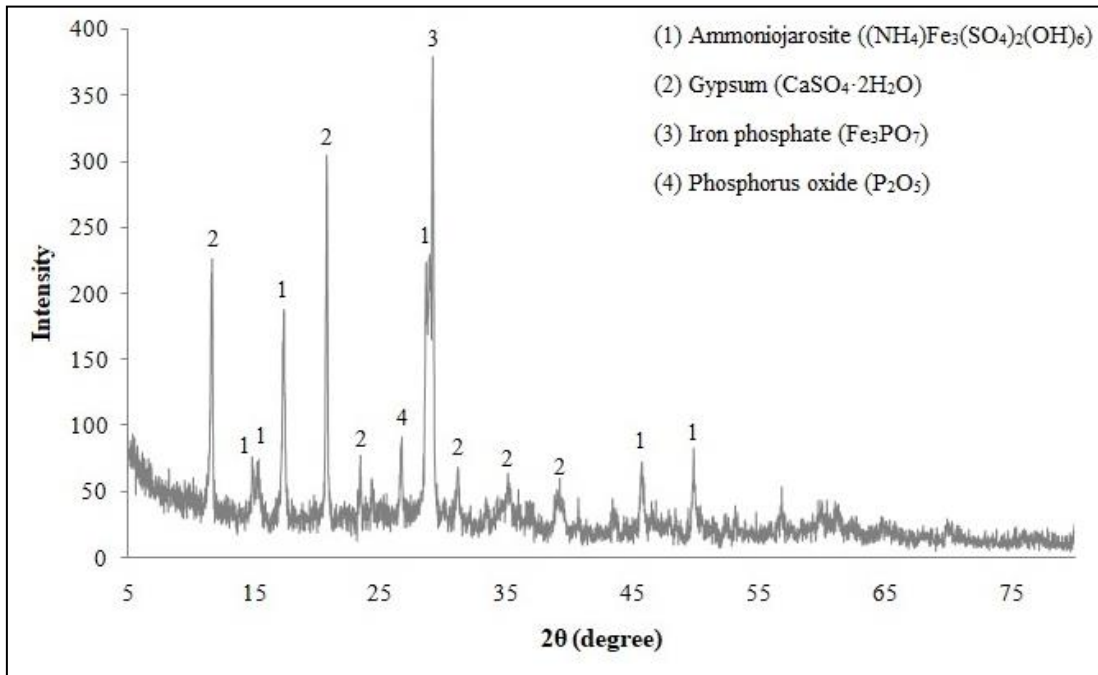


Figure 3.6. X-Ray diffractogram of the residue obtained after the bioleaching of the sewage sludge ash with Iron oxidizing bacteria

3.3.1.2. Bioleaching with Sulfur oxidizing bacteria

This trial was performed with Sulfur oxidizing bacteria with inocula volume of 20% and 2, 4, 8 grams of ash. This bioleaching experiments were lasted 29 days.

The pH profile of this trial was given in Figure 3.7. Initial pHs of the batches were adjusted to 7 in this bioleaching experiments after the addition of medium, inocula and ash. However, after 1 day, there were increases in pH except the 2 g ash batch. This might be because of the dissolution of ash. When the acid produced by Sulfur oxidizing bacteria was not enough to decrease the pH that was increased by ash dissolution, pH of the batches increased. However, this did not last so much and at the 2nd day, pH decreased in all of the batches. The pH decrease was highest in the 2 g ash batch and at the 5th day, pH of this batch was 1.2. The change in pHs were not significant for the control batch of 2 g ash and also for the 8 g ash batch between the days 5 and 29. There was decrease in pH for the 4 g ash batch, it decreased to below 2 at the 15th day of bioleaching and it was 0.5 at the 29th day. At the 15th day of bioleaching, pH decreased to 1 in the 2 g ash batch and it continued to decrease after this days and it reached to 0.3 at the 29th day.

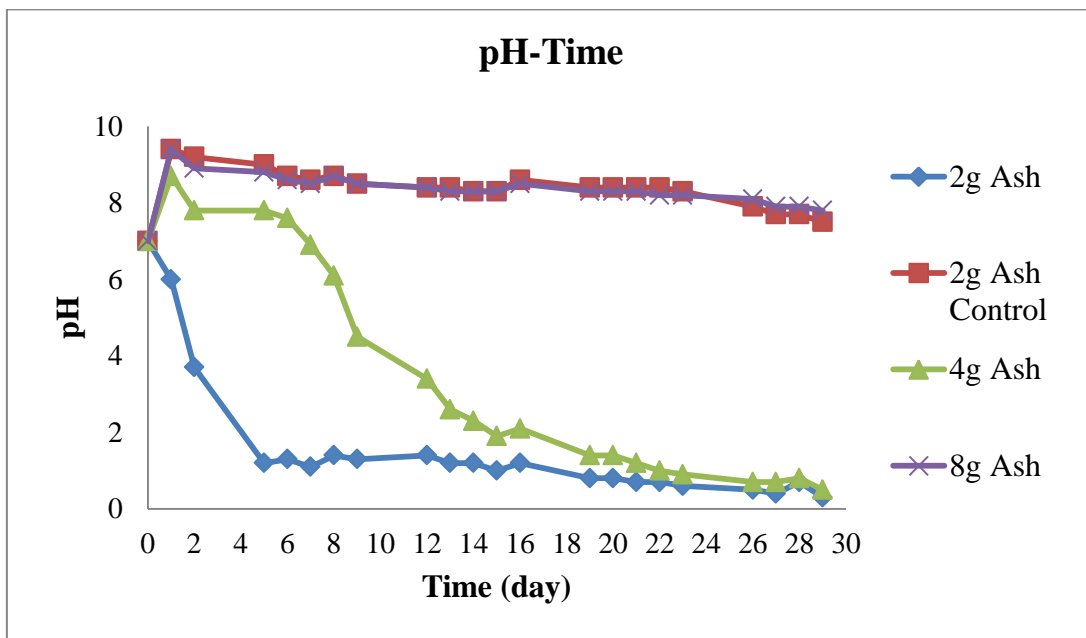


Figure 3.7. pH profile of trial with Sulfur oxidizing bacteria

The conductivity profile of this trial was given in Figure 3.8. Initial conductivities of the batches were 3.4, 3.61, 4.77 and 2 mS/cm for 2 g ash, 4 g ash, 8 g ash and 2 g ash control, respectively. Conductivity of the 2 g ash batch increased from the first day till the last day of bioleaching and it reached to 86.6 mS/cm. This was because of the decrease of pH levels and production of sulfuric acid by bacteria. Conductivity of the 4 g ash batch did not change significantly between the days 1 to 15; however after the 15th day, it started to increase and reached to 41 mS/cm at the last day (day 29) of bioleaching. The increase in the conductivity after 15 days might be due to the decrease in pH levels to below 2 that meant more acid production and more dissolution from the ash. There were no significant changes in conductivity for the batches that had 8 g of ash and 2 g ash control. The reason for the control batch might be the absence of the bacteria that produce sulfuric acid and therefore there was no dissolution from the ash. The reason for the 8 g ash batch might be the amount of ash that may cause inhibition of bacteria.

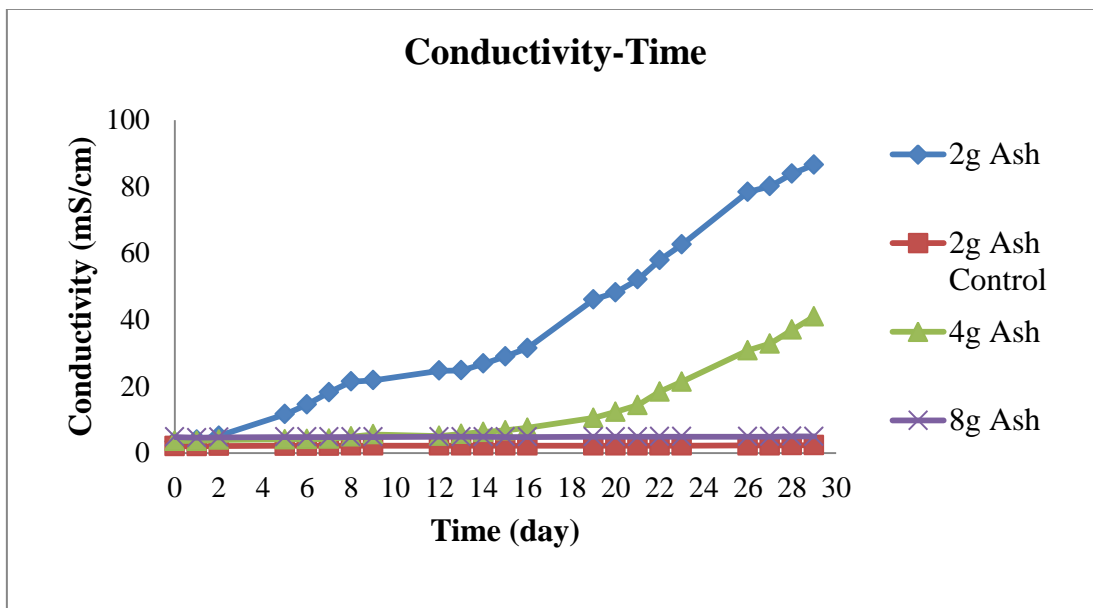


Figure 3.8. Conductivity profile of trial with Sulfur oxidizing bacteria

Sulfate concentration is an indicator for sulfuric acid production by bacteria and in a properly working bioleaching process sulfate concentration increases with time and this results in decrease in pH and increase in conductivity. Therefore sulfate concentration of the batches were measured and its graph was given in Figure 3.9. As it is seen from this graph, sulfate concentration increased with time for the batches that had 2 g and 4 g

of ash. As it was in the case of pH and conductivity, the highest sulfate production was obtained with the batch that had 2 g of ash. It increased from 1.40 g/L to 26.0 g/L after 29 days which was a significant change. For the 4 g ash batch, sulfate concentration increased from 1.75 g/L to 15.0 g/L after 29 day and the significant change was seen between the days 21 and 29. There were no sulfate concentration change in the batches that had 8 g ash and 2 g ash without bacteria. This result was relevant to pH and conductivity profiles of these batches.

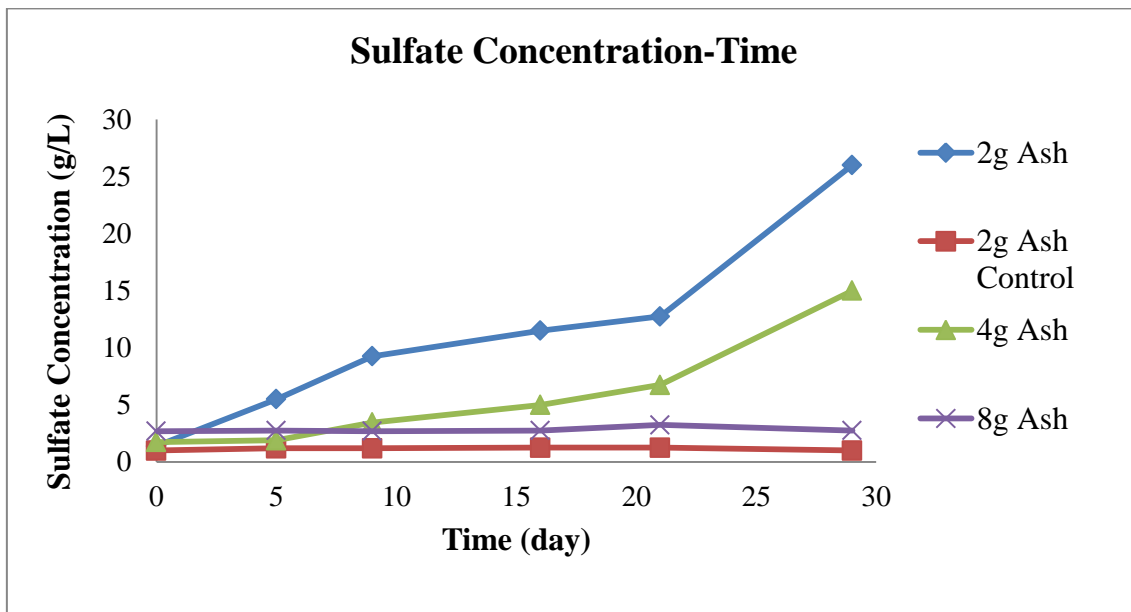


Figure 3.9. Sulfate concentration profile for bioleaching with Sulfur oxidizing bacteria

In Figure 3.10, phosphorus dissolution percentages were given. As it is seen from this Figure 3.10, phosphorus dissolution increased with time for the 2 g and 4 g ash batches. The highest phosphorus dissolution from the sewage sludge ash observed from the 2 g ash batch and it reached to the 68.6% at the 29th day of bioleaching. However it is also seen that between the days 9 and 29, there were no major changes for the 2 g ash batch. For the 4 g ash batch, phosphorus dissolution percentage was 2.9% at the 9th day and there was increase in phosphorus dissolution percentage between the days 9 and 21; at these days major changes in pH and conductivity realized also. The maximum phosphorus dissolution for 4 g ash batch was 50% and it was obtained at the last day of the bioleaching which was 29th day. There were no phosphorus dissolution for the batches that had 8 g ash and 2 g ash without bacteria, this result was relevant to pH and

conductivity profiles of these batches. Because there were no significant change in pH and conductivity of these batches, there were no phosphorus dissolution.

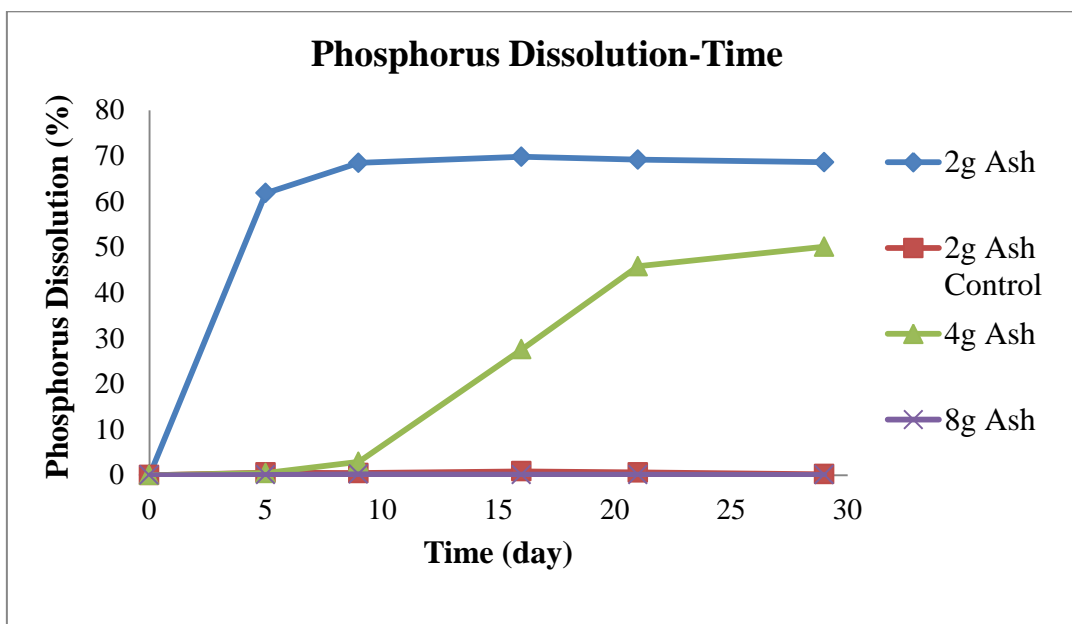


Figure 3.10. Phosphorus dissolution profile for bioleaching with Sulfur oxidizing bacteria

3.3.1.3. Bioleaching with mixture of Sulfur&Iron oxidizing bacteria

This trial was performed with mixture of Sulfur&Iron oxidizing bacteria with inocula volume of 20% and 2, 4, 8 grams of ash. This bioleaching experiments were lasted 29 days.

The pH profile of this trial was given in Figure 3.11. Initial pHs of the batches were adjusted to 2.5 in this bioleaching experiments after the addition of medium, inocula and ash. pHs of the 2 g and 4 g of ash batches started to decrease and it reached to 1.3 for both batches after 16 days. There was a difference in this trial from the previous one that was realized with only Sulfur oxidizing bacteria because pH of the batches that had 8 g ash and 2 g ash without bacteria also decreased. The reason for this pH decrease might be presence of ferrous ion and the reaction shown in Equation (3.1). At the last day of bioleaching, pH levels of all of the batches were almost same and they were all below 1.

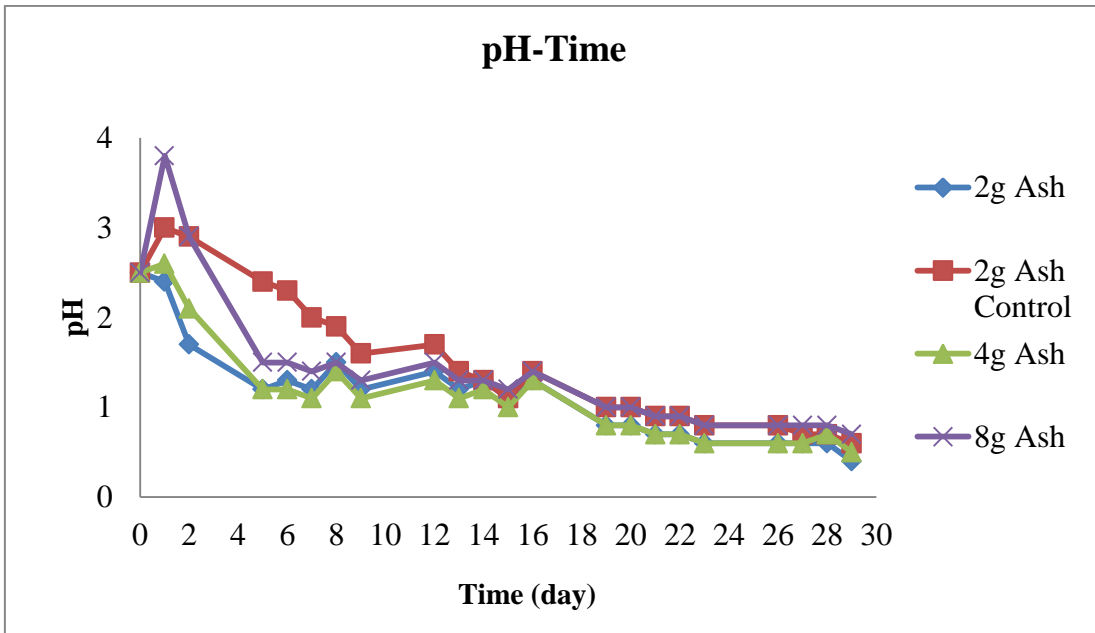


Figure 3.11. pH profile of trial with mixture of Sulfur&Iron oxidizing bacteria

The conductivity profile of this trial was given in Figure 3.12. Starting conductivity levels of the all batches were almost similar and they were between 9.08 and 10.74 mS/cm. In all the batches there were increasing trend and the highest conductivity was obtained from the 2 g ash batch with 72.4 mS/cm at the last day of the bioleaching.

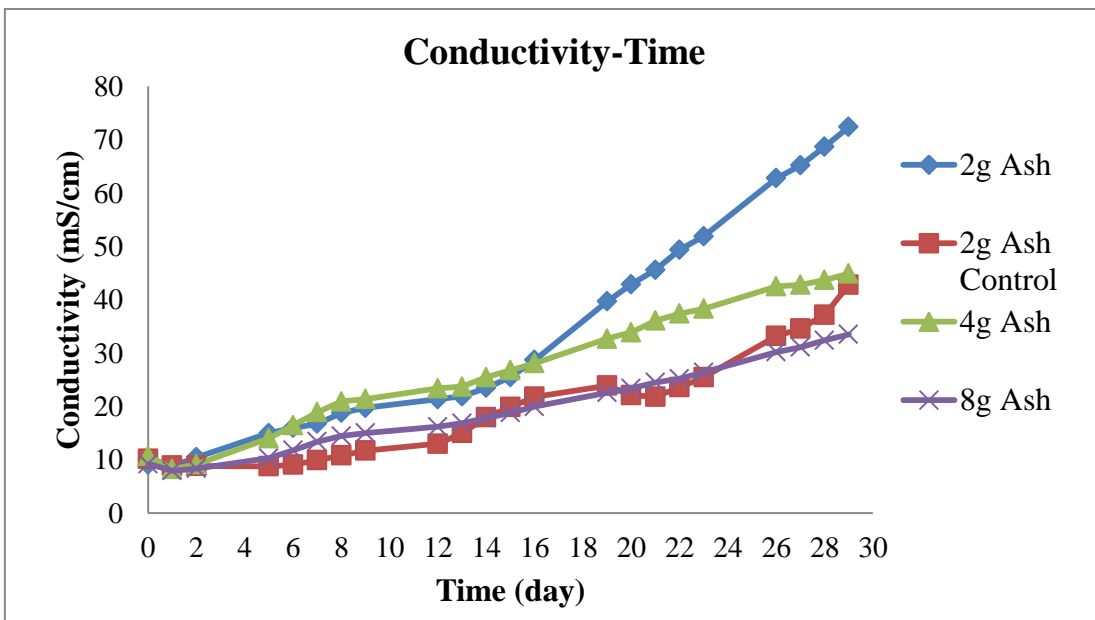


Figure 3.12. Conductivity profile of trial with mixture of Sulfur&Iron oxidizing bacteria

Sulfate concentration profile was given in Figure 3.13. As it is seen from this Figure 3.13, there were increasing trend for all of the batches. The highest sulfate concentration was obtained from the 2 g ash batch and it was increased from 8.50 to 29.5 g/L. This high sulfate concentration was result of more acid production. However in all of the batches, the reached sulfate concentrations were similar and it ranged between 24.5 and 29.5 g/L.

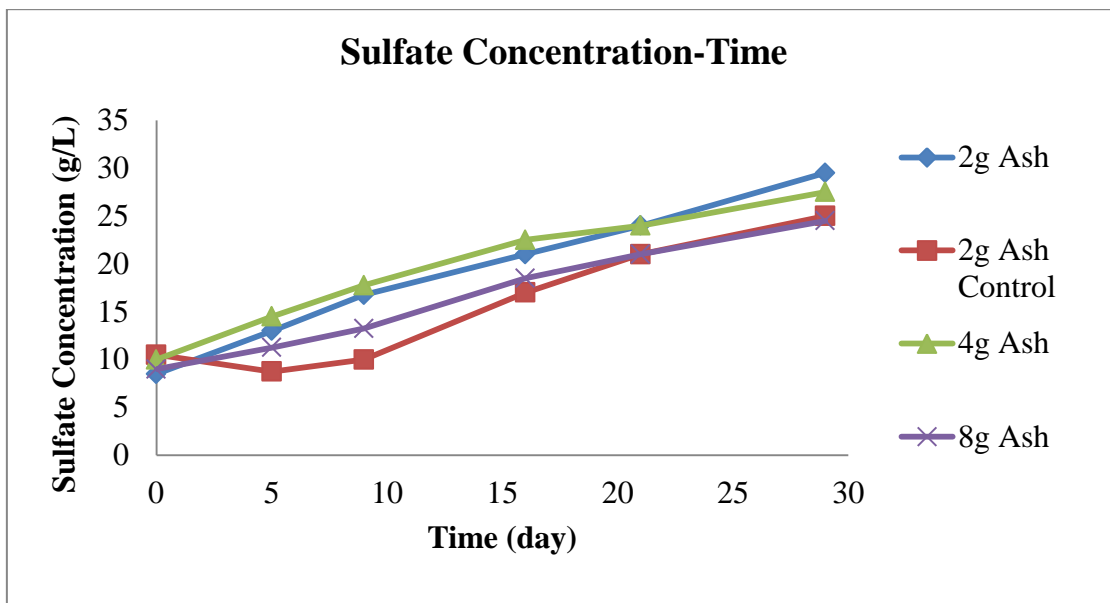


Figure 3.13. Sulfate concentration profile for bioleaching with mixture of Sulfur&Iron oxidizing bacteria

Phosphorus dissolution percentages were not linear and its graph was given in Figure 3.14. The reason for this situation might be the complexity of iron-phosphate chemistry. The highest phosphorus dissolution was obtained from the 2 g ash batch and it reached to 55.8% after 21 days. At the 29th day, it was 54.2%. This small decrease might be because of the bacterial usage of phosphate or again iron-phosphate chemistry. For the 4 g ash batch, highest phosphorus dissolution was obtained at the 21th day and it was 45.15%. There were also dissolution of phosphorus at the batches that had 8 g ash and 2 g ash without bacteria. This dissolution was a result of pH decrease in these batches because of the ferrous ion.

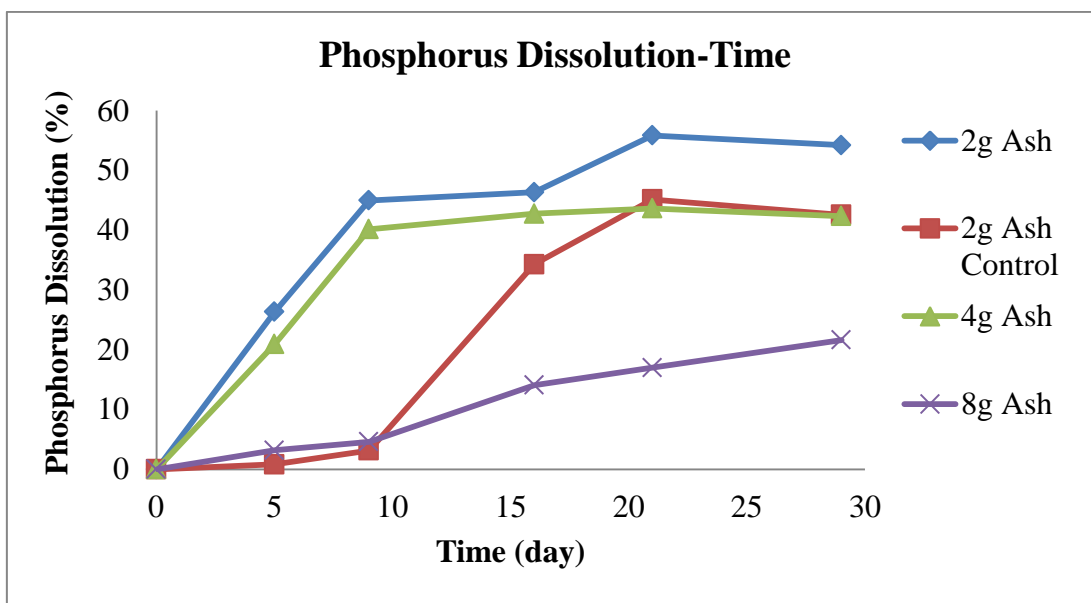


Figure 3.14. Phosphorus dissolution profile for bioleaching with mixture of Sulfur&Iron oxidizing bacteria

3.3.1.4. Optimum ash amount

After the 3 sets of experiments realized for the determination of the optimum ash amount for phosphorus bioleaching, it was seen that the 2 g of ash was the optimum amount because highest phosphorus dissolution percentages were obtained with this amount. Therefore, for the experiments realized to find optimum inocula volume and optimum sulfur amount, ash amount of 2 g was used.

3.3.2. Determination of optimum inocula volume

Optimum inocula volume was determined by 2 sets of experiments and the conditions for these experiments were given in Table 2.2. These 2 sets were performed with Sulfur oxidizing bacteria and mixture of Sulfur&Iron oxidizing bacteria. For the determination of the optimum inocula volume, study with only Iron oxidizing bacteria was not performed because of the low dissolution percentages obtained from previous studies.

3.3.2.1. Bioleaching with Sulfur oxidizing bacteria

This trial was performed with Sulfur oxidizing bacteria with inocula volume of 25, 30, 35, 40% and 2 grams of ash to see the effect of inocula volume and also to find the optimum inocula volume. This set of bioleaching experiments were lasted 29 days.

The pH profile of this trial was given in Figure 3.15. Initial pHs of the batches are different from each other because pHs were not adjusted and they ranged between 6.2 and 7. In all of the batches, pHs started to decrease rapidly and after 5 days of bioleaching pHs were 1.6, 1.6, 1.4, 1.4 for 25, 30, 35, 40% inocula volume, respectively. At the day 12, all of the pHs were below 1 and they were 0.8. Although decrease in pHs continued in all batches, because change in pHs were so rapid from the beginning to 5th day, after 12th day, there were no significant change in pH levels. At the last day of the bioleaching, 29th day, all of the batches had the pH of 0.3.

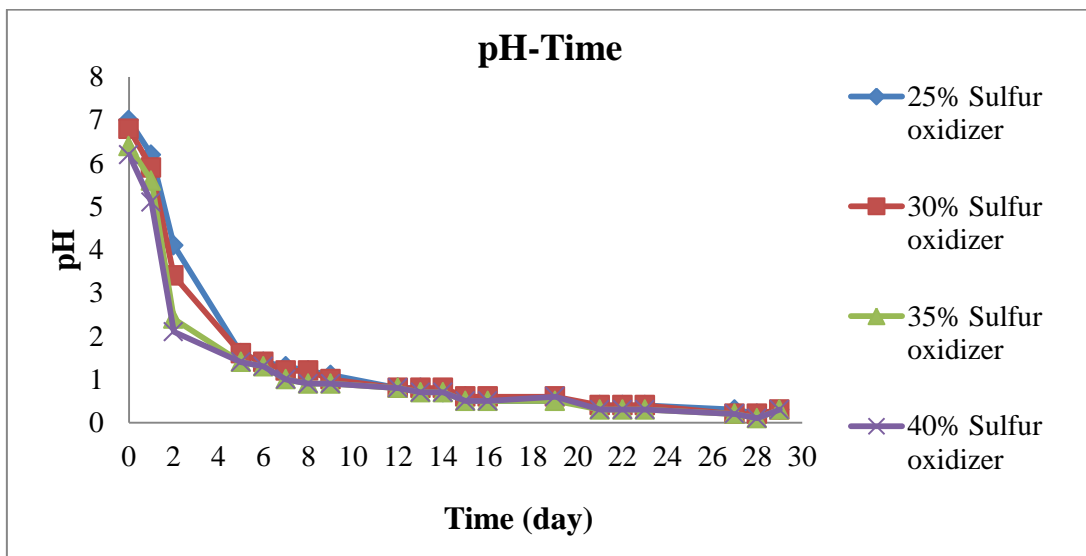


Figure 3.15. pH profile for bioleaching with different Sulfur oxidizing bacteria inocula volumes

The conductivity profile of this trial was given in Figure 3.16. Initial conductivity levels of the all batches were similar and between 2.63 and 3.45 mS/cm. Conductivities of all the batches increased with time linearly. This was because of the production of sulfate by the bacteria and dissolution of ions from the ash. The highest conductivity was obtained from the batch that had 40% of inocula with 96.1 mS/cm at the last day of bioleaching.

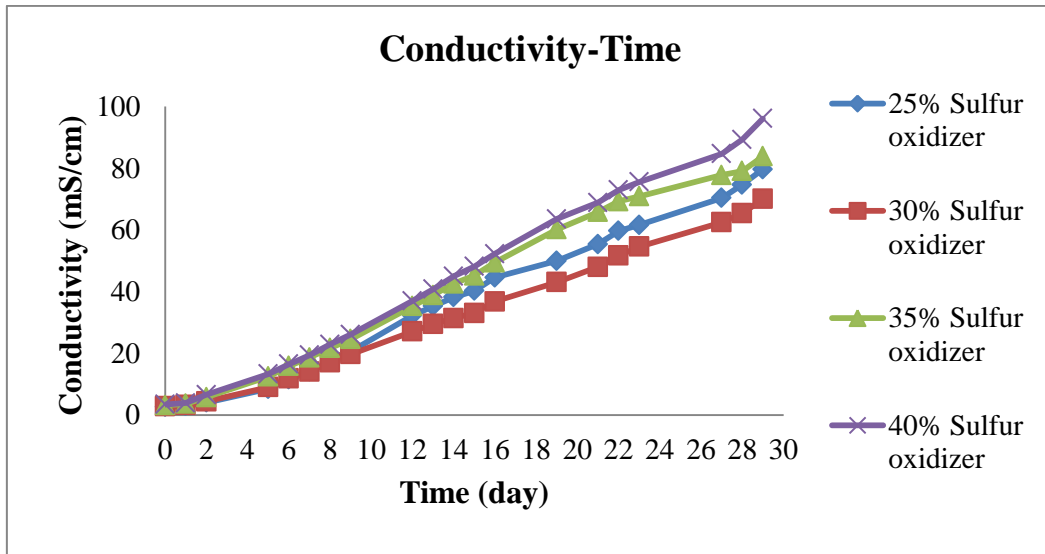


Figure 3.16. Conductivity profile for bioleaching with different Sulfur oxidizing bacteria inocula volumes

Change of sulfate concentrations with time was shown in Figure 3.17. As it is seen from the Figure 3.17, sulfate concentrations increased linearly for all of the batches. This indicated the sulfuric acid production by the bacteria. The initial sulfate concentrations were similar and 1.15, 1.20, 1.45, 1.45 g/L for inocula volumes of 25, 30, 35, 40%, respectively. At the last day, day 29, the highest sulfate concentration was at the batch that had 40% of inocula with 28.5 g/L and the lowest sulfate concentration was at the batch that had 25% of inocula with 23 g/L.

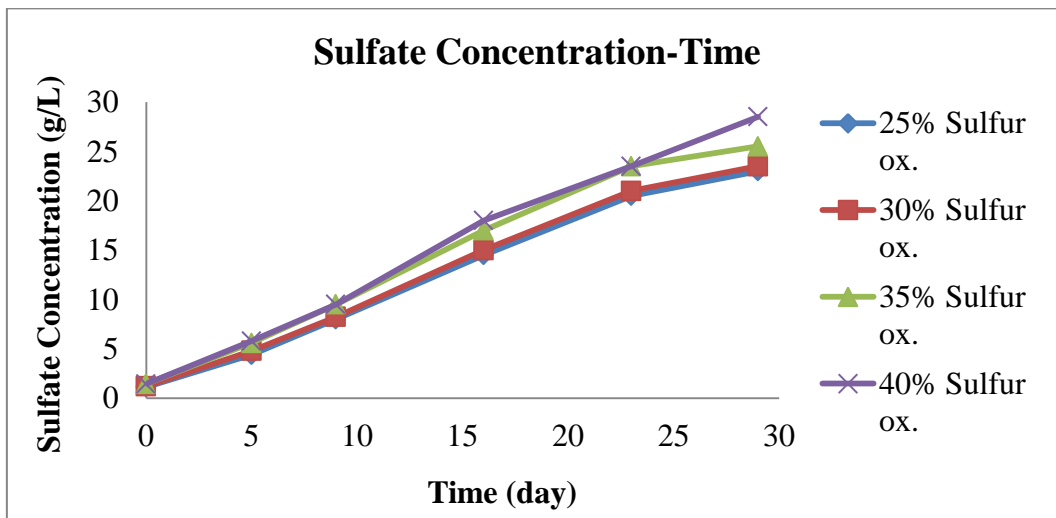


Figure 3.17. Sulfate concentration profile for bioleaching with different Sulfur oxidizing bacteria inocula volumes

Phosphorus dissolution percentages were given in Figure 3.18. As it is seen from the Figure 3.18, as the time passes dissolution of phosphorus increased. The most rapid increase was between the days 0-5 and 69.7% of phosphorus dissolution was obtained from the 40% inocula batch. After the 5th day of bioleaching, there were increases also; however these increases were not as high as they were at the first 5 days. The highest dissolution was obtained from the 40% inocula batch with 76.6% after 16 days. At the last day (day 29); the highest dissolution was seen at the 40% inocula batch with 76% and the lowest dissolution was seen at the 25% inocula batch with 55%. Thus, it can be concluded that inocula volume directly affected the phosphorus dissolution.

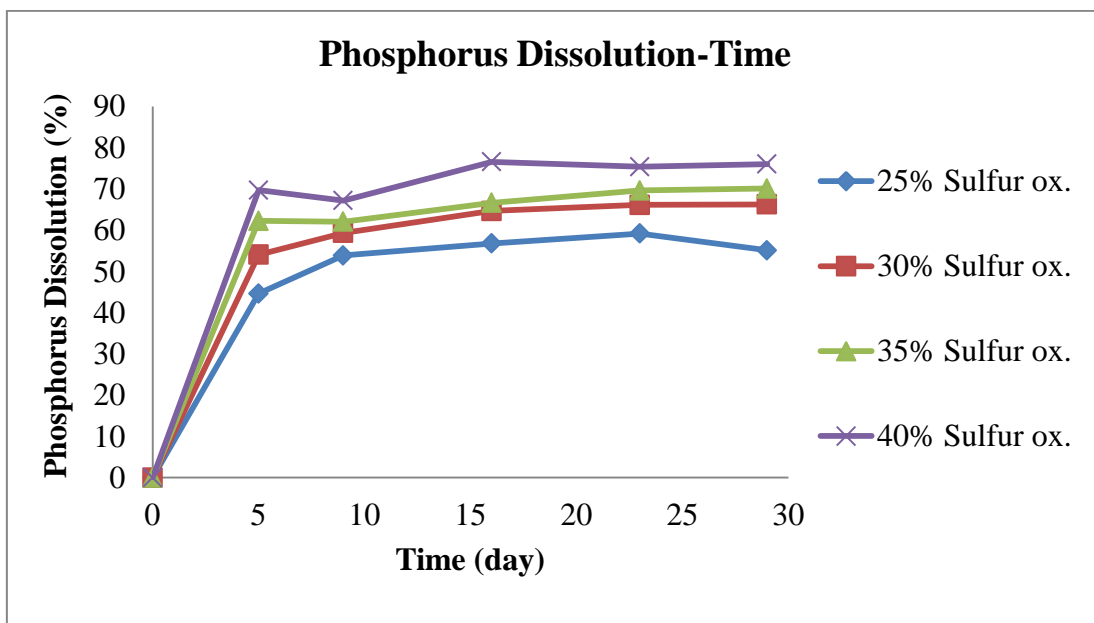


Figure 3.18. Phosphorus dissolution profile for bioleaching with different Sulfur oxidizing bacteria inocula volumes

3.3.2.2. Bioleaching with mixture of Sulfur&Iron oxidizing bacteria

This trial was performed with mixture of Sulfur&Iron oxidizing bacteria with inocula volume of 25, 30, 35, 40% and 2 grams of ash to see the effect of inocula volume and also to find the optimum inocula volume. This set of bioleaching experiments were lasted 29 days.

Initial pH values of the batches were 5.5, 5, 4.9, 4.3 for the inocula volumes of 25, 30, 35, 40%, respectively. The reason for the lower initial pH levels from the previous trial realized with only Sulfur oxidizing bacteria was the presence of the Iron oxidizing

bacteria because pH of the Iron oxidizing bacteria inocula was lower than the Sulfur oxidizing bacteria inocula. As it seen from the Figure 3.19, the pH values of all the batches started to decrease from the first day of bioleaching. At the 12th day, pH values were below 1 and 0.8, 0.9, 0.8, 0.9 for 25, 30, 35, 40% of inocula volumes, respectively. After this day, decreases of pH values continued but it couldn't be as much as it was at first 12 day, because pH values were already too low. At the last day, day 29, pH values were 0.3, 0.4, 0.3, 0.4 for 25, 30, 35, 40% inocula volumes, respectively.

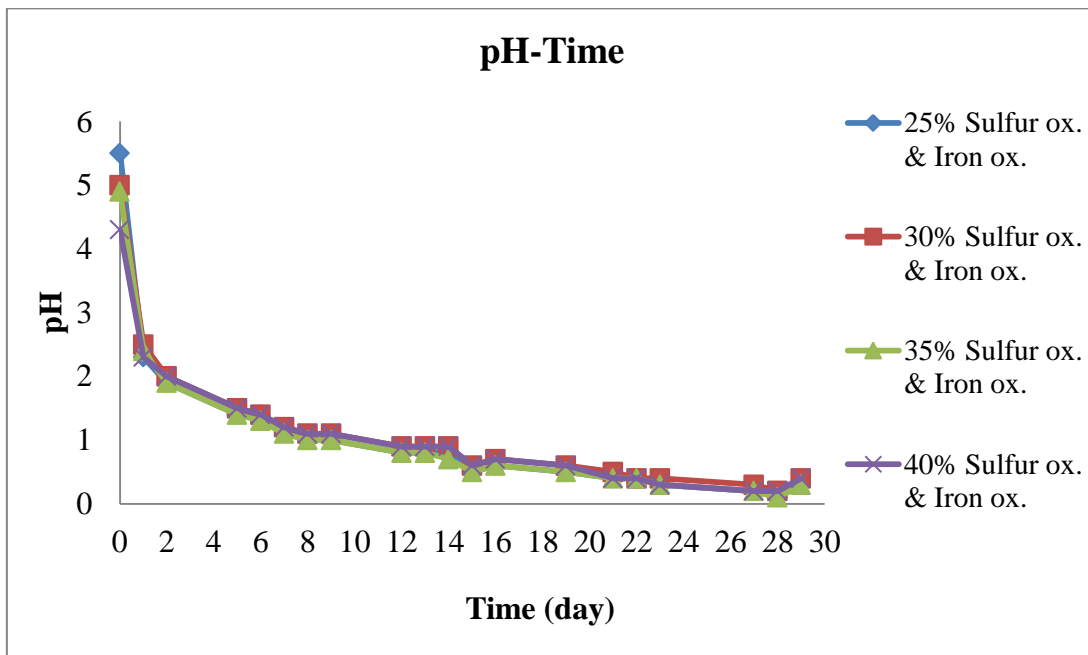


Figure 3.19. pH profile for bioleaching with mixture of Sulfur&Iron oxidizing bacteria with different inocula volumes

Figure 3.20 shows the conductivity profile of this trial and it is seen that initial conductivity values were similar and ranged between 6.45 and 6.83 mS/cm. From first day to 5th day of bioleaching, there were no significant change in conductivity levels. This might be because of the adaptation of the Sulfur and Iron oxidizing bacteria or conversion of ferrous iron ions to ferric iron ions. However, after 5th day, conductivities of all the batches started to increase. At the last day of bioleaching, the highest conductivity was at the batch that had 35% inocula volume with 79.8 mS/cm.

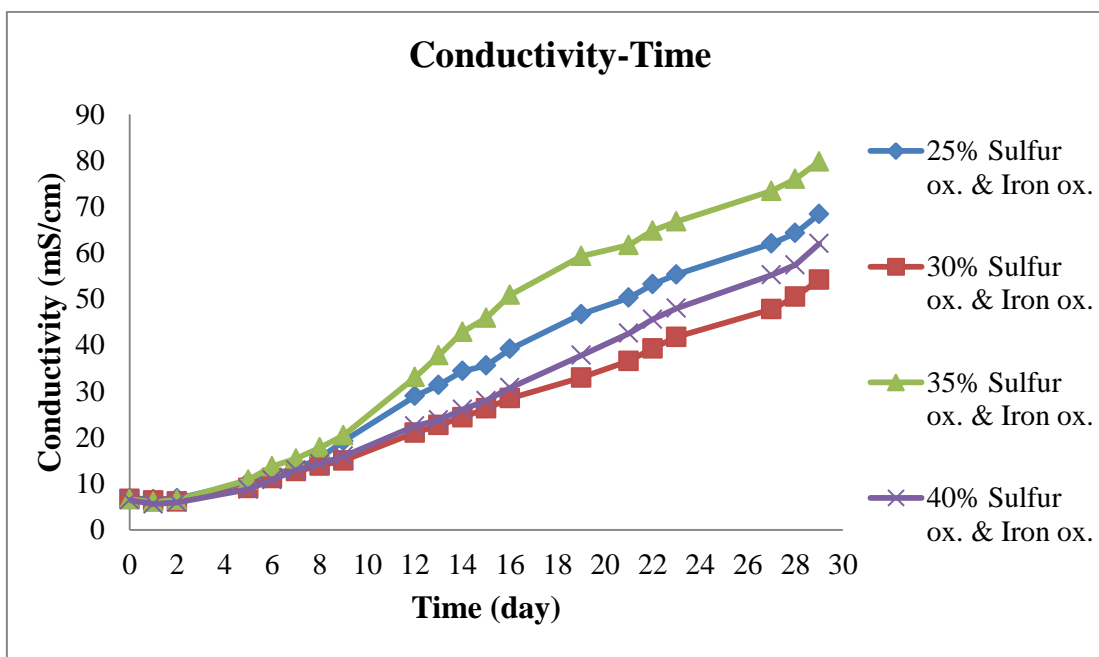


Figure 3.20. Conductivity profile for bioleaching with mixture of Sulfur&Iron oxidizing bacteria with different inocula volumes

Sulfate concentration profile was given in Figure 3.21. Initial sulfate concentrations were 5.5, 6, 6, 6 g/L for 25, 30, 35, 40% of inocula volumes, respectively. As the time passed, bacteria produced sulfuric acid and sulfate concentrations increased. The increase rate was slower at first 5 day when it compared with the rate after 5th day. This might be because of the adaptation of the sulfur and iron oxidizing bacteria as it was in the pH change at first 5 days. Between the days 5 and 29, there were linear increases in sulfate concentrations of all the batches. After 29 days, the highest sulfate concentration was at the 40% inocula volume batch with 36 g/L and the lowest sulfate concentration was at the 25% inocula volume batch with 32 g/L.

Phosphorus dissolution profile was shown in Figure 3.22. As it is seen from this Figure 3.22, there were some fluctuations, there were not linear increases in phosphorus dissolution. This might be because of the iron-phosphate chemistry (e.g. precipitation, complexation). This situation was not seen when only sulfur oxidizing bacteria was used. Significant phosphorus dissolutions were seen between the days 5 and 16 and the highest dissolution was at the 40% inocula volume batch with 57.8% after 16 days. After 16th day, no significant changes were seen. At the last day, the highest dissolution was at the 35% inocula volume batch with 67.1% and the lowest dissolution was at the 25% inocula volume batch with 50.6%.

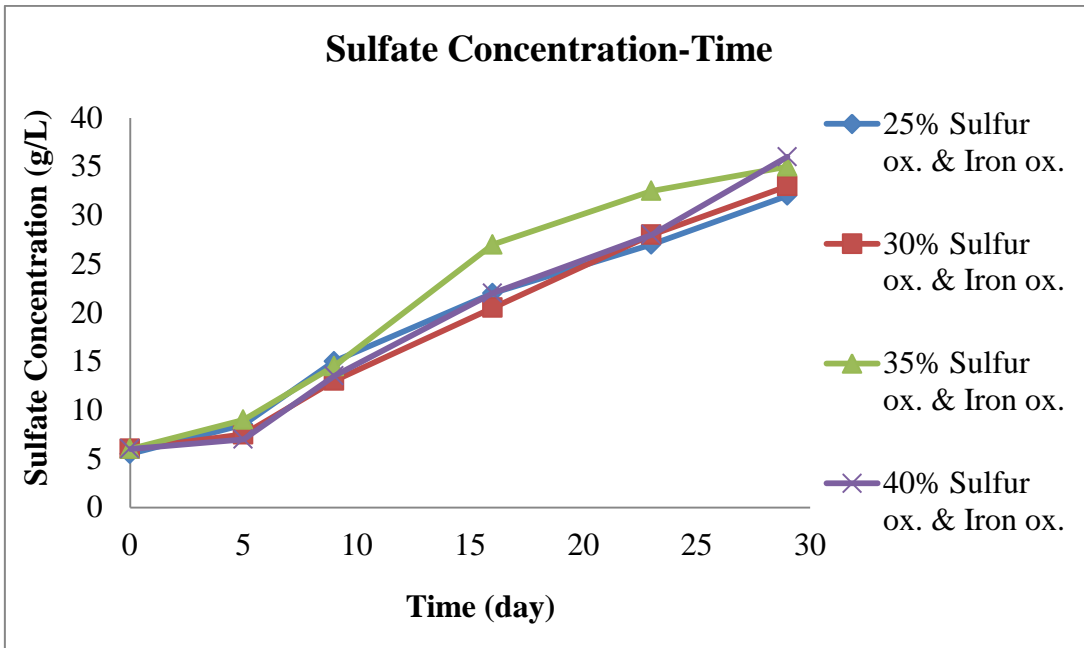


Figure 3.21. Sulfate concentration profile for bioleaching with mixture of Sulfur&Iron oxidizing bacteria with different inocula volumes

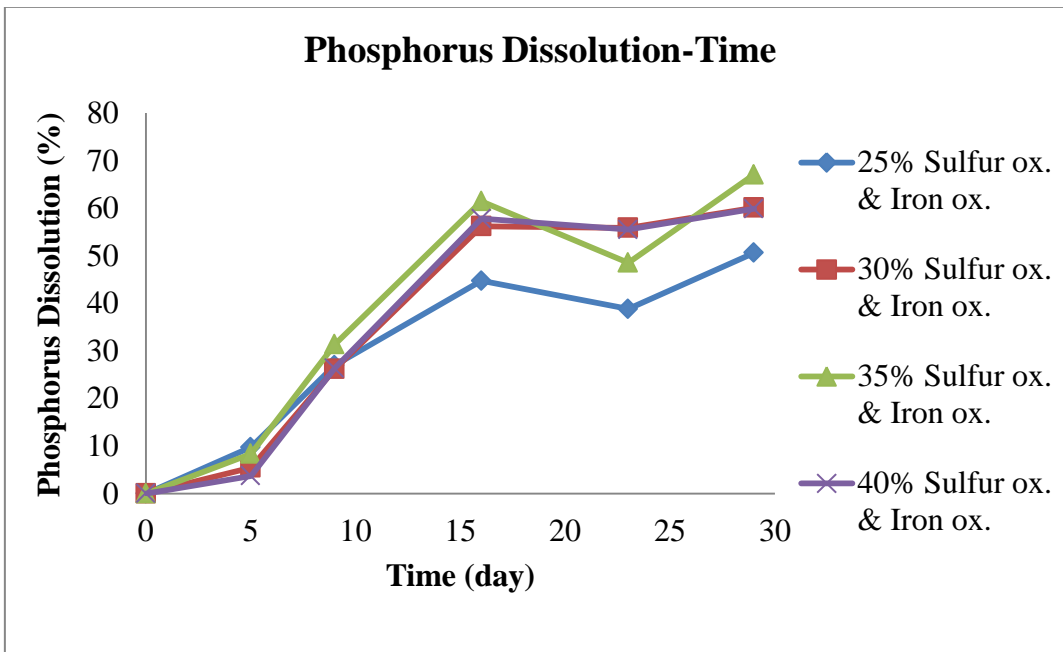


Figure 3.22. Phosphorus dissolution profile for bioleaching with mixture of Sulfur&Iron oxidizing bacteria with different inocula volumes

3.3.2.3. Optimum inocula volume

After the 2 sets of experiments realized for the determination of the optimum inocula volume for phosphorus bioleaching, it was seen that the 40% inocula volume was the optimum because highest phosphorus dissolution percentages were obtained with this percentage. Thus, for the experiments realized to find optimum sulfur amount, inocula volume of 40% was used.

3.3.3. Determination of optimum amount of sulfur

Optimum sulfur amount was determined by the 1 set of experiment and conditions for this set were given in Table 2.3. This 1 set was performed with Sulfur oxidizing bacteria with different sulfur concentrations.

pH profile for batches with different sulfur amounts was given in Figure 3.23. The initial pH of all the batches were 6.1. After 1 day, there were significant change in pH values of all the batches; pH values were 2.7, 2.5, 2.6, 2.7 for the batches that had 10, 15, 20, 25 g/L sulfur, respectively. After this day, the pH changes were similar for all the batches. At the last day, day 29, pH values were 0.4, 0.3, 0.3, 0.3 for the batches that had 10, 15, 20, 25 g/L sulfur, respectively.

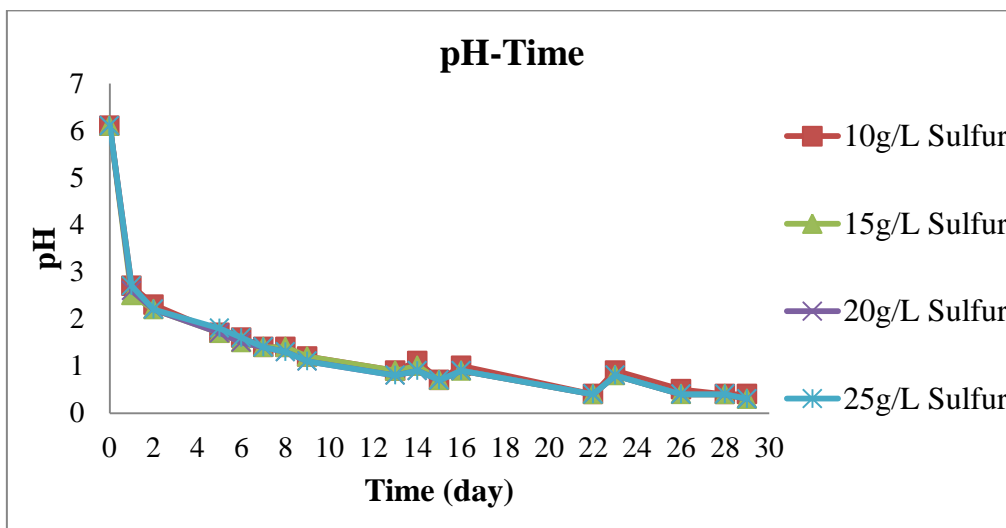


Figure 3.23. pH profile for bioleaching with different sulfur amounts

Conductivity profile for batches with different sulfur amounts was given in Figure 3.24. Initial conductivity values were similar and 2.71, 2.73, 2.73, 2.69 for the 10, 15, 20, 25 g/L sulfur batches, respectively. There were increase in conductivities from the first day

to the last day. However the rate of increase in first 9 day was lower than the rate of increase between the days 9 and 29. This might be because of the adaptation of the bacteria to sewage sludge ash. At the last day the highest conductivity was at the 25 g/L sulfur batch with 125.6 mS/cm and the lowest conductivity was at the 10 g/L sulfur batch with 92.3 mS/cm.

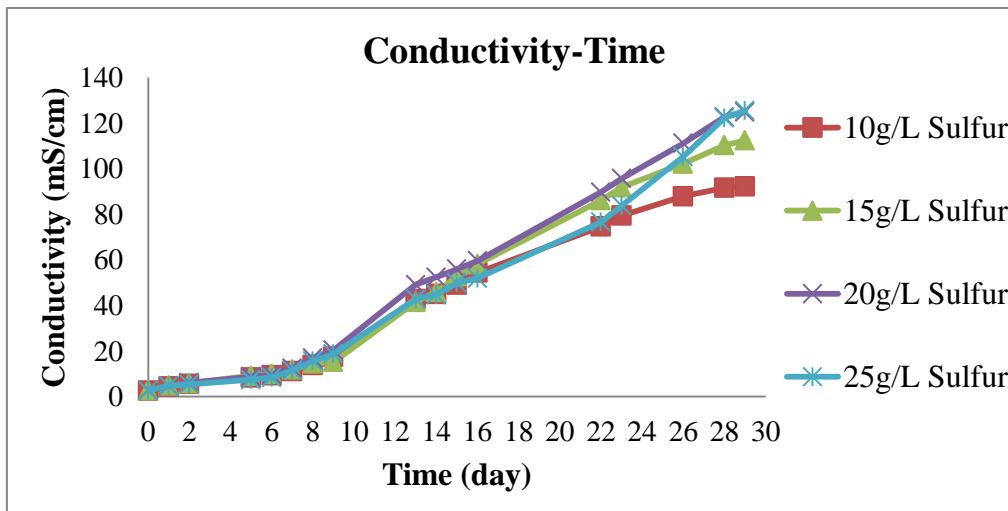


Figure 3.24. Conductivity profile for bioleaching with different sulfur amounts

Sulfate concentration profile was given in Figure 3.25. Initial sulfate concentrations were equal to each other and 1.3 g/L for all the batches. At the day 6, again the sulfate concentrations were same and equal to 5 g/L. After day 6, increase in sulfate concentrations continued which means production of more sulfuric acid. At the last day (day 29), the highest sulfate concentration was at the 25 g/L sulfur batch with 45 g/L sulfate and the lowest sulfate concentration was at the 10 g/L sulfur batch with 33 g/L sulfate.

Phosphorus dissolution profile was given in Figure 3.26. As it is seen from the Figure 3.26, at the first 5 day phosphorus dissolution reached to 57.3, 59.6, 55.2, 55.0% for the 10, 15, 20, 25 g/L sulfur batches, respectively. After this day, dissolution of phosphorus continued and changes were very similar for all the batches. At the last day of bioleaching, the highest dissolution was at the 15 g/L sulfur batch with 72.9% and the lowest dissolution was at the 20 g/L sulfur batch with 67.7%. From all these results, it can be concluded that sulfur concentrations between 10 and 25 g/L did not change the phosphorus dissolution too much because dissolution percentages were very similar to each other.

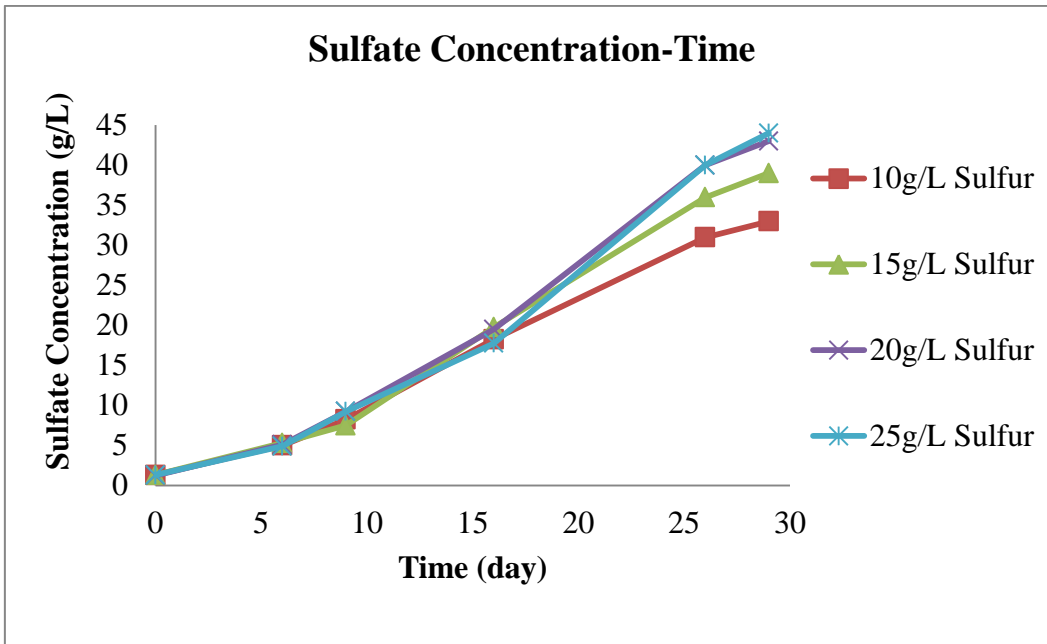


Figure 3.25. Sulfate concentration profile for bioleaching with different sulfur amounts

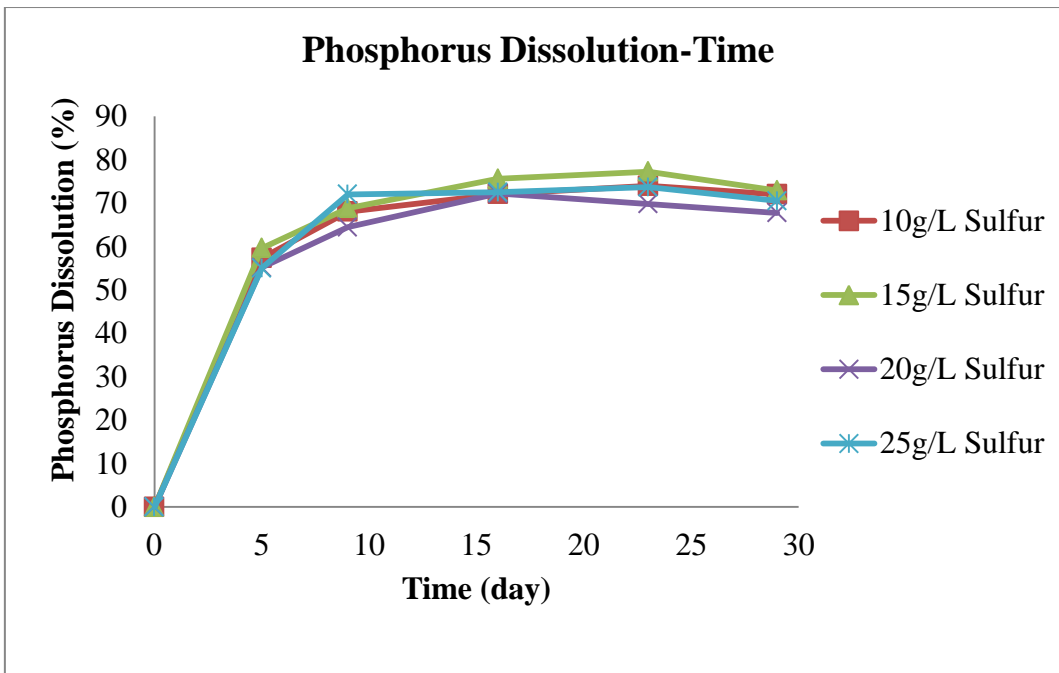


Figure 3.26. Phosphorus dissolution profile for bioleaching with different sulfur amounts

3.3.4. Bioleaching in 2 L reactor

After the determination of optimum ash amount, inocula volume and sulfur amount for sulfur oxidizing bacteria, this trial was realized in 2 L reactor. This trial lasted 30 days and other information about this trial were given in Table 2.4.

The pH and conductivity profiles of this trial were given in Figure 3.27. As it is seen from the Figure 3.27, there was decrease in pH levels and increase in conductivity levels. The starting pH was 6.1 and it dropped to below 2 at day 14, which is important for phosphorus dissolution. After day 14, pH continued to decrease and it dropped to 1 at the last day of bioleaching (day 30). Initial conductivity was 2.16 mS/cm and till the day 14 there were small increases in conductivity. After day 14, conductivity increase was faster which is probably because of the pH change. Because decrease of pH causes dissolution of ions from the ash and this increases the conductivity. At the last day of bioleaching, conductivity reached to 17.65 mS/cm.

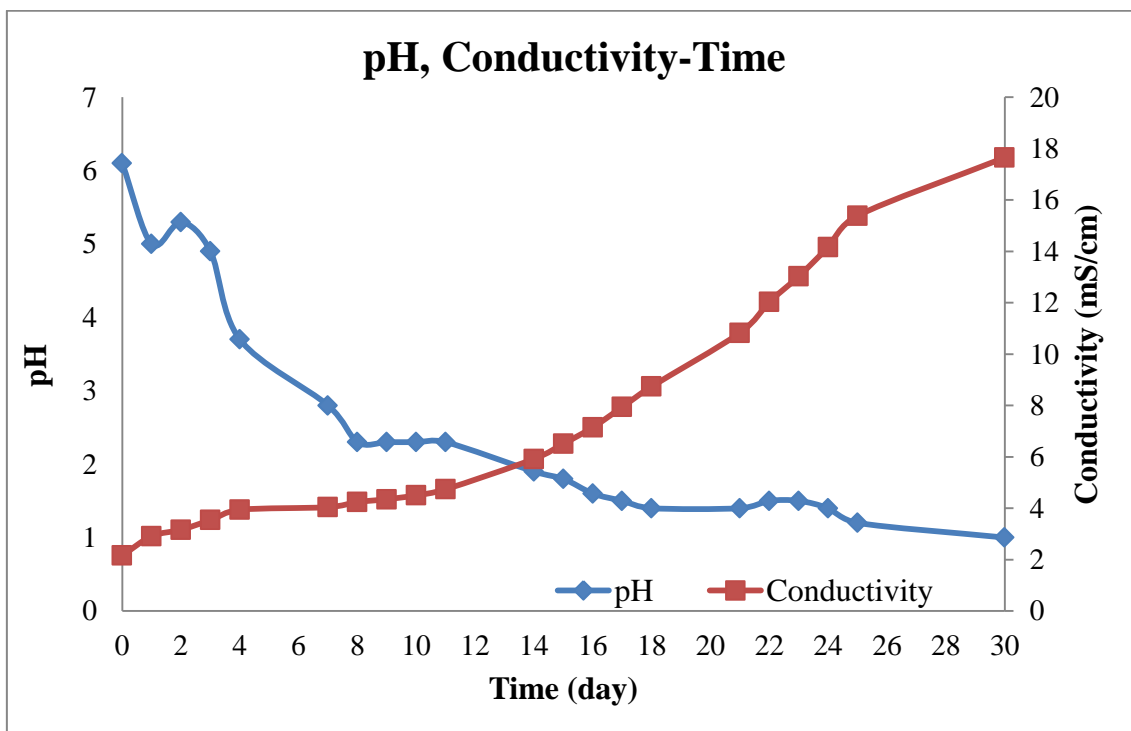


Figure 3.27. pH and conductivity profiles for bioleaching in 2 L reactor

Sulfate concentration profile was given in Figure 3.28. As it is seen from this Figure 3.28, the sulfate concentration increased with time. The initial sulfate concentration was 0.9 g/L and at the day 11 it reached to 3.2 g/L. Between the days 0 and 11 there was

not a significant change in sulfate concentration. The reason for this minor change might be the adaptation of sulfur oxidizing bacteria to sewage sludge ash. After this 11th day, the rate of increase in sulfate concentration was faster and it reached to 12 g/L at the last day of bioleaching.

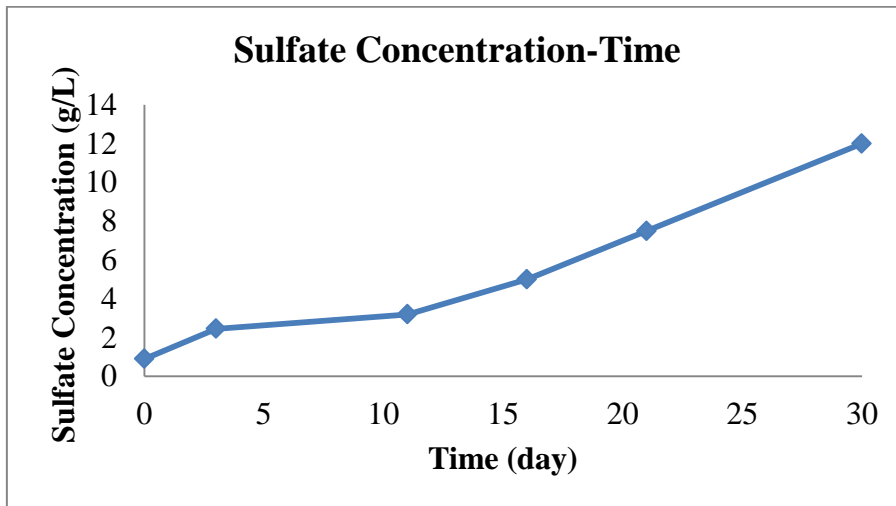


Figure 3.28. Sulfate concentration profile for bioleaching in 2 L reactor

Phosphorus dissolution profile was given in Figure 3.29. Phosphorus dissolution was slower at the first 11 days. The reason for this slow dissolution was the pH levels at these days. Because phosphorus dissolution needs pH levels below 2 and when pH levels reached to this levels, phosphorus dissolution increased after 11th day. While dissolution was 23.5% at the 11th day, it was 79.2% at the day 21. After day 21, there was no significant change in phosphorus dissolution and it was 81.7 at day 30. Thus, 21 days seem to enough for the bioleaching of the phosphorus.

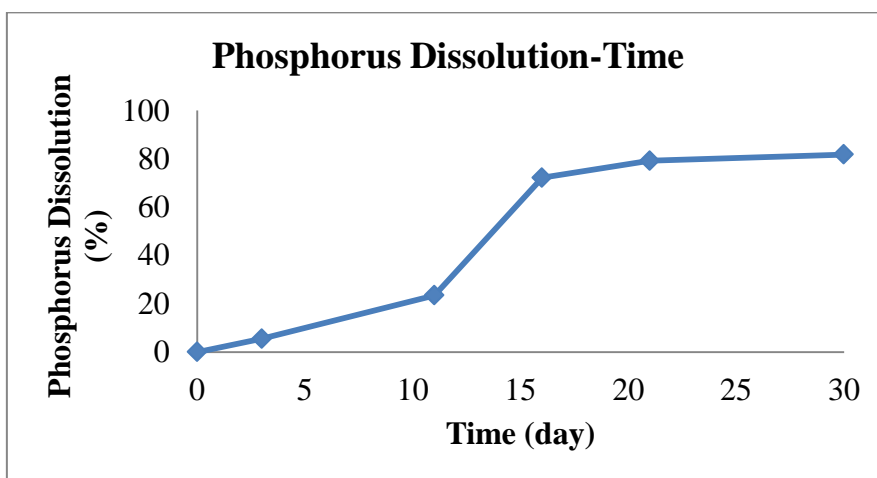


Figure 3.29. Phosphorus dissolution profile for bioleaching in 2 L reactor

Zimmermann and Dott (2009) performed experiments for the recovery of phosphorus from sewage sludge ash with bioleaching process and they obtained 93% phosphorus release with the mixed culture of *Acidithiobacillus ferrooxidans* and *Acidithiobacillus thiooxidans*. The reason for the lower phosphorus percentages in this study with mixed culture might be the energy source of the *Acidithiobacillus ferrooxidans*. Because ferrous sulfate heptahydrate ($\text{FeSO}_4 \cdot 7\text{H}_2\text{O}$) was used as energy source for the Iron oxidizing bacteria in this study. However in the study of Zimmermann and Dott (2009), they have used elemental sulfur. Another reason might be related with the way that bioleaching experiments performed. Because they have used 25 mL/min constant flow of the media, 500 mL of medium volume, 20 L/min ambient air aeration and ash amount of 2 g. Unlike the study of Zimmermann and Dott (2009), there were no circulation of the media and there was no aeration in this study.

Fang et al. (2018) studied chemical leaching of the phosphorus and trace elements from incinerated sewage sludge ash. They have obtained 94% of the phosphorus dissolution with using 0.2 mol/L H_2SO_4 with 20:1 liquid to solid ratio in 2 hour reaction time.

Heavy metal dissolution percentages of this study and Zimmermann and Dott (2009) were given in Table 3.4. Although dissolution of the Al was similar in both studies, dissolution of Zn, Fe, Pb, Cu and Ni was higher in this study.

Table 3.4. Heavy metal dissolution percentages after bioleaching

	This study	Zimmermann and Dott, 2009
Zn (%)	37.5	20
Fe (%)	78.5	16
Al (%)	61.8	61
Pb (%)	32.9	-
Cu (%)	98.1	41
Ni (%)	66.0	-
Cr (%)	31.8	13

In the study of Li et al. (2017), they have studied the chemical extraction of the heavy metals from sewage sludge ash. They have used 0.5 mol/L H_2SO_4 as extractant. When their dissolution percentages were compared with this study, they have seen Zn dissolution around 40%, like this study. Their Pb dissolution result was also similar with 38.4%. However they obtained higher dissolution for Cr with 57.7%.

3.4. Electrodialysis Studies

3.4.1. Electrodialysis with graphite electrodes

One of the electrodialysis experiments was realized with graphite electrodes. In this experiment, middle solution was the solution that obtained from bioleaching experiments and it contained 2175 mg/L PO_4^{3-} and 10250 mg/L SO_4^{2-} . This trial was lasted 11 days which can be considered as 2 different parts. Because, during the first 9 days of the electrodialysis process, it was observed that while there was no passage of the phosphate ions to anode part, some portion of the sulfate passed to the anode part. The reason for this situation was the problem related with the connections of the electric circuit to the electrodialysis reactor. When this problem was realized and solved at the day 9, phosphate anions started to pass to the anode part.

pH profile of this trial were given in Figure 3.30. As it is seen from this Figure 3.30, there were no significant changes in pH values during first 9 days and after electrical problem was solved, pH of the anode part decreased from 1.4 to 0.9. This decrease was because of the acidification reaction takes place at the anode and also might be because of the passage of the sulfate ions to the anode. Moreover, pH of the cathode part increased from 1.6 to 12.5; because the reactions that take place at the cathode produce OH^- ions. Also, pH of the middle part increased from 1.3 to 2.2 because of the lost sulfate ions.

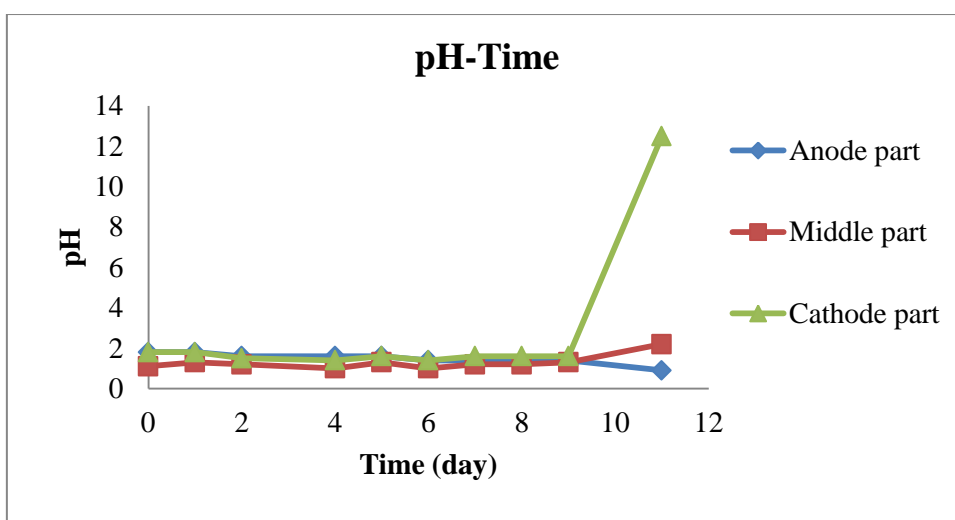


Figure 3.30. pH profile for electrodialysis realized with bioleaching solution and graphite electrodes

Conductivity profile of this trial was given in Figure 3.31. As it is seen from this Figure 3.31, during first 9 days of electro dialysis, there was decrease in conductivity of middle part and increase in conductivity of anode part. During first 9 day, the conductivity of the anode part increased from 3.96 to 9.93 mS/cm and conductivity of the middle part decreased from 20.54 to 14.25 mS/cm. The reason for this situation was the sulfate ion passage to the anode part even there was no electricity entrance to the reactor and this passage can be explained by the concentration difference between the middle part and anode part. However, significant changes were observed after day 9, after solving the electricity problem of the reactor, migration of the ions from the middle part to the anode part was realized faster; thus, conductivity of the anode part reached to 24.6 mS/cm and conductivity of the middle part decreased to 3.96 mS/cm.

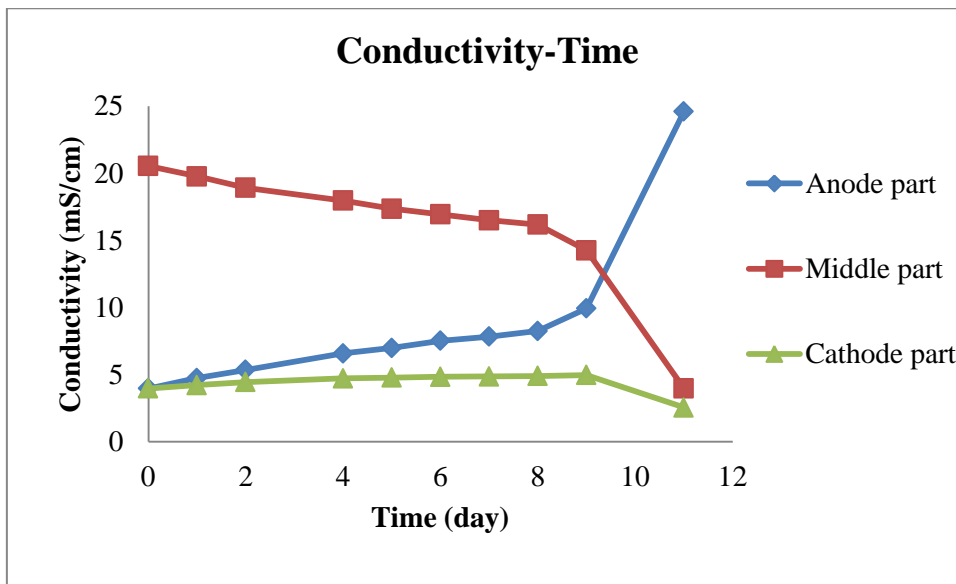


Figure 3.31. Conductivity profile for electro dialysis realized with bioleaching solution and graphite electrodes

Sulfate concentration profile for the middle part of the electro dialysis reactor was shown in Figure 3.32. As it was mentioned before, there was migration of the sulfate ions from the middle part to the anode part between the days 0 and 9; sulfate ion concentration decreased from 10250 to 8250 mg/L and this corresponds to 32.5% passage to the anode part. However, between the days 9 and 11, migration of the sulfate ions became faster because of the application of the electricity and it decreased from 8250 to 3250 mg/L which corresponds to 77.2% passage to the anode part.

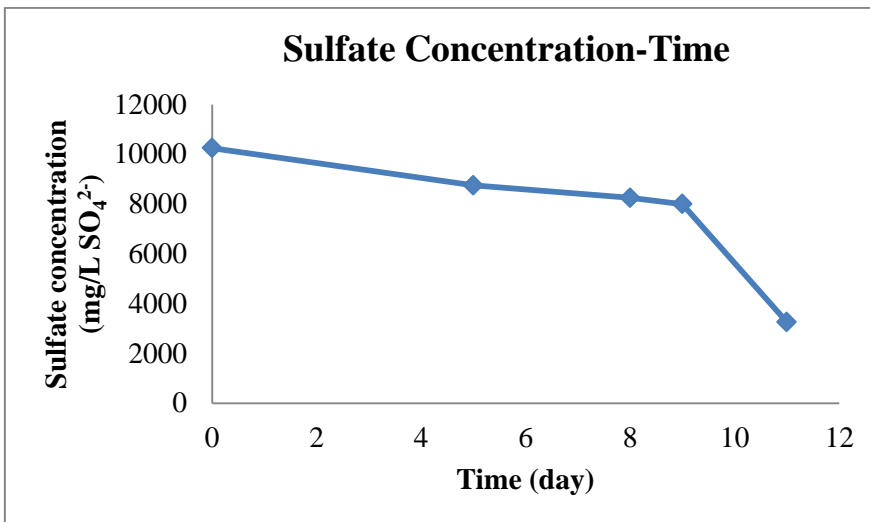


Figure 3.32. Sulfate concentration profile for middle part

Phosphate concentration profiles for the middle and anode parts were shown in Figure 3.33. As it is seen from this Figure 3.33, between the days 0 and 9, there were no significant changes of the phosphate concentrations of both middle and anode parts. However, between the days 9 and 11, there was sharp decrease of phosphate concentration at the middle part. The reasons for this decrease were the passage to the anode part and precipitation that took place at the middle part caused by the pH increase at the cathode part. Between the days 9 and 11, phosphate concentration at the anode part increased and between these days passage to the anode part was 6.6%. From this result, it can be concluded that phosphate ion migration is strongly dependent to applied electricity and not realized with concentration difference.

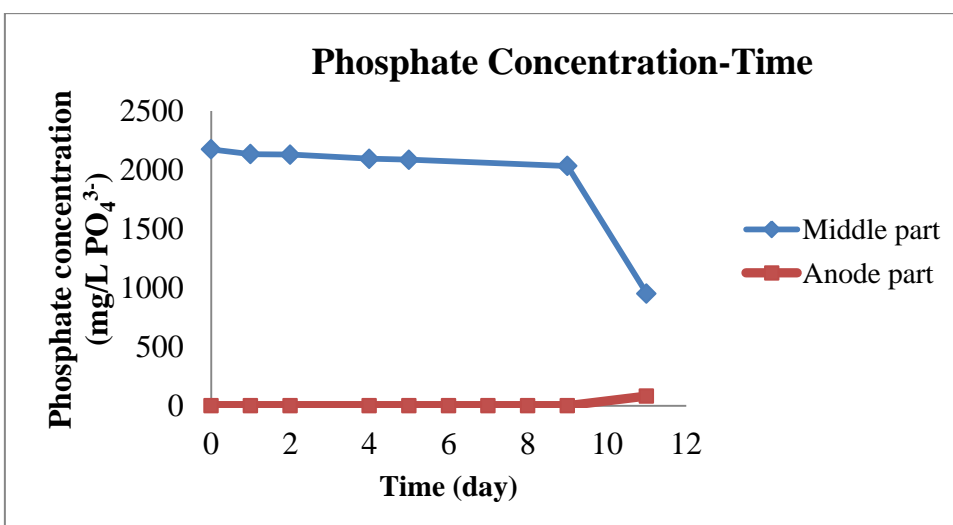


Figure 3.33. Phosphate concentration profiles for the middle and anode parts

During the electro dialysis trial with the graphite electrodes; electrical problem was realized, it was solved at the day 9 and phosphate migration to anode part was achieved. However, at the end of the day 11, graphite electrodes were damaged unexpectedly at the anode part as it is shown at Figure 3.34. Therefore this electro dialysis trial was ended at the day 11 and other trials of electro dialysis were realized with gold coated copper electrodes.

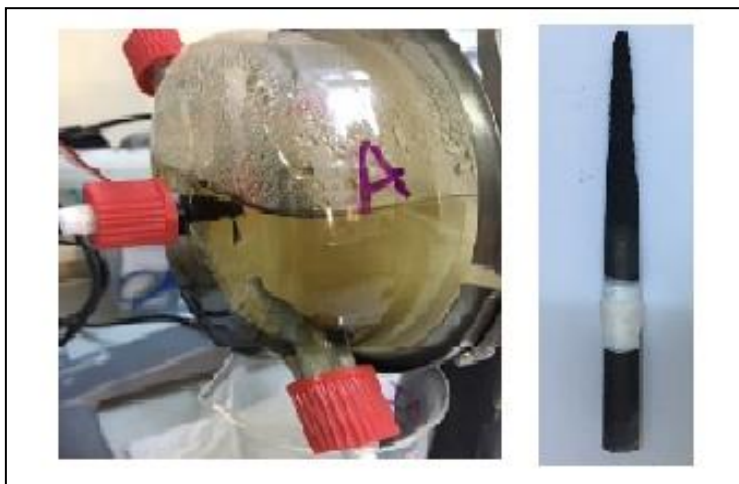


Figure 3.34. Graphite electrode of the anode part after electro dialysis

3.4.2. Electro dialysis with gold coated copper electrodes

3.4.2.1. Electro dialysis with the synthetic phosphate containing solution

Electro dialysis experiment was performed with the synthetic phosphate containing solution which was 2000 mg/L K_2HPO_4 solution and it lasted 2 days until the phosphate at the middle part decreased to low levels. During these 2 days, phosphate concentration at the middle part decreased because of the passages to anode and cathode parts that led to increase in phosphate concentrations at the anode and cathode parts. Figure 3.35. shows the phosphate concentration profiles for the middle, anode and cathode part.

Figure 3.36. shows the phosphorus passage percentages to the anode part during electro dialysis process. After 1 day, phosphorus passage to the anode part was 64.2% and at the end of the 2 days of electro dialysis process it reached to 86.5%.

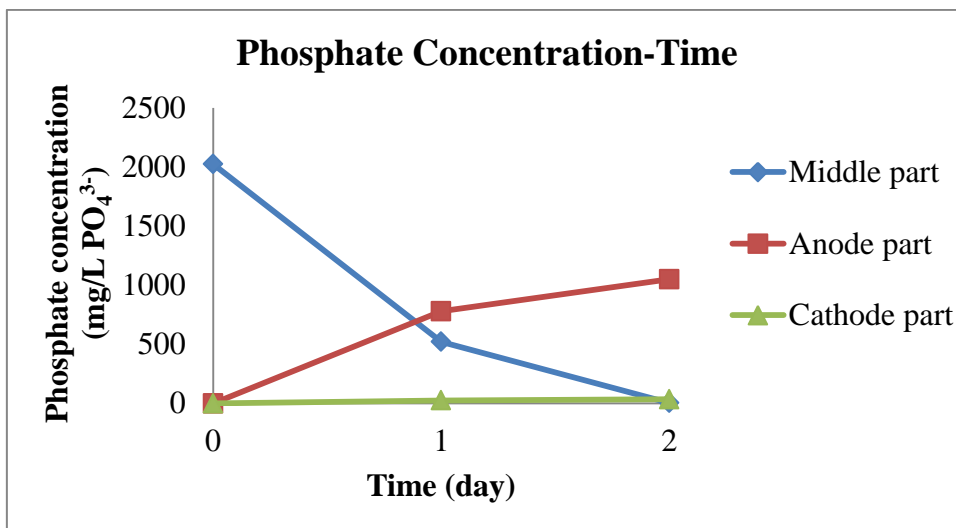


Figure 3.35. Phosphate concentration profiles for the middle, anode and cathode parts

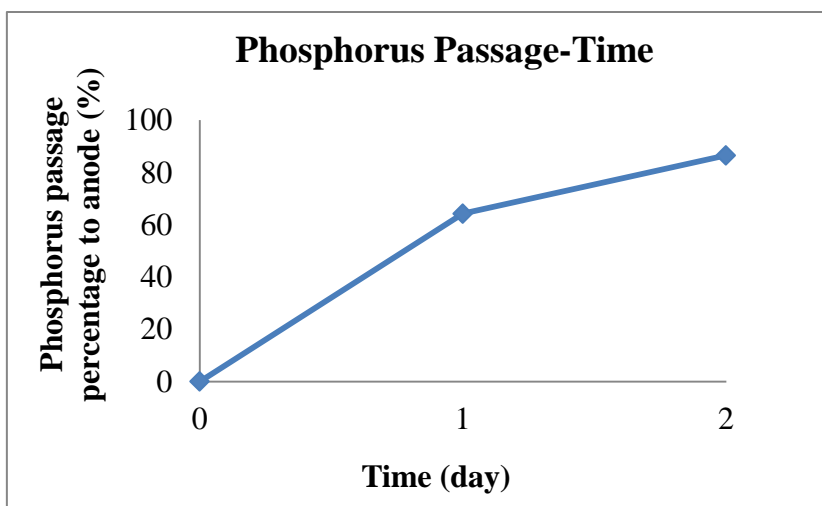


Figure 3.36. Phosphorus passage percentages to anode part

At the end of this trial, phosphate mass balance was done to see the distributions of the phosphate on the anode part, cathode part, middle part, anion exchange membrane and cation exchange membrane. This mass balance was shown in Figure 3.37. After electro dialysis process, most of the phosphate ions were at the anode part of the reactor with 86.5%. Phosphate at the middle part was only 0.2% and at the cathode part this percentage was 2.96%. There were also phosphate on the anion and cation exchange membranes in very small amounts, 0.3% at the anion exchange membrane and 0.2% at the cation exchange membrane. Also, 9.8% of the phosphate was shown as ‘lost’ at the mass balance because the sum of the masses at the anode part, cathode part, middle part and membranes were 90.2%. The reason for this ‘lost’ part might be the precipitation of

the phosphorus because mass balance was done with soluble portions, digestion was not applied.

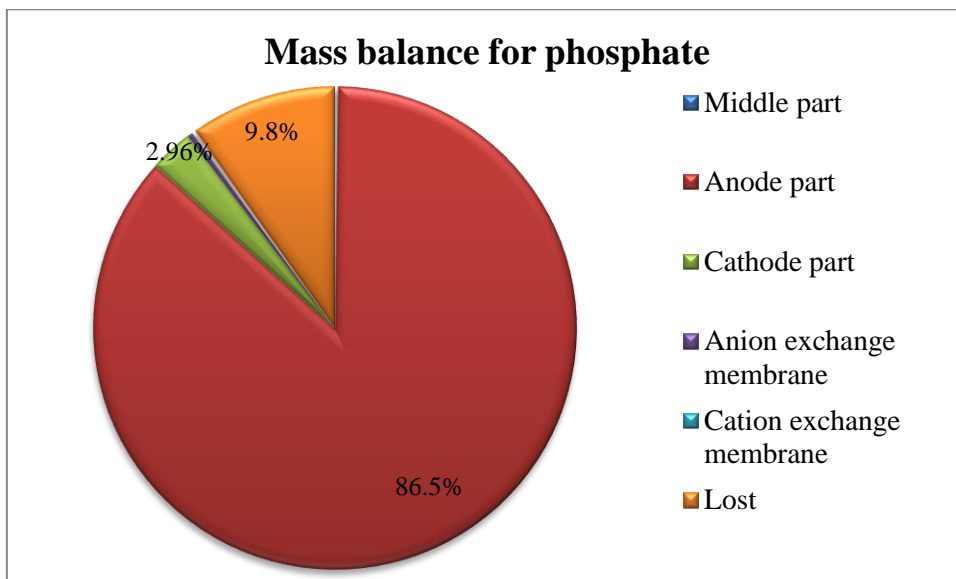


Figure 3.37. Mass balance for phosphate ion after electro dialysis

3.4.2.2. Electro dialysis with bioleaching solution

Another electro dialysis trial was realized with bioleaching solution that contained 1000 mg/L PO_4^{3-} and 10500 mg/L SO_4^{2-} . The content of the bioleaching solution was given in Table 3.5. This electro dialysis trial was lasted 14 days.

Table 3.5. Content of the bioleaching solution

	Concentration (mg/L)
Zn	12.2
Fe	47
Al	230
Cu	5.2
Ni	2.5
Cr	2.3
Ca	354
Mg	114

During this trial, pH increase at the middle part was observed. The reasons of this situation might be the sulfate ion passage to the anode part and also the reactions that take place at the cathode side. Interestingly, there was one advantage and one drawback

of this situation. The advantage was related with the distribution of the phosphate ions as a function of pH. This distribution was given in Figure 3.38. From this Figure 3.38, it is seen that at low pHs ($\text{pH} < 2$), some portion of the phosphate ions are in the form of phosphoric acid (H_3PO_4) which has no electrical charge and uncharged species cannot be separated in electro dialysis process. Thus, higher pHs were better for electro dialysis process. The drawback was the phosphorus concentration decrease at the middle part due to precipitation. Therefore, a balance must be established to prevent precipitation while keeping phosphate ions in the ionized form. Therefore, Visual MINTEQ 3.1 program was used to decide the pH. Results of the Visual MINTEQ 3.1 program were given in Figure 3.39. As it was seen from Figure 3.39, when pH was 1, 90% of the phosphate was in the form of H_3PO_4 . However when it was increased to 2, the dominant phosphate specie was H_2PO_4^- and H_3PO_4 percentage decreased to 47%. When pH was further increased after 2, H_2PO_4^- percentage was around 90%; however, when pH was increased to these levels precipitation was also seen. Thus it was decided to keep the pH of the middle part around 2 to be sure that dominant phosphate specie was not H_3PO_4 .

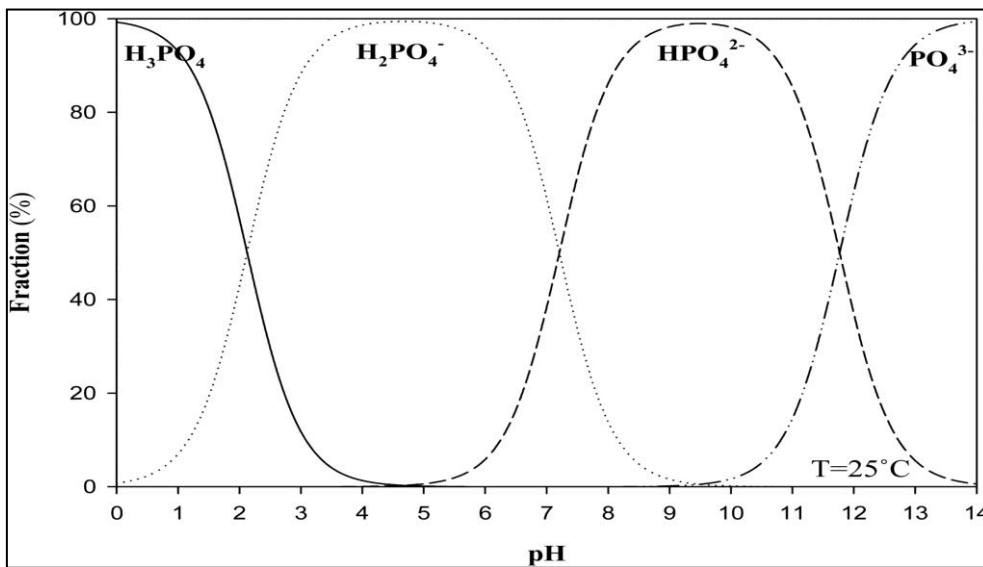


Figure 3.38. Distribution of phosphate species as a function of pH (Thanh and Liu, 2017)

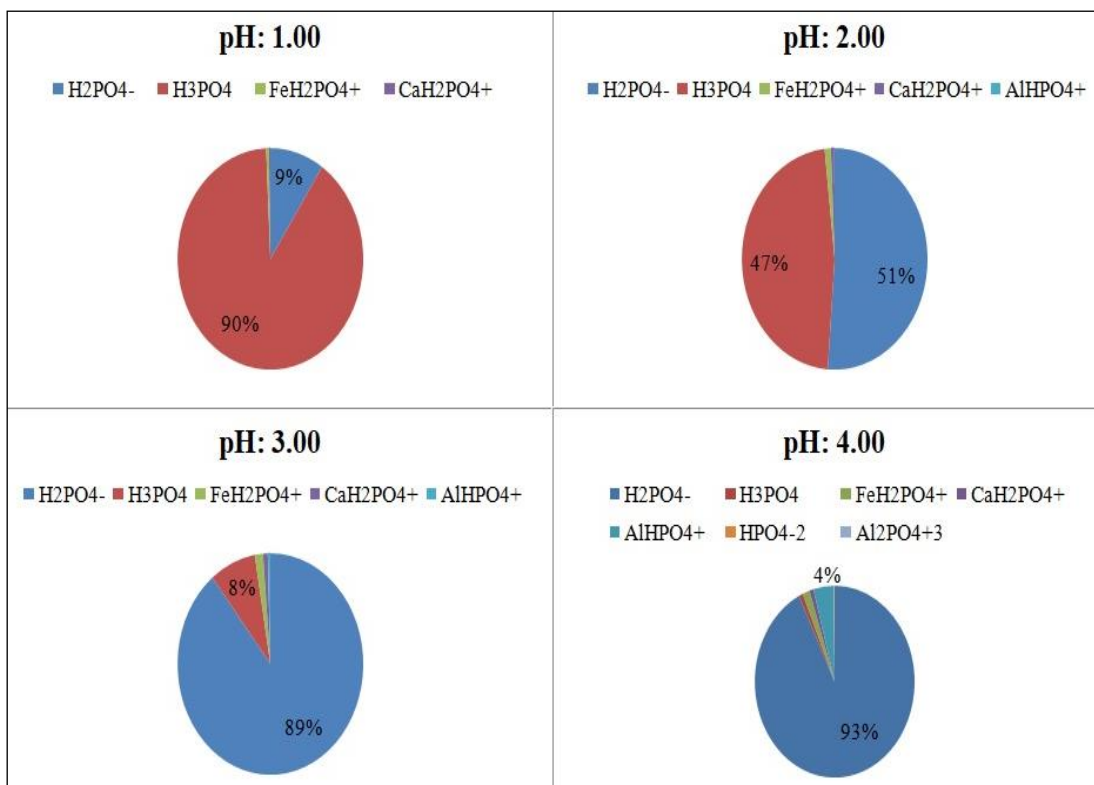


Figure 3.39. Phosphate species for different pH values

pH profile of this trial was given in Figure 3.40. Initial pH of the middle part was 1.9 and it increased to 2.3 at the 2nd day and after this day pH was decreased to around 2 by adding HNO₃ to the middle part of the reactor. Therefore, there are pH increases and decreases for the middle part as it is seen from Figure 3.40. Similar situation was seen for the cathode part between the days 0 and 6. Initial pH of the cathode part was 1.8 and it increased to 13.6 after 1 day because of the cathode reactions. To prevent precipitations at the cation exchange membrane, pH of the catholyte was adjusted to below 2 by adding HNO₃. Therefore, for the cathode part, there were pH increases and decreases till the day 6. After this day, pH of the catholyte did not increase. The reason for this situation might be the destruction of the electrode. pH of the anode part did not change significantly as in the case of the cathode and middle parts. Initial pH for the anode part was 1.8 and it increased to 3.7 after 9 days and some precipitations were seen on the anion exchange membrane. To prevent these precipitations, pH of the anolyte was decreased to below 2, and it did not change between the days 10-14.

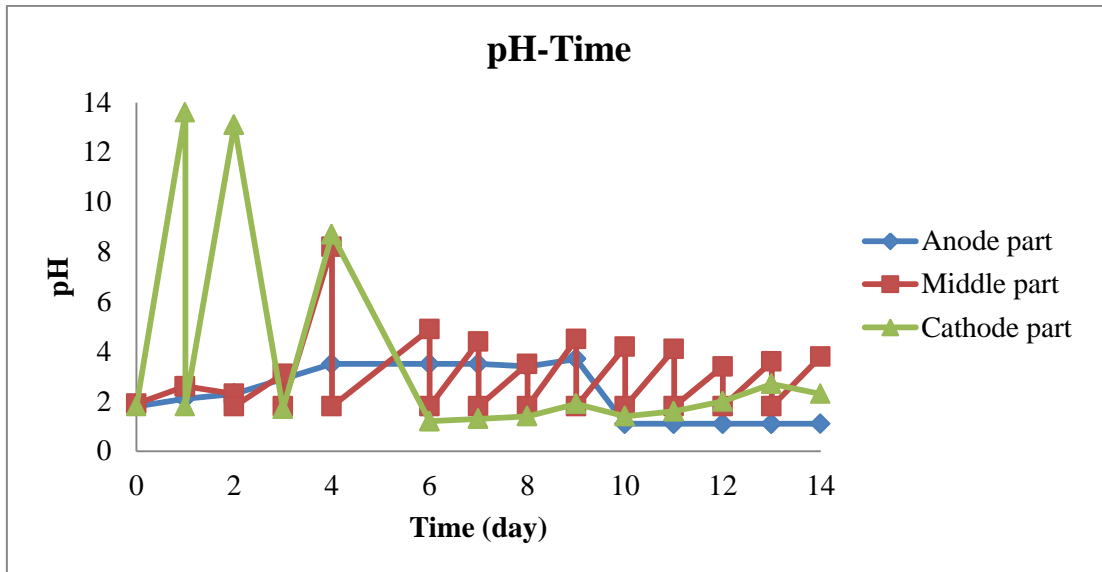


Figure 3.40. pH profile for electro dialysis realized with bioleaching solution and gold coated copper electrodes

During this trial, conductivity of the anode side increased gradually because of the passage of the PO_4^{3-} and SO_4^{2-} ions. Figure 3.41 shows the conductivity profile of the anode part.

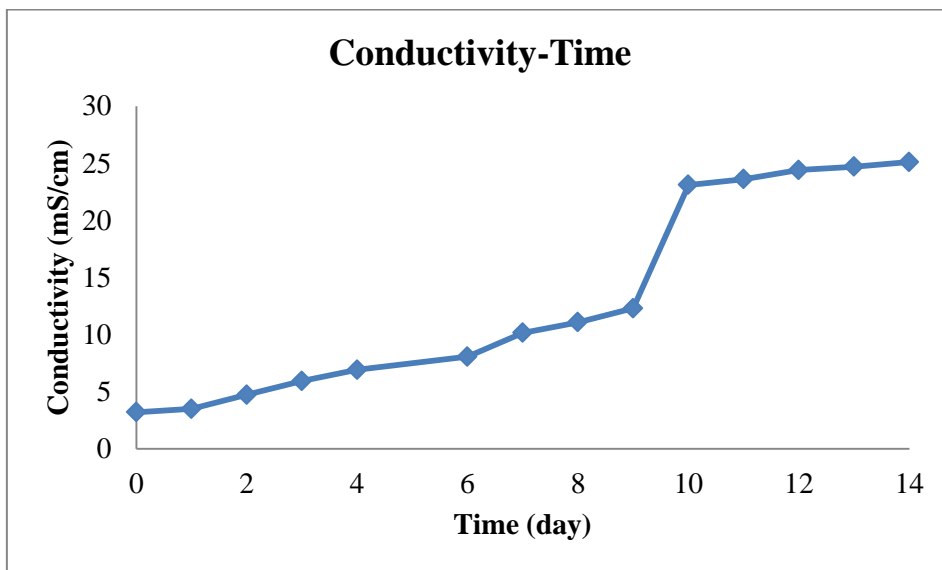


Figure 3.41. Conductivity profile for the anode part

Figure 3.42 shows the phosphate concentrations for the middle part and anode part. During the electro dialysis of the bioleaching solution, phosphate concentration of the anode side increased gradually. For the middle part, the expected situation was the decrease of the phosphate concentration. However as it is seen from the Figure 3.42,

there were increases for the middle part. This was because of the addition of the acid to solubilize the precipitates and also to prevent precipitations. Solubilization of the precipitates increased the concentration of the phosphate at the middle part.

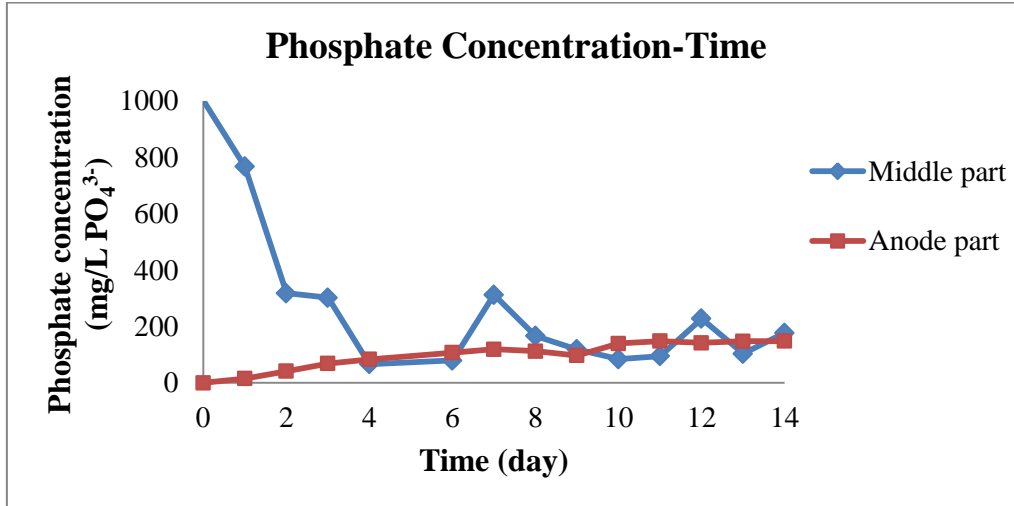


Figure 3.42. Phosphate concentrations for the middle part and anode part

Figure 3.43 shows the phosphorus passage percentages to anode part. As the time passed, phosphate concentration increased at the anode side and its recovery percentage too. At the 10th day, phosphorus passage to anode side reached to 23.2% and after this point it did not change too much and it was 24.6% at the last day of electro dialysis.

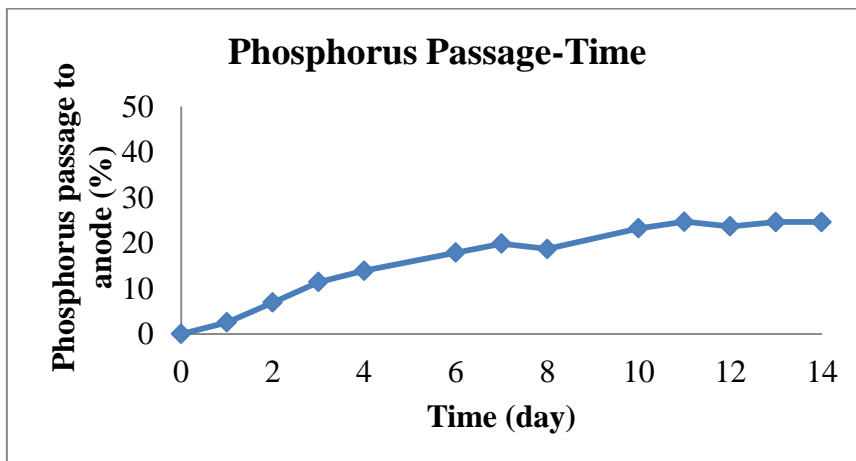


Figure 3.43. Phosphorus passage percentages to anode part

At the end of this trial, phosphate mass balance was done to see the distributions of the phosphate on the anode part, cathode part, middle part, anion exchange membrane, cation exchange membrane and mechanical mixer. This mass balance was shown in Figure 3.44. After electro dialysis process, most of the phosphate ion was at the

precipitated form with the percentage of 54.7%. This precipitated form was found from the difference between the acid digested phosphate concentration and soluble phosphate concentration. As it was mentioned before, 24.6% of the phosphate ion was at the anode part and 17.7% was at the middle part of the electro dialysis reactor at the end of the 14th day. 4.7% of the phosphate was at the catholyte because of the formation of positively charged phosphorus complexes. Also, very small percentages of the phosphate ion were found on the anion and cation exchange membranes with the percentages of 0.07% and 0.6%, respectively. Lastly, 0.01% of the phosphorus was on the mechanical mixer.

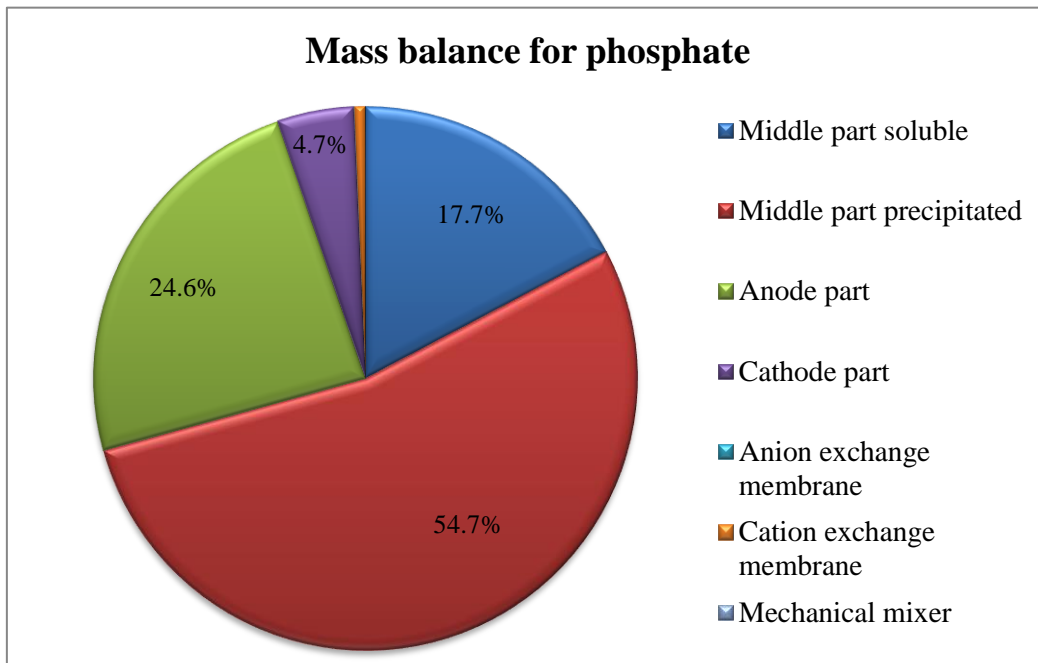


Figure 3.44. Mass balance for phosphate ion after electro dialysis

After the electro dialysis with copper coated electrodes, it was seen that the electrode at the anode part was damaged as it was shown in Figure 3.45. The reason for this situation was the corrosive nature of the anode part.



Figure 3.45. Gold coated copper electrodes at the anode part before and after the electro dialysis (left side: before electro dialysis, right side: after electro dialysis)

In the study of Guedes et al. (2014), they studied the recovery of phosphorus from two different sewage sludge ashes with chemical leaching and electro dialysis processes. They have recovered 20% of the phosphorus from the sewage sludge ashes after 7 days. This result was very similar with the result obtained from this study; 19.9% of phosphorus was at the anode part after 7 days. However, Guedes et al. (2014) obtained 59% and 69% of phosphorus transportation to the anode part after 14 days. In this study, 24.6% of the phosphorus was at the anode part after 14 days. The reason for this difference might be the usage of different electrodes. Because copper electrode at the anode side was damaged and this might cause decrease in efficiency of the electrical conductance to the electro dialysis reactor. To prevent such situations, platinum coated electrodes can be used like Guedes et al. (2014).

Heavy metal passage percentages were given in Table 3.6 with the percentages from the study of Guedes et al. (2014). When passage percentages were compared, passage of the Zn was almost same with the Guedes et al. (2014). However; Fe, Al and Cr passages were higher in Guedes et al. (2014). The reason for this difference might be precipitation at the cathode part or might be usage of the different ashes. Also, while Cu

passage was 95.4% in this study, it was around 80% in the study of Guedes et al. (2014).

Table 3.6. Heavy metals, Ca and Mg passage percentages to the cathode part

	This study	Guedes et al., 2014 for 2 different ashes	
Zn (%)	54.6	~50	~50
Fe (%)	0	~6	~6
Al (%)	6.0	~50	~50
Cu (%)	95.4	79	82
Ni (%)	58.4	-	-
Cr (%)	0	12	15
Ca (%)	83.6	-	-
Mg (%)	85.8	-	-

4. CONCLUSIONS

In this MSc. study, phosphorus recovery from sewage sludge ash with sequencing bioleaching and electro dialysis was realized. Batch bioleaching experiments were conducted to obtain the maximum phosphorus dissolution from the sewage sludge ash and again batch electro dialysis experiments were conducted to separate dissolved phosphorus from the heavy metals.

Bioleaching experiments performed to find the optimum ash amount for 200 mL total volume resulted in different phosphorus dissolution percentages depending on the conditions of the experiments. Trial realized with the Iron oxidizing bacteria was not successful because only 14.9% of the phosphorus inside the sewage sludge ash was dissolved after 48 days for the 2 g ash batch. This was because of the iron-phosphate chemistry and it was also proved with the XRD results. Trial with the Sulfur oxidizing bacteria was more successful and 68.5% of the phosphorus became soluble after 9 days of bioleaching for the 2 g ash batch. After 29 days, there was no significant difference and it was 68.6%. Trial with the mixture of Sulfur&Iron oxidizing bacteria yielded lower than the only Sulfur oxidizing bacteria. After 29 days of bioleaching, 54.2% phosphorus dissolution was obtained. This lower dissolution compared with the only Sulfur oxidizing bacteria might be again the iron-phosphate chemistry. After all these experiments 2 g ash was found as the optimum amount for 200 mL volume.

Sulfur oxidizing bacteria and mixture of Sulfur&Iron oxidizing bacteria were used to determine the optimum inocula volume for the maximum phosphorus dissolution. 40% inocula volume resulted in 76.6% phosphorus dissolution with the Sulfur oxidizing bacteria after 16 days. Mixture of Sulfur&Iron oxidizing bacteria had the lower yields in terms of phosphorus dissolution and 67% was obtained from the 35% inocula volume after 29 days. Thus, 40% inocula volume with Sulfur oxidizing bacteria was the optimum for the phosphorus bioleaching from sewage sludge ash.

Sulfur oxidizing bacteria with 2 g ash for 200 mL total volume and 40% inocula volume were used to find the optimum amount of energy source (elemental sulfur) for the bacteria. Sulfur concentration range of 10 and 25 g/L were investigated and it was seen that there were no significant differences between these concentrations in terms of

phosphorus dissolution. After 29 day of bioleaching, phosphorus dissolution percentages were between 67.7 and 72.9%.

Last bioleaching trial was realized in 2 L reactor with the optimum conditions obtained from previous studies. At the 21th day 79.2% phosphorus dissolution was seen and at the 29th day there was no significant change and it was 81.7%.

Electrodialysis experiments were performed with two different electrodes: graphite electrodes and gold coated copper electrodes. Both electrodes damaged because of the corrosive effect of the anode part. However, graphite electrodes damaged earlier than the copper ones. In two days, 6.6% of the phosphate migrated to anode part from the middle part of the reactor in the case of graphite electrodes but experiment was not lasted so much because electrodes could not be used so much after this point. Experiments with gold coated copper electrodes lasted 14 days and 24.6% of the phosphorus passage to the anode part was obtained. Thus, usage of another types of electrodes like platinum coated titanium can be suggested. Also, continuous pH control at the middle and cathode parts can increase the phosphorus migration to anode part by preventing precipitations.

REFERENCES

- Abuşoğlu, A., Özahi, E., Kutlar, A. İ., Al-jaf, H. (2017). Life cycle assessment (LCA) of digested sewage sludge incineration for heat and power production. *Journal of Cleaner Production*, 142 (2017), 1684-1692.
- Adam, C., Peplinski, B., Michaelis, M., Kley, G., Simon, F. -G. (2009). Thermochemical treatment of sewage sludge ashes for phosphorus recovery. *Waste Management*, 29 (2009), 1122-1128.
- AirPrex[®], 2015. Technical factsheet,
http://p-rex.eu/uploads/media/PREX_Factsheet_AIRPREX.pdf (28.7.2017).
- Altin, S., Oztekin, E., Altin, A. (2017). Comparison of electro dialysis and reverse electro dialysis process in the removal of Cu(II) from dilute solutions. *Korean Journal of Chemical Engineering*, 34 (2017), 2218-2224.
- Arnout, S., Nagels, E. (2016). Modelling thermal phosphorus recovery from sewage sludge ash. *CALPHAD: Computer Coupling of Phase Diagrams and Thermochemistry*, 55 (2016), 26-31.
- AshDec[®], 2015. Technical factsheet,
http://p-rex.eu/uploads/media/PREX_Factsheet_ASHDEC.pdf (29.7.2017).
- Atienza-Martínez, M., Gea, G., Arauzo, J., Kersten, S. R. A., Kootstra, A. M. J. (2014). Phosphorus recovery from sewage sludge char ash. *Biomass and Bioenergy*, 65 (2014), 42-50.
- Avdalovic, J., Beskoski, V., Gojgic-Cvijovic, G., Mattinen, M. L., Stojanovic, M., Zildzovic, S., Vrvic, M. M. (2015). Microbial solubilization of phosphorus from phosphate rock by iron-oxidizing *Acidithiobacillus* sp. B2. *Minerals Engineering*, 72 (2015), 17-22.
- Berg, U., Knoll, G., Kaschka, E., Kreutzer, V., Donnert, D., Weidler, P. G., Nüesch, R. (2005). P-RoC-Phosphorus Recovery from Wastewater by Crystallisation of Calcium Phosphate Compounds. *Journal of Residual Science and Technology*.

Bernardes, A. M., Rodrigues, M. A. S., Ferreira, J. Z. (2014). General Aspects of Electrodialysis. *Electrodialysis and Water Reuse, Topics in Mining, Metallurgy and Materials Engineering*, Springer.

Bewer, G., Debrodt, H., Herbst, H. (1982). Titanium for electrochemical processes. *Journal of Metals*, January 1982, 37-41.

Chi, R., Xiao, C., Gao, H. (2006). Bioleaching of phosphorus from rock phosphate containing pyrites by *Acidithiobacillus ferrooxidans*. *Minerals Engineering*, 19 (2006), 979-981.

Cieślak, B. M., Namieśnik, J., Konieczka, P. (2015). Review of sewage sludge management: standards, regulations and analytical methods. *Journal of Cleaner Production*, 90 (2015), 1-15.

Cieślak, B., Konieczka, P. (2017). A review of phosphorus recovery methods at various steps of wastewater treatment and sewage sludge management. The concept of “no solid waste generation” and analytical methods. *Journal of Cleaner Production*, 142 (2017), 1728-1740.

Cordell, D., Drangert, J., White, S. (2009). The story of phosphorus: Global food security and food for thought. *Global Environmental Change*, 19 (2009), 292-305.

Cordell, D., Rosemarin, A., Schröder, J. J., Smit, A. L. (2011). Towards global phosphorus security: A systems framework for phosphorus recovery and reuse options. *Chemosphere*, 84 (2011), 747-758.

Coutand, M., Cyr, M., Deydier, E., Guilet, R., Clastres, P. (2008). Characteristics of industrial and laboratory meat and bone meal ashes and their potential applications. *Journal of Hazardous Materials*, 150 (2008), 522-532.

Darwish, M., Aris, A., Puteh, M. H., Jusoh, M. N. H., Kadir, A. A. (2016a). Waste bones ash as an alternative source of P for struvite precipitation. *Journal of Environmental Management*, In Press.

Darwish, M., Aris, A., Puteh, M. H., Abideen, M. Z., Othman, M. N. (2016b). Ammonium-Nitrogen Recovery from Wastewater by Struvite Crystallization Technology. *Separation & Purification Reviews*, 45:4, 261-274.

- Davis, M. L. (2010). *Water and Wastewater Engineering: Design Principles and Practise*, McGraw-Hill.
- Demirbas, A. (2009). *Biofuels- Securing the Planet's Future Energy Needs*. Springer.
- Desmidt, E., Ghyselbrecht, K., Zhang, Y., Pinoy, L., Van der Bruggen, B., Verstraete, W., Rabaey, K., Meesschaert, B. (2015). Global Phosphorus Scarcity and Full-Scale P-Recovery Techniques: A Review. *Critical Reviews in Environmental Science and Technology*, 45:4, 336-384.
- Díaz-Tena, E., Gallastegui, G., Hipperdinger, M., Donati, E. R., Ramírez, M., Rodríguez, A., López de Lacalle, L. N., Elías, A. (2016). New advances in copper biomachining by iron-oxidizing bacteria. *Corrosion Science*, 112 (2016), 385-392.
- Donatello, S., Cheeseman, C. R. (2013). Recycling and recovery routes for incinerated sewage sludge ash (ISSA): A review. *Waste Management*, 33 (2013), 2328-2340.
- Ebbers, B., Ottosen, L. M., Jensen, P. E. (2015a). Comparison of two different electro-dialytic cells for separation of phosphorus and heavy metals from sewage sludge ash. *Chemosphere*, 125 (2015), 122-129.
- Ebbers, B., Ottosen, L. M., Jensen, P. E. (2015b). Electro-dialytic treatment of municipal wastewater and sludge for the removal of heavy metals and recovery of phosphorus. *Electrochimica Acta*, 181 (2015), 90-99.
- Egle, L., Rechberger, H., Zessner, M. (2015). Overview and description of technologies for recovering phosphorus from municipal wastewater. *Resources, Conservation and Recycling*, 105 (2015), 325-346.
- Egle, L., Rechberger, H., Krampe, J., Zessner, M. (2016). Phosphorus recovery from municipal wastewater: An integrated comparative technological, environmental and economic assessment of P recovery technologies. *Science of the Total Environment*, 571 (2016), 522-542.
- Ekpo, U., Ross, A. B., Camargo-Valero, M. A., Fletcher, L. A. (2016). Influence of pH on hydrothermal treatment of swine manure: Impact on extraction of nitrogen and phosphorus in process water. *Bioresource Technology*, 214 (2016), 637-644.

- Fang, D., Zhou, L. X. (2006). Effect of sludge dissolved organic matter on oxidation of ferrous iron and sulfur by *Acidithiobacillus ferrooxidans* and *Acidithiobacillus thiooxidans*. *Water, Air, and Soil Pollution*, 171 (2006), 81-94.
- Fang, L., Li, J., Guo, M. Z., Cheeseman, C. R., Tsang, D. C. W., Donatello, S., Poon, C. S. (2018). Phosphorus recovery and leaching of trace elements from incinerated sewage sludge ash (ISSA). *Chemosphere*, 193 (2018), 278-287.
- Feng, S., Yang, H., Xin, Y., Zhang, L., Kang, W., Wang, W. (2012). Isolation of an extremely acidophilic and highly efficient strain *Acidithiobacillus sp.* for chalcopyrite bioleaching. *Journal of Industrial Microbiology and Biotechnology*, 39 (2012), 1625-1635.
- Franz, M. (2008). Phosphate fertilizer from sewage sludge ash (SSA). *Waste Management*, 28 (2008), 1809-1818.
- Fytali, D., Zabaniotou, A. (2008). Utilization of sewage sludge in EU application of old and new methods- A review. *Renewable and Sustainable Energy Reviews*, 12 (2008), 116-140.
- Gantner, O., Schipper, W., Weigand, J. J. (2014). *Technological Use of Phosphorus: The Non-fertilizer, Non-feed and Non-detergent Domain. Sustainable Phosphorus Management: A Global Transdisciplinary Roadmap*, Springer.
- George, T. S., Hinsinger, P., Turner, B. L. (2016). Phosphorus in soils and plants-facing phosphorus scarcity. *Plant Soil*, 401 (2016), 1-6.
- Giesen, A., Erwee, H., Wilson, R., Botha, M., Fourie, S. (2009). Experience with crystallisation as sustainable, zero-waste technology for treatment of wastewater. *Abstracts of the International Mine Water Conference*, 401-406.
- Gifhorn, 2015. Technical factsheet,
http://p-rex.eu/uploads/media/PREX_Factsheet_GIFHORN.pdf (29.7.2017).
- Gonçalves, A. R. S. (2015). Analysis of chromium behaviour and speciation during the electro-dialytic process. MSc Thesis, New University of Lisbon, Lisbon, Portugal.

- Guedes, P., Couto, N., Ottosen, L. M., Ribeiro, A. B. (2014). Phosphorus recovery from sewage sludge ash through an electrolysytic process. *Waste Management*, 34 (2014), 886-892.
- Havukainen, J., Nguyen, M. T., Hermann, L., Horttanainen, M., Mikkilä, M., Deviatkin, I., Linnanen, L. (2016). Potential of phosphorus recovery from sewage sludge and manure ash by thermochemical treatment. *Waste Management*, 49 (2016), 221-229.
- He, Z., Liu, W., Wang, L., Tang, C., Guo, Z., Yang, C., Wang, A. (2016). Clarification of phosphorus fractions and phosphorus release enhancement mechanism related to pH during waste activated sludge treatment. *Bioresource Technology*, 222 (2016), 217-225.
- Hem, J. D., Cropper, W. H. (1962). Survey of ferrous-ferric chemical equilibria and redox potentials. *Chemistry of Iron in Natural Waters*, Geological Survey Water-Supply Paper, United States Government Printing Office, Washington.
- Henze, M., van Loosdrecht, M. C. M., Ekama, G. A., Brdjanovic, D. (2008). *Biological Wastewater Treatment: Principles, Modelling and Design*, IWA Publishing.
- Herzel, H., Krüger, O., Hermann, L., Adam, C. (2016). Sewage sludge ash- A promising secondary phosphorus source for fertilizer production. *Science of the Total Environment*, 542 (2016), 1136-1143.
- Huang, C., Xu, T., Zhang, Y., Xue, Y., Chen, G. (2007). Application of electrodialysis to the production of organic acids: State-of-the-art and recent developments. *Journal of Membrane Science*, 288 (2007), 1-12.
- Jindarom, C., Meeyoo, V., Kitiyanan, B., Rirksomboon, T., Rangsunvigit, P. (2007). Surface characterization and dye adsorptive capacities of char obtained from pyrolysis/gasification of sewage sludge. *Chemical Engineering Journal*, 133 (2007), 239-246.
- Kaikake, K., Sekito, T., Dote, Y. (2009). Phosphate recovery from phosphorus-rich solution obtained from chicken manure incineration ash. *Waste Management*, 29 (2009), 1084-1088.
- Káňanová, N., Machuča, L., Tvrzník, D. (2014). Determination of limiting current density for different electrodialysis modules. *Chemical Papers*, 68 (2014), 324-329.

- Kataki, S., West, H., Clarke, M., Baruah, D. C. (2016). Phosphorus recovery as struvite from farm, municipal and industrial waste: Feedstock suitability, methods and pre-treatments. *Waste Management*, 49 (2016), 437-454.
- Kleemann, R., Chenoweth, J., Clift, R., Morse, S., Pearce, P., Saroj, D. (2017). Comparison of phosphorus recovery from incinerated sewage sludge ash (ISSA) and pyrolyzed sewage sludge char (PSSC). *Waste Management*, 60 (2017), 201-210.
- LEACHPHOS[®], 2015. Technical factsheet,
http://p-rex.eu/uploads/media/PREX_Factsheet_LEACHPHOS.pdf (29.7.2017).
- Le Corre, K. S., Valsami-Jones, E., Hobbs, P., Parsons, S. A. (2009). Phosphorus Recovery from Wastewater by Struvite Crystallization: A Review. *Critical Reviews in Environmental Science and Technology*, 39:6, 433-477.
- Lee, M., Kim, D. -J. (2017). Identification of phosphorus forms in sewage sludge ash during acid pre-treatment for phosphorus recovery by chemical fractionation and spectroscopy. *Journal of Industrial and Engineering Chemistry*, 51 (2017), 64-70.
- Li, J., Tsang, D. C. W., Wang, Q., Fang, L., Xue, Q., Poon, C. S. (2017). Fate of metals before and after chemical extraction of incinerated sewage sludge ash. *Chemosphere*, 186 (2017), 350-359.
- Li, L., Lv, Z., Zuo, Z., Yang, Z., Yuan, X. (2016). Effect of energy source and leaching method on bio-leaching of rock phosphates by *Acidithiobacillus ferrooxidans*. *Hydrometallurgy*, 164 (2016), 238-247.
- Liberti, L., Petruzzelli, D., De Florio, L. (2001). REM NUT Ion Exchange Plus Struvite Precipitation Process. *Environmental Technology*, 22:11, 1313-1324.
- Liu, Y., Villalba, G., Ayres, R. U., Schroder, H. (2008). Global Phosphorus Flows and Environmental Impacts from a Consumption Perspective. *Journal of Industrial Ecology*, 12 (2008), 229-247.
- Liu, Y., Kumar, S., Hoon-Kwag, J., Ra, C. (2013). Magnesium ammonium phosphate formation, recovery and its application as valuable resources: a review. *Journal of Chemical Technology & Biotechnology*, 88 (2013), 181-189.

- Lynn, C. J., Dhir, R. K., Ghataora, G. S., West, R. P. (2015). Sewage sludge ash characteristics and potential for use in concrete. *Construction and Building Materials*, 98 (2015), 767-779.
- Magro, C. J. C. (2014). Electrolytic remediation of two types of air pollution control residues and their applicability in construction materials. MSc Thesis, New University of Lisbon, Lisbon, Portugal.
- Mehta, C. M., Khunjar, W. O., Nguyen, V., Tait, S., Batstone, D. J. (2015). Technologies to Recover Nutrients from Waste Streams: A Critical Review. *Critical Reviews in Environmental Science and Technology*, 45:4, 385-427.
- Melia, P. M., Cundy, A. B., Sohi, S. P., Hooda, P. S., Busquets, R. (2017). Trends in the recovery of phosphorus in bioavailable forms from wastewater. *Chemosphere*, 186 (2017), 381-395.
- Mephrec®, (2015). Technical factsheet,
http://p-rex.eu/uploads/media/PREX_Factsheet_MEPHREC.pdf (29.7.2017).
- Metcalf & Eddy (2004). *Wastewater Engineering: Treatment and Reuse*, Fourth Edition, McGraw-Hill.
- Metcalf & Eddy (2014). *Wastewater Engineering: Treatment and Resource Recovery*, Fifth Edition, McGraw-Hill.
- Montastruc, L., Azzaro-Pantel, C., Biscans, B., Cabassud, M., Domenech, S. (2003). A thermochemical approach for calcium phosphate precipitation modeling in a pellet reactor. *Chemical Engineering Journal*, 94 (2003), 41-50.
- Murakami, T., Suzuki, Y., Nagasawa, H., Yamamoto, T., Koseki, T., Hirose, H., Okamoto, S. (2009). Combustion characteristics of sewage sludge in an incineration plant for energy recovery. *Fuel Processing Technology*, 90 (2009), 778-783.
- Nguyen, T. A. H., Ngo, H. H., Guo, W. S., Zhang, J., Liang, S., Lee, D. J., Nguyen, P. D., Bui, X. T. (2014). Modification of agricultural waste/by-products for enhanced phosphate removal and recovery: Potential and obstacles. *Bioresource Technology*, 169 (2014), 750-762.

- Ottosen, L. M., Jensen, P. E., Kirkelund, G. M. (2014). Electrodialytic Separation of Phosphorus and Heavy Metals from Two Types of Sewage Sludge Ash. *Separation Science and Technology*, 49:12, 1910-1920.
- Ottosen, L. M., Jensen, P. E., Kirkelund, G. M. (2016). Phosphorus recovery from sewage sludge ash suspended in water in a two-compartment electrodialytic cell. *Waste Management*, 51 (2016), 142-148.
- Pathak, A., Dastidar, M. G., Sreekrishnan, T. R. (2009). Bioleaching of heavy metals from sewage sludge: A review. *Journal of Environmental Management*, 90 (2009), 2343-2353.
- Pearce, B. J. (2015). Phosphorus Recovery Transition Tool (PRTT): a transdisciplinary framework for implementing a regenerative urban phosphorus cycle. *Journal of Cleaner Production*, 109 (2015), 203-215.
- Pedersen, K. B., Lejon, T., Jensen, P. E., Ottosen, L. M. (2016). Degradation of oil products in a soil from a Russian Barents hot-spot during electrodialytic remediation. *Springer Plus*, 5:168.
- Peng, G., Tian, G., Liu, J., Bao, Q., Zang, L. (2011). Removal of heavy metals from sewage sludge with a combination of bioleaching and electrokinetic remediation technology. *Desalination*, 271 (2011), 100-104.
- Petzet, S., Peplinski, B., Cornel, P. (2012). On wet chemical phosphorus recovery from sewage sludge ash by acidic or alkaline leaching and an optimized combination of both. *Water Research*, 46 (2012), 3769-3780.
- Pradhan, N., Nathsarma, K. C., Srinivasa Rao, K., Sukla, L. B., Mishra, B. K. (2008). Heap bioleaching of chalcopyrite: A review. *Minerals Engineering*, 21 (2008), 355-365.
- Priha, O., Sarlin, T., Blomberg, P., Wendling, L., Mäkinen, J., Arnold, M., Kinnunen, P. (2014). Bioleaching of phosphorus from fluorapatites with acidophilic bacteria. *Hydrometallurgy*, 150 (2014), 269-275.
- Samolada, M. C., Zabaniotou, A. A. (2014). Comparative assessment of municipal sewage sludge incineration, gasification and pyrolysis for a sustainable sludge-to-energy management in Greece. *Waste Management*, 34 (2014), 411-420.

- Schippers, A. (2007). Microorganisms involved in bioleaching and nucleic acid-based molecular methods for their identification and quantification. *Microbial Processing of Metal Sulfides*, Springer, 3-33.
- Scholz, R. W., Roy, A. H., Brand, F. S., Hellums, D. T., Ulrich, A. E. (2014). *Sustainable Phosphorus Management: A Global Transdisciplinary Roadmap*, Springer.
- Sengupta, S., Nawaz, T., Beaudry, J. (2015). Nitrogen and Phosphorus Recovery from Wastewater. *Current Pollution Reports*, 1 (2015), 155-166.
- Spångberg, J., Hansson, P. -A., Tidåker, P., Jönsson, H. (2011). Environmental impact of meat meal fertilizer vs. chemical fertilizer. *Resources, Conservation and Recycling*, 55 (2011), 1078-1086.
- Stendahl, K., Jäfverström, S., (2004). Recycling of sludge with the Aqua Reci process. *Water Science and Technology*, 49 (2004), 233–240.
- Sun, T. R. (2013). Effect of pulse current on energy consumption and removal of heavy metals during electro-dialytic soil remediation. PhD Thesis, Technical University of Denmark.
- Szögi, A. A., Vanotti, M. B., Hunt, P. G. (2015). Phosphorus recovery from pig manure solids prior to land application. *Journal of Environmental Management*, 157 (2015), 1-7.
- Tan, Z., Lagerkvist, A. (2011). Phosphorus recovery from the biomass ash: A review. *Renewable and Sustainable Energy Reviews*, 15 (2011), 3588-3602.
- Tao, W., Fattah, K. P., Huchzermeier, M. P. (2016). Struvite recovery from anaerobically digested dairy manure: A review of application potential and hindrances. *Journal of Environmental Management*, 169 (2016), 46-57.
- Thomsen, T. P., Sárossy, Z., Ahrenfeldt, J., Henriksen, U. B., Frandsen, F. J., Müller-Stöver, D. S. (2017a). Changes imposed by pyrolysis, thermal gasification and incineration on composition and phosphorus fertilizer quality of municipal wastewater sludge. *Journal of Environmental Management*, 198 (2017), 308-318.
- Thanh, L. H. V., Liu, J. C. (2017). Flotation separation of strontium via phosphate precipitation. *Water Science and Technology*, 75 (2017), 2520-2526.

- Thomsen, T. P., Hauggaard-Nielsen, H., Gøbel, B., Stoholm, P., Ahrenfeldt, J., Henriksen, U. B., Müller-Stöver, D. S. (2017b). Low temperature circulating fluidized bed gasification and co-gasification of municipal sewage sludge. Part 2: Evaluation of as materials as phosphorus fertilizer. *Waste Management*, 66 (2017), 145-154.
- Toldrá, F., Mora, L., Reig, M. (2016). New insights into meat by-product utilization. *Meat Science*, 120 (2016), 54-59.
- Töre, G. Y., Kar, Y. B. (2017). Evaluation of Gasification Efficiency of Miscellaneous Industrial Sewage Sludges in a Down Draft Fluidized Bed Reactor. *Environmental Processes*, 4 (2017), 223-237.
- Udaeta, M. C., Dodbiba, G., Ponou, J., Sone, K., Fujita, T. (2017). Recovery of Phosphorus from Sewage Sludge Ash (SSA) by heat treatment followed by high gradient magnetic separation and flotation. *Advanced Powder Technology*, 28 (2017), 755-762.
- United States Geological Survey, Mineral Commodity Summaries, January 2017, <https://minerals.usgs.gov/minerals/pubs/commodity/phosphaterock/mcs-2017-phosp.pdf> (30.6.2017).
- Valero, F., Barceló, A., Arbós, R. (2011). Electrodialysis Technology - Theory and Applications. *Desalination, Trends and Technologies, In Tech*.
- van Dijk, K. C., Lesschen, J. P., Oenema, O. (2016). Phosphorus flows and balances of the European Union Member States. *Science of the Total Environment*, 542 (2016), 1078-1093.
- Viader, R. P., Jensen, P. E., Ottosen, L. M., Ahrenfeldt, J., Hauggaard-Nielsen, H. (2015). Electrodialytic extraction of phosphorus from ash of low-temperature gasification of sewage sludge. *Electrochimica Acta*, 181 (2015), 100-108.
- Villalba, G., Liu, Y., Schroder, H., Ayres, R. U. (2008). Global Phosphorus Flows in the Industrial Economy From a Production Perspective. *Journal of Industrial Ecology*, 12 (2008), 557-569.
- Vogel, C., Adam, C., Unger, M. (2011). Heavy metal removal from sewage sludge ash analyzed by thermogravimetry. *Journal of Thermal Analysis and Calorimetry*, 103 (2011), 243-248.

- Wang, J., Shen, S., Kang, J., Li, H., Guo, Z. (2010). Effect of ore solid concentration on the bioleaching of phosphorus from high-phosphorus iron ores using indigenous sulfur-oxidizing bacteria from municipal wastewater. *Process Biochemistry*, 45 (2010), 1624-1631.
- Weigand, H., Bertau, M., Hübner, W., Bohndick, F., Bruckert, A. (2013). RecoPhos: Full-scale fertilizer production from sewage sludge ash. *Waste Management*, 33 (2013), 540-544.
- Wen, Y. -M., Wang, Q. -P., Tang, C., Chen, Z. -L. (2012). Bioleaching of heavy metals from sewage sludge by *Acidithiobacillus thiooxidans*—a comparative study. *Journal of Soils and Sediments*, 12 (2012), 900–908.
- Wen, Y. -M., Cheng, Y., Tang, C., Chen, Z. -L. (2013). Bioleaching of heavy metals from sewage sludge using indigenous iron-oxidizing microorganisms. *Journal of Soils and Sediments*, 13 (2013), 166-175.
- Wilfert, P., Kumar, P. S., Korving, L., Witkamp, G. J., van Loosdrecht, M. C. M. (2015). The Relevance of Phosphorus and Iron Chemistry to the Recovery of Phosphorus from Wastewater: A Review. *Environmental Science and Technology*, 49 (2015), 9400-9414.
- Wilhelmy, R. B., Patel, R. C., Matijevic, E. (1985). Thermodynamics and Kinetics of Aqueous Ferric Phosphate Complex Formation. *Inorganic Chemistry*, 24 (1985), 3290-3297.
- Worsfold, P., McKelvie, I., Monbet, P. (2016). Determination of phosphorus in natural waters: A historical review. *Analytica Chimica Acta*, 918 (2016), 8-20.
- Wu, D., Xiao, L., Ba, Y., Wang, H., Zhang, A., Wu, X., Niu, M., Fang, K. (2017). The recovery of energy, nitrogen and phosphorus from three agricultural wastes by pyrolysis. *Energy Procedia*, 105 (2017), 1263-1269.
- Xiao, C. Q., Chi, R. A., Li, W. S., Zheng, Y. (2011). Biosolubilization of phosphorus from rock phosphate by moderately thermophilic and mesophilic bacteria. *Minerals Engineering*, 24 (2011), 956-958.

- Ye, Y., Ngo, H. H., Guo, W., Liu, Y., Zhang, X., Guo, J., Ni, B., Chang, S. W., Nguyen, D. D. (2016). Insight into biological phosphate recovery from sewage. *Bioresource Technology*, 218 (2016), 874-881.
- Ye, Y., Ngo, H. H., Guo, W., Liu, Y., Li, J., Liu, Y., Zhang, X., Jia, H. (2017). Insight into chemical phosphate recovery from municipal wastewater. *Science of the Total Environment*, 576 (2017), 159-171.
- Zhang, P., Zhu, Y., Zhang, G., Zou, S., Zeng, G., Wu, Z. (2009). Sewage sludge bioleaching by indigenous sulfur-oxidizing bacteria: Effects of ratio of substrate dosage to solid content. *Bioresource Technology*, 100 (2009), 1394–1398.
- Zhou, K., Barjenbruch, M., Kabbe, C., Inial, G., Remy, C. (2017). Phosphorus recovery from municipal and fertilizer wastewater: China's potential and perspective. *Journal of Environmental Sciences*, 52 (2017), 151-159.
- Zhu, J., Yao, Y., Lu, Q., Gao, M., Ouyang, Z. (2015). Experimental investigation of gasification and incineration characteristics of dried sewage sludge in a circulating fluidized bed. *Fuel*, 150 (2015), 441-447.
- Zimmermann, J., Dott, W. (2009). Sequenced bioleaching and bioaccumulation of phosphorus from sludge combustion- A new way of resource reclaiming. *Advanced Materials Research*, Volumes (71-73), 625-628.

CURRICULUM VITAE

Name and Surname : Büşra KUNT

Birth Location and Date : Kadıköy, 10.06.1991

E-mail : kuntbusra@gmail.com

Education

Degree	Department/ Program	University/ High School	Graduation Year
High School	Science	T.E.B. Ataşehir High School	2009
BSc Degree	Environmental Engineering	Marmara University	2014
BSc Degree	Chemical Engineering	Marmara University	2015